Spatio-temporal Distribution Mapping of Invasive Weed *Lantana camara* Using Satellite Imageries in Chitwan Annapurna Landscape, Nepal

A Dissertation submitted for partial fulfillment of the requirements for the Master's Degree in Science, Central Department of Botany
Tribhuvan University

Submitted by

Sandeep Dhakal

T.U. Regd. No.: 5-2-33-57-2012

Exam Roll No.: 426

Batch: 2073/075

Ecology and Resource Management Unit

Central Department of Botany

Institute of Science and Technology

Tribhuvan University, Kirtipur, Kathmandu, Nepal

July, 2021

Letter of Recommendation

This is to certify that the dissertation work entitled "**Spatio-temporal distribution mapping of invasive weed *Lantana camara* using satellite imageries in Chitwan Annapurna Landscape, Nepal**" has been completed by **Mr. Sandeep Dhakal** under our supervision. This entire work was accomplished on the basis of candidate's original research work. To the best of our knowledge, the work has not been submitted to any other academic degree. We hereby recommend for acceptance of this dissertation as a partial fulfillment of the requirement of Master's Degree in Botany at the Institute of Science and Technology, Tribhuvan University, Nepal.

…….....

Supervisor

Assoc. Prof. Dr. Bharat Babu Shrestha

Central Department of Botany

Tribhuvan University

Kirtipur, Kathmandu, Nepal

…….....……

Co- Supervisor

Prof. Emeritus Dr. Pramod Kumar Jha

Central Department of Botany

Tribhuvan University

Kirtipur, Kathmandu, Nepal

…….....

Co- Supervisor

Prof. Dr. Krishna Prasad Poudel

Central Department of Education

Tribhuvan University

Kirtipur, Kathmandu, Nepal

Date: 21 July 2021

Letter of Approval

The M.Sc. dissertation entitled **"Spatio-temporal distribution mapping of invasive weed *Lantana camara* using satellite imageries in Chitwan Annapurna Landscape, Nepal "** submitted to the Central Department of Botany, Tribhuvan University, Kirtipur, Kathmandu by Mr. Sandeep Dhakal has been accepted as partial fulfillment of the requirement of Masters of Science in Botany.

Examination Committee

…….....…

External Examiner
Prof. Dr. Mukesh Kumar Chhetri
Amrit Science Campus
Tribhuvan University

…….....…

Internal Examiner
Asst. Prof. Dr. Achyut Tiwari
Central Department of Botany
Tribhuvan University

…….....

Supervisor
Assoc. Prof. Dr. Bharat Babu Shrestha
Central Department of Botany
Tribhuvan University

…….....…….

Co- Supervisor
Prof. Emeritus Dr. Pramod Kumar Jha
Central Department of Botany
Tribhuvan University

…….....

Co- Supervisor
Prof. Dr. Krishna Prasad Poudel
Central Department of Education
Tribhuvan University

…….....

Prof. Dr. Ram Kailash Prasad Yadav
Head
Central Department of Botany
Tribhuvan University

Date: 21 July 2021

Declaration

I, Sandeep Dhakal, hereby declare that this dissertation entitled "**Spatio-temporal distribution mapping of invasive weed *Lantana camara* using satellite imageries in Chitwan Annapurna Landscape, Nepal**" is my original work and all other sources of the information used are duly acknowledged. I have not submitted it or any of its part to any other universities for any academic award.

.....

Sandeep Dhakal
Central Department of Botany
Tribhuvan University, Kirtipur
Kathmandu, Nepal
Email: sandeepdhakal29@gmail.com

Date: 21 July 2021

Acknowledgements

I would like to express my sincere gratitude to my respected supervisor Dr. Bharat Babu Shrestha (Associate Professor), Co-supervisors Dr. Pramod Kumar Jha (Professor Emeritus) and Dr. Krishna Prasad Paudel (Professor) for their invaluable time, suggestions and guidance throughout my dissertation work. Their devotion regarding biological invasion inspired and offered me to step my pathway in this field.

I am also thankful to Head of the Department Prof. Dr. Ram Kailash Parsad Yadav and Former Head of the Department Prof. Dr. Mohan Siwakoti for their academic and administrative supports.

I am also grateful to USAID IPM Innovation Lab for providing me financial support to conduct this research. Similarly, I am thankful to Department of Hydrology and Meteorology (DHM) and Department of Survey for providing essential information/data required for my research.

I am equally thankful to Mr. Anil Kumar Chaudhary for his support and encouragement to complete this work. My thanks also go to all the academic and administrative staff of Central Department of Botany, Tribhuvan University for their direct and indirect support and help. Likewise, I would like to express my sincere thanks to my seniors Mr. Dol Raj Luital, Ms. Shreejana Maharjan and Ms. Anju Sharma Poudel for their suggestions and help.

I am heartily thankful to my friends Sita Gyawali, Srijana Poudel, Himal Yonjan and Abhishek Singh for their kind support and help during the field work. Similarly, I am thankful to Pradeep Shrestha for his support in the transportation during the field visit.

Lastly, I am greatly indebted to my whole family, for their overall support and inspiration throughout my academic career.

Date: 21 July 2021 **Sandeep Dhakal**

Abstract

One of the major environmental concerns in Nepal is spread of the invasive alien plants and its threat to biodiversity. The detection of invasive alien plant species (IAPS) at landscape level can aid in monitoring and managing their invasion in ecosystem. Remote sensing has been an important tool for large scale ecological studies of IAPS. In the present study knowledge-based classification using Landsat images was employed to determine the distribution of *Lantana camara* in Chitwan Annapurna Landscape (CHAL), Nepal. Maximum Likelihood Classification (MLC) technique was used for the extraction of land use/land cover types from remotely sensed data. Variables like elevation, aspect, slope, land use/land cover, temperature, rainfall and normalized difference vegetation index (NDVI) were used for the knowledge based classification approach. For the comparison of satellite data, World View-2 (WV2) of fine spatial resolution (2x2) m and Landsat of coarse spatial resolutions (30x30)m multispectral data of same area of interest were used. The results using Landsat image showed that weed covered 0.24, 0.9, 1.45 and 2.74 % area of CHAL in the year 1992, 2000, 2009 and 2018, respectively. The cover of the weed estimated using Landsat images was comparatively higher than the cover obtained from the World view-2 images. After evaluating all the available results the knowledge-based algorithm using Landsat produced very promising results, with >77% overall accuracy and a Kappa index of 0.54 in CHAL. The overall accuracy varied between 78 and 83% and Kappa indices of 0.56 and 0.66 for Landsat; the highest overall accuracy was achieved in Makwanpur district where as the lowest was achieved in Kaski district. The overall accuracy varied between 81 and 88% and Kappa indices of 0.62 and 0.76 for the WV2. The highest overall accuracy was achieved in Nawalparasi district where as the lowest was achieved in Kaski district. When compared, the accuracy was higher in the WV2 image than in the Landsat image. The largest area of distribution was found in Middle Mountain followed by Siwalik and High Mountains. The methods adopted in this study can be used for testing other types of satellite data or other classification algorithms. This investigation revealed the strength of mapping shrub weed using Landsat images which is freely available in the archives.

Keywords: Supervised classification, Landsat imageries, World view 2, Digital number, Confusion matrix, Kappa index

TABLE OF CONTENTS

List of Figures

List of Tables

List of Acronyms and Abbreviations

ASTER	Advanced Space borne Thermal Emission and Reflection
CBD	Convention on Biological Diversity
CHAL	Chitwan Annapurna Landscape
DEM	Digital Elevation Model
DN	Digital Number
ERDAS	Earth Resources Data Analysis System
ETM+	Enhanced Thematic Mapper +
FCC	False Color Composite
GIS	Geographic Information System
GPS	Global Positioning System
IAPS	Invasive Alien Plant Species
ICIMOD	International Centre for Integrated Mountain Development
IUCN	International Union for Conservation of Nature
K	Kappa
KII	Key Informants Interview
LiDAR	Light Detection and Ranging
LULC	Land Use and Land Cover
MCTCA	Ministry of Culture, Tourism and Civil Aviation
MFSC	Ministry of Forest and Soil Conservation
MIR	Mid Infra Red
MLC	Maximum Likelihood Classification
NDVI	Normalized Difference Vegetation Index
NIR	Near Infra Red
RS	Remote Sensing
SPOT	Satellite Pour l'Observation de la Terre
TIN	Triangulated Irregular Networks
TM	Thematic Mapper
USGS	United States Geological Survey
UTM	Universal Transverse Mercator
VHR	Very High Resolution
WGS	World Geodetic System
WV2	World view-2

1. INTRODUCTION

1.1 Background

Invasive species are the alien species that sustain self-replacing populations over several life cycles; produce reproductive off spring, often in very large numbers at considerable distances from the parent and/or site of introduction; and have the potential to spread over long distances (Pyšek *et al.,* 2004). Invasive alien plant species (IAPS) displace indigenous species and have detrimental environmental impacts (Bradley *et al.,* 2011). Biological invasions occur at rapid rates within diverse habitats across the globe, from grasslands to dense forests, and spread over large areas (Mack *et al.,* 2007). Despite several efforts to manage biological invasions, the number of alien species has been ever increasing across all taxonomic groups and geographic regions of the world (Seebens *et al.,* 2017). Furthermore, the biological invasions are likely to be exacerbated by climate change (Bellard *et al.,* 2013; Tittensor *et al.,* 2014; IUCN, 2017) and by further international trade (Levine and D'antonio, 2003). Invasive species are major threats to biodiversity because of their negative effects on floral and faunal species, food web, ecosystems and their habitat (Vila *et al.,* 2010). Invasive species are of great concern because of their capability of spreading fast, high competitiveness and ability to colonize new areas within short periods (Reichard and White, 2001).

Systematic repeated observations and monitoring are essential for ecosystem management to enable managers to detect, document, and respond to changes. Monitoring of the invasion process involves repeated observations for recording the advance of the invasion over different seasons and across years, which is made possible by affording a general view of a whole (synoptic) and frequently repeated observations of large and small landscapes by remote sensing. Mapping invasion over long temporal periods has been possible due to the long history of the availability of remote sensing (RS) data across many regions in the world (Gavier-Pizarro *et al.,* 2012).

Remote sensing is the science and art of obtaining information about an object, area, or phenomenon through the analysis of data acquired by a device that is not in contact with the object, area, or phenomenon under investigation (Lillesand *et al.,* 2008).

Remote sensing techniques for vegetation mapping and monitoring is a function of scale, resolution, season of imagery, kind of vegetation, sensor and spectral sensitivity, processing of the remote sensing product, and speed and precision of transfer of information into a map product (van den Berg *et al.,* 2014). Recent advances in RS technology now provides very high resolution (VHR-multispectral resolution 2 m × 2 m or lower (Nagendra *et al.,* 2008) data for land cover mapping. The use of these data for remote detection of invasive plants has proved useful in several different ecosystems, and for a variety of species (Doody *et al.,* 2014). The study undertaken by Noonan and Chafer (2007) in Australia has utilized remote sensing specifically to map willow distribution. Comparative studies of VHR data and medium resolution data for detection of invasive species have often proved that VHR data were extremely effective (Everitt *et al.,* 2008), although medium resolution data could be used in areas where invasive species stands are contiguous and large to allow detection at stand level (Mullerova *et al.,* 2013). Medium resolution data can be effective specifically in areas where monitoring of very large regions demands investment in several images which may prove expensive and process-intensive if VHR data were used. However, VHR data are increasingly proving to be of much use in the process of invasion mapping specifically because of the precision and detail that these data provide in separating signatures of different land cover types (Nagendra and Rocchini, 2008). Integration of satellite-derived information in Geographical Information Systems (GIS) can be useful in modeling and predicting the spread of invasive species (Kimothi and Dasari, 2010).

The integration of remote sensing and GIS has been used historically in mapping plant and vegetation distributions. This practice has increased with focus shifting to mapping IAPS (Joshi *et al.,* 2005). This current shift toward IAPS mapping using these geospatial technologies has been enhanced by advancement in sensor development, spatial statistics and modelling (Evangelista *et al.,* 2009). Effective mapping of IAPS extent and determining the risk they pose for future invasions and impact requires an accurate study of species distributions (Joshi *et al.,* 2005), and an insight into density and impacts of IAPS (van den Berg *et al.,* 2014).

1.2 Rationale

There are interests in distribution mapping of invasive species for several reasons: First, once an invader has been recognized as problematic, it is essential to locate its distribution and monitor its eventual further spread for managing IAPS. Secondly, ecological knowledge is required to assess their density and impact. Distribution maps have been used since long to acquire such knowledge. Thirdly, it has been argued that spatial information is needed to develop policies aimed at invasive species management (Wittenberg and Cock, 2001). Monitoring and assessing the environment have become more reliant on remote sensing as it has the capacity to assess large spatial extents and examine historic distribution of IAPS (Mutanga *et al.*, 2009). In order to successfully remove IAPS, they need to be mapped (Rowlinson *et al.*, 1999). While manual field surveys as a method of mapping are time consuming and labor intensive, the remote sensing is a more feasible alternative as it can reach inaccessible locations and assess large areas rapidly and comprehensively (Calviño-Cancela *et al.*, 2014). The CHAL is an ecologically unique (confluence of eastern and central Himalaya) and socio-culturally diverse region with high potential and needs for conservation. This region has a higher number of naturalized plant species than those found in eastern and western Nepal (Bhattarai *et al.*, 2014). Any study on invasive plants covering the entire range of CHAL using satellite images is lacking. There is a need for tools that can simultaneously determine species expansion and monitor invaded area.

Lantana camara is a widespread and problematic invasive plant with negative effects in over 60 countries globally (Day *et al.*, 2003). *L. camara* is one of the 100 of the world's worst invasive species (Lowe *et al.*, 2000). This weed can easily colonize degraded/open forests, tree plantations, and shrub land forming impenetrable bush and replacing almost all other herbaceous and shrub species. Management of this weed has remained a challenge in Asia, Africa, and Australia (Bhagwat *et al.*, 2012).

1.3 Research questions

This research aimed to answer following questions:

- How the area invaded by *Lantana camara* has changed in Chitwan-Annapurna Landscape over the period between 1992 and 2018?
- Does a coarse satellite image provide the same level of accuracy as the fine satellite image does in detecting invasive weed at the landscape level?

1.4 Objective

The general objective of this research work was:

- To assess the spatial and temporal distribution of *Lantana camara* in CHAL area.

Specific objectives

- To analyze the distribution pattern and direction of invasion in the study area since 1992.
- To compare the accuracy of the classification in Landsat and WV2 images for same area of interest of CHAL.

1.5 Limitation

A major limitation of this study was the lack of high spatial and spectral resolution images for whole CHAL area which is time consuming to decipher the complexity of natural environment and further delineate the distribution of IAPS. Moderate spatial resolution sensors like Landsat are not able to detect IAPS within a heterogeneous vegetation type and are only effective when targeting homogenous stands over a large area (Huang and Asner, 2009).

Due to the limitation of spatial resolution, Landsat products are usually used to map vegetation at community level. It is a challenging task to use Landsat images for mapping at species level, especially in a heterogeneous environment. However, when integrating with GPS information and other ancillary data (elevation, aspect, slope, tmax, tmin, ndvi, luses, reflectance value) it becomes possible to map species.

Most of the GPS points in the study area are collected along the roadside which seems a convenience method of data collection but it may not represent all the area.

2. LITERATURE REVIEW

2.1 Invasive alien plant species monitoring

An essential element of invasive plant management is observing changes in weed populations over time and monitoring. Biodiversity monitoring methods can be broadly split into field-based and remote sensing methods. Survey methods for monitoring invasive species along roadsides could be valuable for understanding the roles of human influences and disturbance regimes in the spread of invasive plants (Hartzler and Buhler, 2000).

Citizen science is the involvement of volunteers in the scientific process. Although this term is new, people have been monitoring biodiversity in a voluntary capacity for centuries (Pocock *et al.,* 2015). Anyone can get involved with citizen science and there are so many ways people can contribute to monitoring alien species, from simple mass participation initiatives to systematic repeat surveys mass participation. citizen science can rapidly provide invaluable data on spatial scales that would otherwise be unachievable (Roy, 2015)

An important principle in biodiversity observation and monitoring is to ensure that the methods used are transparent and repeatable. In other words the methods should be well documented, well archived and readily accessible to anyone that may want to repeat them or apply the same methods elsewhere. Decisions can be made to optimize the cost effectiveness and efficiency of surveys for invasive alien species, by selecting particular spatial arrangements, sampling density and using fixed versus temporally dynamic survey designs for particular areas.(Berec *et al.,* 2015).

Remote sensing is successful at detecting IAPS as long as the target IAPS exhibit distinctive characteristics when compared to surrounding indigenous species (Huang and Asner, 2009). The launch of a variety of new sensors coupled with Geographical Information Systems (GIS) and advanced modelling has resulted in many methods and tools in IAPS detection (Evangelista *et al.,* 2009). However remote sensing techniques differ due to spatial and spectral variations of sensors (Calviño-Cancela *et al.,* 2014).

2.2 Detection of IAPS using remote sensing

Monitoring and assessing the environment has become more reliant on remote sensing as it has the capacity to assess large spatial extents and examine historic distribution of IAPS (Mutanga *et al.,* 2009). In order to successfully remove IAPS, they need to be mapped (Rowlinson *et al.,* 1999). Manual field surveys as a method of mapping are time consuming and labour intensive, remote sensing is a more feasible alternative as it can reach inaccessible locations and assess large areas rapidly and comprehensively (Calviño-Cancela *et al.,* 2014). Mapping through remote sensing technology has become more feasible in the field of biological invasions, with the availability of high-resolution multi-spectral and multi-temporal data (Joshi *et al.,* 2006). Satellite imagery of temporal series helps in monitoring of phenological changes occurring in the vegetation. Integration of remote sensing and Geographical Information Systems (GIS) can be useful in modelling and predicting the spread of invasive species.

Various satellites provide multispectral imagery, however, the choice of satellite imagery is dependent on spectral resolution (number of bands), spatial resolution (pixel size), spatial coverage (area covered by image) and the cost of images (Cuneo *et al.,* 2009). Spatial resolution is crucial as it determines the target feature's level of accuracy in terms of classification and the scale of the study. Finer spatial resolution increases classification accuracy but can make it difficult to separate spectral classes due to intra-pixel variability (He *et al.,* 2011). Hyperspectral imagery is more useful at mapping species with a low density and a scattered distribution, and therefore more effective in a heterogeneous community (He *et al.,* 2011).

Moderate spatial resolution satellites such as Landsat and Satellite Pour l'Observation de la Terre (SPOT) are only effective at detecting a species if they form large stands (Huang and Asner, 2009). Other satellite imageries such as Quickbird and World view 2 are better suited at IAPS detection as these are considered high spatial resolution multispectral data (Bradley, 2014). World view 2 is a very high spatial resolution sensor which collects data in the visible and infrared spectrum (Doody *et al.,* 2014). However, high spatial resolution imagery may be inadequate when the spectral resolution is low, therefore hyperspectral imagery would be required (Huang and Asner, 2009).

Plant detection of single species using remote sensing is a challenging task, where large scale infestations are generally easier to detect compared to small scale invasions (Evangelista *et al.,* 2009). Therefore the use of remote sensing to detect IAPS using multispectral imagery would be feasible if the target IAPS form dense stands and have distinct spectral signatures (Cuneo *et al.,* 2009).

Light absorption by vegetation produces a unique spectral signature which is influenced by leaf biochemistry (He *et al.,* 2011) and canopy structure (Cuneo *et al.,* 2009). Solar radiation interacts with leaf properties in different ways which is dependent on wavelength. Absorption is high in the visible spectra due to pigments (e.g., chlorophyll a and b) and in the mid infrared (MIR) due to water content, while reflectance is high in the near infrared (NIR) due to spongy mesophyll (Shouse *et al.,* 2013). These properties allow for the spectral differentiation between species and in some cases spectral signatures of IAPS may be unique to the signature of indigenous species (He *et al.,* 2011).

A number of invasive species have also been identified based on the uniqueness in leaf chemistry using multispectral (Becker *et al.,* 2005) analyses. Underwood *et al.* (2003) were able to use airborne visible/infrared imaging spectrometer (AVIRIS) imagery with 4 m resolution to detect iceplant (*Carpobrotus edulis*) and jubata grass (*Cortaderia jubata)* in mediterranean-type ecosystems of California because such invasive species showed higher leaf water content than native co-occurring species.

Carter *et al.* (2009) demonstrated the power of using Quickbird data (4 bands, spatial resolution 2.44 m at nadir) to detect *Tamarix* spp along the Colorado river (USA) attaining a classification accuracy of 91%. However, there were large errors of commission since the moderate spectral resolution used was not sufficient to discriminate tamarisk and non-tamarisk riparian vegetation.

Shouse *et al.* (2013) examined the feasibility and tradeoffs of species level invasive exotic plant (IEP) mapping using multiple remote sensing techniques in a highly complex urban forest setting. Analysis using both medium spatial resolution (Landsat 5 TM) and high spatial resolution (0.3 m color aerial photo) imagery provided viable results for IEP distribution mapping with overall mapping accuracy ranged from 89.8% to 94.9% for high spatial resolution techniques and from 74.6% to 79.7% for medium spatial resolution techniques.

2.3 Other detection approaches and challenges

Management of IAPS is best done in the early stages of invasion, however, detection may be difficult due to invaders being sparse and occupying the sub-canopy (Ghulam *et al.,* 2014). Conventional remote sensing currently has been restricted to mapping canopy dominant species, as these determine the spectral signature. In the forest, sub-canopy invaders are difficult to detect. The use of multiple sensors such as multi-angle sensors can determine the forest vertical profile, and IAPS can be indirectly detected (Huang and Asner, 2009; Ghulam *et al.,* 2014). One of the methods of detecting sub-canopy invaders at the time when there is a temporal variation in senescence between the invader and the canopy species. Another method employed for IAPS detection within indigenous vegetation is to take into consideration the vegetation dynamics of an area. This can be tracked via time series analysis using high temporal resolution imagery (Huang and Asner, 2009) which will infer on the presence of an IAPS.

2.4 Invasive alien plants in Nepal

Nepal lies at the cross-road of six floristic provinces of Asia (Sino-Japanese, Southeastern Asiatic, Indian, Sudano-Zambian, Irano-Turranean and Central Asiatic) and the floral elements of all provinces are represented in Nepal (Dobremez, 1976). Naturalized species mostly enter Nepal through India because of land connected open border, high trade with India. Moreover, the southern half of the country which includes Tarai and Siwalik with tropical to subtropical climate, is more vulnerable to biological invasions because $3/4^{th}$ of the naturalized plant species (including IAPS) of Nepal are native to tropical and subtropical regions of the World (Bhattarai *et al.,* 2014). Nepal's agriculture sector has been ranked third among the most threatened countries out of the 124 countries assessed (Paini *et al.,* 2016). Now there are at least 179 alien species of flowering plants that are naturalized in Nepal (Shrestha *et al.,* 2019) and of them 26 are IAPS (Shrestha, 2019). Among them four IAPS, i.e., *Chromolaena odorata, Eichhornia crassipes*, *Lantana camara* and *Mikania micrantha* are considered as the worst invasive species of the world and listed in 100 of the world's worst invasive alien species (Lowe *et al.,* 2000). Of 26 IAPS, *Ageratum houstonianum, Alternanthera philoxeroides, Erigeron karvinskianus, Oxalis latifolia, Parthenium hysterophorus,* and *Spergula arvensis* were considered highly

troublesome by farmers with toxicity and low palatability. Similarly *Ageratina adenophora, Lantana camara, Chromolaena odorata* and *Mikania micrantha* are the most problematic in forests and shrublands; *Parthenium hysterophorus* in grasslands and residential areas and *Eichhornia crassipes* in wetlands (Shrestha, 2016).

As invasive species already exist in the area, biodiversity and human life are threatened. The invasion of *Mikania micrantha* in the Chitwan National Park located in the lowland areas of Tarai and Siwalik regions causes the degradation of habitats for the endangered one-horn rhino (Murphy *et al.*, 2013) while the Ramsar sites of this region become vulnerable due to rapid expansion of *Eichhornia crassipes*. Similarly, rapid expansion of *Parthenium hysterophorus* in residential areas has negative impacts on forage supply as well as on the health of humans and livestock (Shrestha *et al.*, 2015). IAPS is not only a problem in the low land areas, but also becomes an issue of environmental challenge in the mountain regions of this landscape (Baral *et al.*, 2017). The increase in temperature due to changing climate leads to encroachment of IAPs, which will ultimately affect the biodiversity of CHAL (WWF, 2013).

Study performed by Maharjan *et al.* (2019) suggests that the suitable habitat of *Parthenium hysterophorus* in CHAL will expand by 10% in the future, causing potential threats to the native vegetation. Their findings further suggest that global warming resulting from climate change is likely to facilitate invasion of this weed into new areas.

Among the four physiographic regions in CHAL, the Middle Mountain region currently has the highest proportion and the High Himalaya region currently has the lowest proportion of climatically suitable areas for *Ageratina adenophora*, and this is projected to continue under future projected climate scenarios using Maxent modeling (Poudel *et al.*,2020).

Focus group discussions and prioritization methods conducted by Shrestha *et al. (*2019) in CHAL suggests that *Ageratum houstonianum* was the top-ranked worst invasive species in agroecosystems while *Chromolaena odorata* and *Ageratina adenophora* were the top-ranked worst species in natural ecosystems.

2.5 Research gap

Invasive plants are non-native species that establish and spread in their new location, generating a negative impact on the local ecosystem and representing one of the most important causes of the extinction of local species (Morais *et al.*, 2007). The initial step for the control of invasion should be focused on understanding and quantification of their location, extent and evolution, namely the monitoring of the phenomenon. In this sense, the techniques and methods of remote sensing can be very useful. The aim of this study was to identify the distribution pattern of invasive plant *L. camara* using Landsat images and World view 2 images (high resolution).

Invasion research, although it has been around for a few years, is comparatively a new field for the remote sensing methodology. Most of the literature reviewed are based on either vegetation level using coarse spatial resolution (Landsat) images or species level using fine spatial resolution (WV2). Mapping at species level are limited to fine resolution images; however, very few research were done on the species level using moderate spatial resolution. This study tries to solve the limitation of previous studies, using moderate spatial resolution image (Landsat) and high resolution image (World view 2) to map the species using knowledge based approach.

3. MATERIALS AND METHODS

3.1 Study area

The study was done in Chitwan-Annapurna Landscape (CHAL), which lies in central Nepal and covers 19 of the country's 77 districts (Figs. 1 and 2). The landscape represents four of the five physiographic regions of Nepal, i.e., Siwalik (200-1500 m), middle mountain (1000-2500 m), high mountain (2200-4000 m) and high himal (>4000 m) (DHM, 2017). Siwalik represents southern lowland and relatively plain area of the country with tropical to subtropical climate. Middle mountain is a hilly region with subtropical to temperate climate. High mountain and high himal represents the northern part of the country with rugged topography, deep gorges, glaciers and snow-capped mountain peaks. The present study area covers an area of 32,090 km^2. The CHAL has a higher number of naturalized plant species than those found in eastern and western Nepal due to its unique nature in ecological and socio-culture aspects (Bhattarai *et al.,* 2014). It encompasses a vast elevation gradient ranging from 200 m to 8091 m (Bista *et al.,* 2017), with a climate ranging from tropical, subtropical, temperate, subalpine to alpine (high himal) including trans-himalayan cold and dry climate similar to Tibet. Thus, CHAL has a wide range of the eco-physiographic zones of the Nepal Himalaya, including subtropical forests, temperate broadleaf forests, conifer forests, alpine ecosystems, and semi-desert in the rain shadow of the himalaya. The CHAL has diverse land use types. Forest covers the largest portion of CHAL, followed by agriculture, sand/bare land, snow/ice covered areas, grasslands, and alpine meadow and covers following area by different land uses: Forest - 35.6%, Agriculture - 21.1%, Alpine meadow/scrub - 8.1%, Grasslands - 8.6%, Snow/ice - 9.5%, Sand/bare soil - 16.1 %, Water - 1% (WWF, 2013). The study area comprises seven protected areas including four national parks (Langtang, Chitwan, Shivapuri-Nagarjun and Parsa), Dhorpatan Hunting Reserve and two conservation areas (Annapurna and Manaslu). Twenty eight municipalities including 3 sub-metropolitan cities and business centers (Hetauda, Bharatpur and Pokhara) fall within the CHAL. The average minimum and maximum reported temperatures range from 5°C to 40°C, while the average annual rainfall ranges from 165 mm at to 5,244 mm (MFSC, 2015).

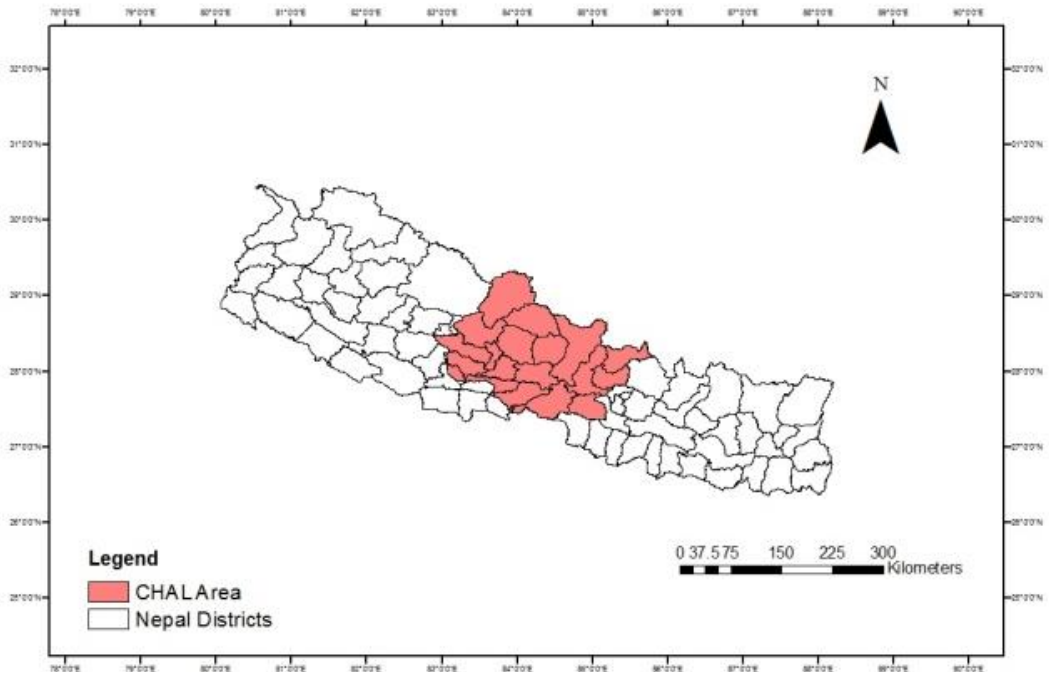

Figure 1: Map of Nepal showing location of Chitwan-Annapurna Landscape (CHAL)

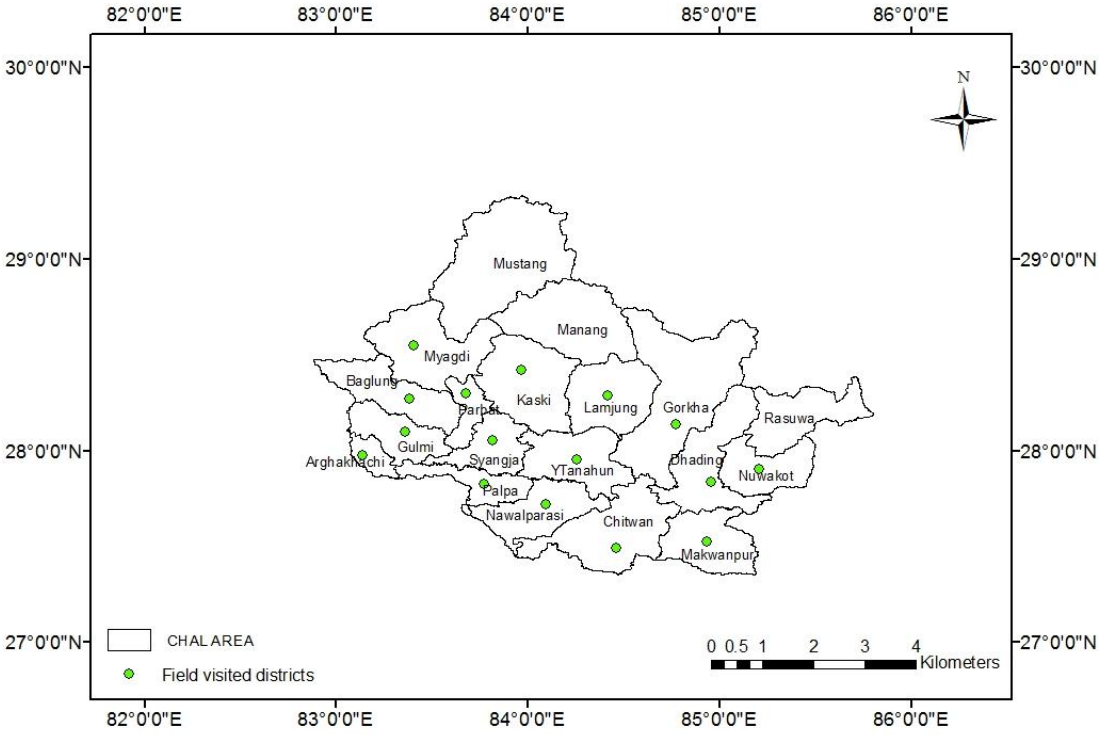

Figure 2: Map of CHAL showing field visited districts.

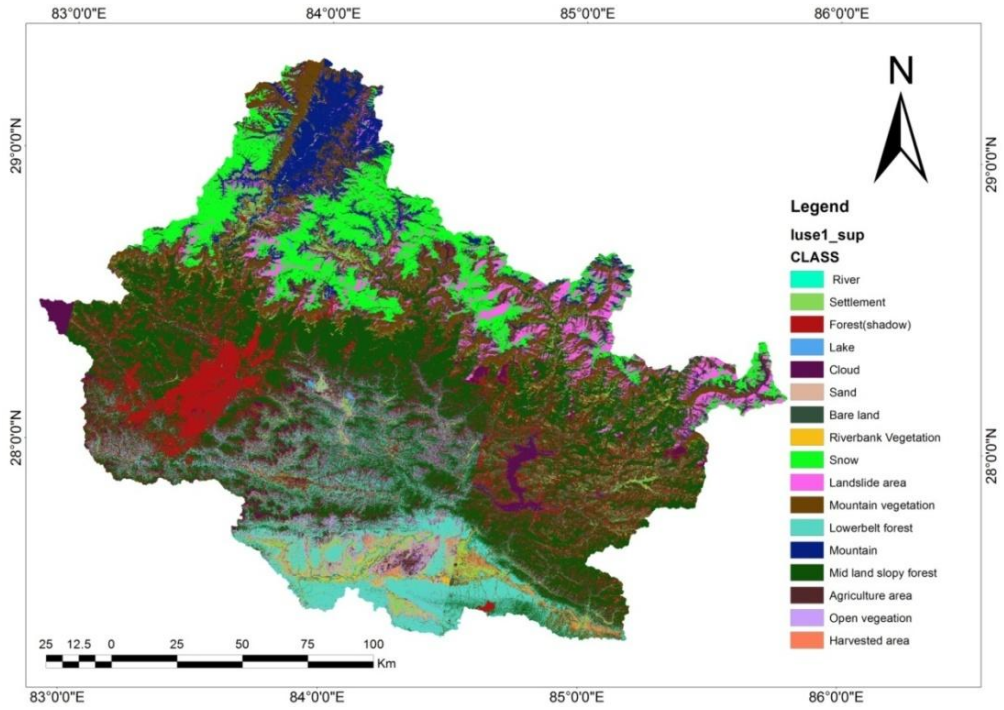

Figure 3: Land use and land cover map of CHAL in the year 2018.

3.2 *Lantana camara*

Lantana camara is a widespread and problematic invasive plant with negative effects in over 60 countries globally (Parsons and Cuthbertson, 2001). It originates from tropical America and was commonly introduced to other countries around the world, mainly by British colonialists, as an ornamental and/or living fence (Kannan *et al.*, 2013). It is now invasive in many parts of Africa, Asia and Oceania (Bhagwat *et al.*, 2012). The distribution and density of *L. camara* is still increasing in many parts of the world, even in areas where it has been present for many years (Day *et al.*, 2003). Lantana is estimated to have invaded 5 million ha in Australia, 13 million ha in India and 2 million ha in South Africa and is continuing to spread in these countries (Bhagwat *et al.*, 2012). *L. camara* has many traits that make it a good invader, including all-year flowering and fruit production in many areas, especially if adequate moisture and light are available; adaptation to long-range dispersal by birds and some mammals; high establishment rates; the ability to coppice; poisonous leaves; high phenotypic plasticity; the ability to hybridize; vegetative reproduction; and allelopathy (Sharma *et al.*, 2005; Priyanka and Joshi, 2013). *L. camara* has been

documented to cause a wide range of negative impacts around the world (Day *et al.,* 2003; Sharma *et al.,* 2005). It is a common weed of pastures where it reduces the grazing value of the land. It is known that widespread and dominant invasive species not only have the potential to replace native flora, but also have direct impacts at other trophic levels by changing the habitat of animals (Te Beest *et al.,* 2012). *L. camara* has invaded large areas in Kenya where it threatens the habitat of the sable antelope (Nanjappa *et al.,* 2005) and affects bird habitats by altering community composition in India (Aravind *et al.*, 2010). In tropical regions, *L. camara* harbors pests that affect human health by providing shelter during the day for tsetse flies (*Glossina* sp.), which are vectors for African sleeping sickness (Mack and Smith, 2011).

L. camara has a negative impact on plant diversity and abundance, by suppressing native vegetation through allelopathy and competition for resources (Bhagwat *et al.,* 2012; Jevon and Shackleton, 2015). Turner and Downey (2010) estimated that 275 native plant species and 24 native animal species are threatened by the presence of this noxious weed in Australia. There is also a growing evidence that *L. camara* has a negative effect on non-timber forest products in India, reducing the abundance of wild bamboos, palms and wild foods through competition (Kent and Dorward, 2015).

L. camara alters ecosystem processes, such as soil nutrient cycling, and changes fire regimes in natural systems, increasing fire intensities and frequency and facilitating fire penetration into habitats that rarely, if ever, burn, such as woodlands and forests (Berry *et al.,* 2011; Ruwanza and Shackleton, 2016). *Lantana* also has social-ecological negative impacts including increased risk of fire, negative impacts on tourism, increased management stress for locals, and decreased aesthetic beauty of landscapes.

3.3 Data acquisition

3.3.1 Satellite imagery

The distribution of *L. camara* in the Chitwan Annapurna Landscape Area (CHAL) was intended for study by using different multispectral satellite imageries (Landsat TM/ETM, and World view 2). Landsat (Landsat 5 and Landsat 8) imagery for 1992 to 2018 in a ten year interval were downloaded from the archives, i.e., United States Geological Survey (USGS) Earth Explorer download client. Landsat 8 OLI/TIRS data

were used for mapping of *L. camara* for 2018 while Landsat 5 TM data were used for 2009, 1999 and 1992 (Annex 3). Images with least cloudiness were downloaded for each year. Though the flowering season was throughout the year, images were selected for June because of least cloudiness; Landsat products have the longest history that have been applied in vegetation mapping (Xie *et al.*, 2008). The spatial resolution of the image is 30 m × 30 m for the multispectral bands. All imageries were received geometrically corrected. Though the time interval of image acquired is ten years but due to the availability and quality of the images the time interval was beyond the expected time interval, i.e., buffering 1-2 year in some of the intervals. A World view 2 satellite imageries of selected area as subset of CHAL having resolution 2 m × 2 m purchased for 2008, 2017 and 2018 (neglecting the changes between the scene of 2017 and 2018, so the scene having common boundary were merged) from the authentic sources were used (Annex 4). Topographic map from Department of Survey, Digital Elevation Model (DEM) file from Shuttle Radar Topography Mission (SRTM) DEM, meteorological data from Department of Hydrology and Meteorology and other documents were also used.

3.3.2 Ground reference data

In image analysis, ground reference data play important roles to determine information classes, interpret decisions, and assess accuracies of the results. Substantial reference data and a thorough knowledge of the geographic area was required at this stage. In this study, we adopted both methods (primary and secondary) for collecting ground truth data. Intensive fieldwork was conducted in between 2018-2019 as the primary data collection method. Global Positioning System (GPS) equipped with a data entry form and road map and a handheld digital camera were used for collecting the geographic data. The geographic locations in points and polygons and their corresponding biophysical attributes were collected in the field. During the field visit, patch size of the weed must be measured before the collection of geographical coordinate. A patch size of 2 m × 2 m, 5 m × 5 m and 10 m × 10 m were considered as low, medium, and large intensity of the weed. The locations of the collected data represent both the homogeneous and the heterogeneous landscape environments of the study area. A total of 630 geographical coordinates were collected for presence data and 630 for the absent data. Using all of these data,

detailed ground reference data of the study area was prepared to support the land use classes scheming, image classification, and subsequent accuracy assessments.

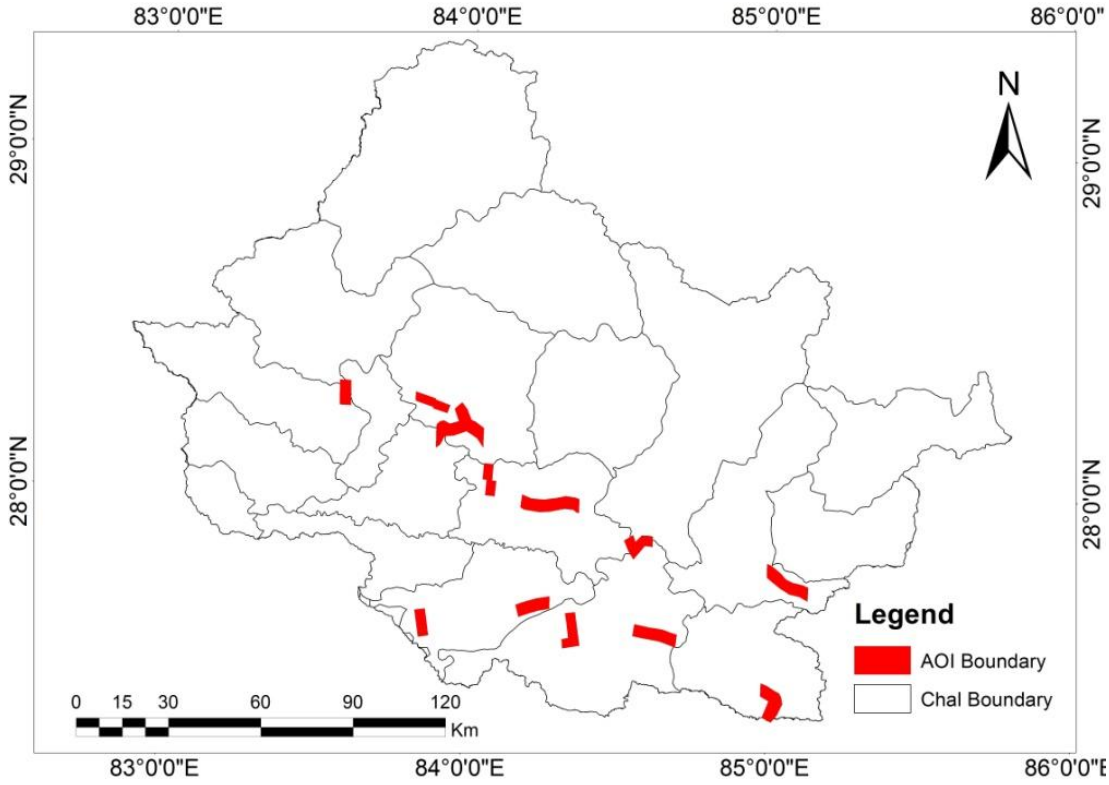

Figure 4: Map showing the area of interest (AOI) for World view 2

3.4 Digital elevation model (DEM)

Digital Elevation Model (DEM) is the most common parameter in GIS application. A DEM can be generated using photogram metrical methods from air photos or satellite images, or can be generated through contour interpolation. The digital elevation model (DEM) used in this study was taken from the Shuttle Radar Topography Mission (SRTM) DEM of resolution 30 m. DEM's can be in raster format, in which each cell display the altitude of the central cell, or in vector format in the form of Triangulated Irregular Networks (TIN). DEMs have a wide range of applications. They can be used to generate slope direction maps, and slope gradient maps (Yang *et al*., 2005). In this study, aspects and slopes are generated from DEM using the field coordinate.

3.5 Software

The segmentation and classification of the satellite images was done with ArcMap 10.2. In this study the process like isoclustering, maximum likelihood classification, interpolation and Masking were done with this software. Another most frequently used software in this study was ERDAS IMAGINE 2014. The processes like image preprocessing and post classification validation was mainly done with this softaware.

3.6 Digital image analysis

Digital image analysis refers to the manipulation of digital images with the aid of a computer. In this study, methods for enhancing digital images, correcting errors, and generally improving image quality prior to further visual interpretation or digital analysis were used. Many of these techniques are broadly applicable to a wide range of types of remotely sensed data which are categorized into the following types of computer-assisted operations:

Pre-processing of satellite images prior to vegetation extraction is essential to make them usable for further analysis. This involves the initial processing of raw image data to eliminate noise present in the data, to calibrate the data radiometrically, to correct for geometric distortions, and to expand or contract the extent of an image via mosaicking or subsetting (Lillesand and Kiefer, 1994). In pre-processing, images were first ortho-rectified. In this study the operation like ortho-rectification are performed by the data provider, before the imagery is provided to the analysts. Some of the operations used in preprocessing were noise removal, image enhancement, image subsetting and mosaicking.

Image noise is any unwanted disturbance in image data that is due to limitations in the sensing, signal digitization, or data recording process. Multispectral sensors data containing systematic striping or banding were particularly prevalent in the collection of early Landsat data. Such stripes were removed through compiling a set of histograms for the image. Since study area covers large area so the Landsat images were obtained in five separate scenes for each year. The Landsat bands were layer stacking to combine multiple separate bands or layers in a single image and it was first mosaiced in ERDAS Imagine software before projecting it to UTM WGS 1984 coordinate system. The study area was extracted by subsetting from the whole image.

After completing the pre-processing of the image, such false color composite (FCC) image was then enhanced using ERDAS imagine 2014 software. Then, such enhanced image was subjected to digital image processing for preparing various classified maps.

3.7 Image classification

Image classification is the process of sorting all the pixels in an image into a finite number of individual classes based on the spectral information and characteristics of these pixels. The classification results in a classified image that is essentially a thematic output of the original image. Target species are typically mapped from digital remotely sensed data through digital image classification and interpretation. The overall objective of the image classification procedure is to automatically categorize all pixels in an image into different land cover classes or themes (Lillesand *et al.,* 2008). In this study, three approaches, i.e., unsupervised, supervised and expert knowledge based (Piyasinghe *et al.,* 2018; Xu *et al.,* 2014) were used for image classification and mapping of the *Lantana camara*.

3.7.1 Unsupervised classification approach

The unsupervised classification approach is an automated classification method that creates a thematic raster layer from a remotely sensed image by letting the software identify statistical patterns in the data without using any ground truth data (Lillesand *et al.,* 2008). In this method, the number of assigned classes (clusters) is 100, of which only 62 spectral clusters are formed to separate the image information into a more readable form by the software itself. After the classification was completed, posterior knowledge was employed to label the spectral classes into information classes. The isoclustering technique was used to cluster the image pixels into groups. Many clusters than actual classes were chosen because the exact number of spectral classes in the dataset was unknown. These clusters were carefully judged using expert knowledge and ground reference data. Spectrally similar classes of identical land cover types were merged. These merged classes were evaluated to whether they belonged to the targeted land use information classes. Finally, a reclassify process was carried out on the landuse map considering 2 for the possible presence area and 1 for the possible absence area.

3.7.2 Supervised classification approach

Supervised classification uses the spectral signatures obtained from training samples to classify an image. Using the "Image Classification" toolbar, representative training data for each predefined number of classes was created. For the selection of training data, usually homogeneous sample pixels should be identified. For each land use and land cover type ten to twenty areas of interest were prepared as the signatures of training samples. These included river, dense forest, lakes, shadow, cloud, agriculture, open scattered vegetation, roadside vegetation, residential etc. Also the different training data of same class were finally merged and a signature file was created from the training samples, which was used by the multivariate classification tools to classify the image. The ground reference data were used to prepare the training signatures. After obtaining satisfactory discrimination between the classes during spectral signature evaluation, supervised classification with the Maximum Likelihood Classifier (MLC) was run. Of the different classes in the classified image, two classes were selected to be used further for mapping presence of *Lantana* within those classes. These include open scattered vegetation and roadside vegetation. A mask (1 = absence, 2 = presence) was generated using reclassify toolbar of Arc GIS.

3.8 Calculation of normalized difference vegetation index (NDVI)

The NDVI is a commonly used index that combines the visible and NIR bands to enhance the signal of photosynthetic vegetation (Huang and Asner, 2009). The notion behind NDVI is that plants' chlorophyll absorbs sunlight, which is captured by the red light region of the electromagnetic spectrum, whereas a plant's spongy mesophyll leaf structure creates considerable reflectance in the near-infrared region of the spectrum (Tucker, 1979). For this reason, greener and dense vegetation has low red-light reflectance and high near-infrared reflectance, and thus high NDVI values. On the other hand, near zero and negative values of the index indicate non-vegetated surface features such as rock, soil, water, ice and clouds (Hishe *et al.*, 2017). It is given by the equation (NIR-RED/NIR+RED), where RED and NIR correspond to channels 1 and 2, respectively. After the acquisition of required satellite imageries from the archives, NDVI was calculated using ERDAS imagine software. The calculated NDVI was further reclassify using ArcGIS in the range of 0.2-0.5 as suitable range for shrubs and grassland (NCAR, 2018).

3.9 Calculation of top of atmospheric (ToA) reflectance

The reflectance value of Operational Land Imager (OLI), Enhanced Thematic Mapper (ETM) and Thematic Mapper (TM) data was calculated for vegetation analysis. For ETM/OLI sensor data of 2018, band 5 and band 4 were used as Near Infra Red (NIR) and Red (R) and for TM sensor data band 4 and band 3 was used as NIR and Red in 2009, 2000 and 1992.

For TM sensor data

a. Conversion of digital number (DN) value to radiance (Landsat 7 data users handbook – USGS)

The raw images of NIR band and Red band was converted to radiances. The formula used in this process is as follows:

$$L\lambda = \frac{LMAX_{\lambda} - LMIN_{\lambda}}{QCALMAX - QCALMIN} \times (QCAL - QCALMIN) + LMIN\lambda$$

Where,

L_{λ} is the cell value as radiance

QCAL = digital number (DN)

$LMIN_{\lambda}$ = spectral radiance scales to QCALMIN

$LMAX_{\lambda}$ = spectral radiance scales to QCALMAX

QCALMIN = the minimum quantized calibrated pixel value (typically = 1)

QCALMAX = the maximum quantized calibrated pixel value (typically = 255)

b. Conversion of radiance to ToA reflectance

After converting DN to radiance the output file was thus converted into reflectance by using following equation:

$$\rho\lambda = \frac{\pi \times L_{\lambda} \times d^2}{ESUN_{\lambda} \times \cos\theta_s}$$

Where,

$\rho\lambda$ = unitless planetary reflectance

$L\lambda$ = spectral radiance (from earlier step)

d = Earth-sun distance in astronomical units

ESUNλ = mean solar exoatmospheric irradiances

θs = solar zenith anle

For ETM/OLI sensor data

Reflective band DN's can be converted to TOA reflectance using the rescaling coefficients in the MTL file. The conversion was performed using parameters provided with the metadata file of the Landsat 8 satellite images and the following formula set:

$\rho\lambda' = M\rho Qcal + A\rho$

Where,

$\rho\lambda'$ = ToA planetary spectral reflectance without correction for the solar angle (unitless)

Mρ = Reflectance multiplicative scaling factor for the band

Aρ = Reflectance additive scaling factor for the band

Qcal = Quantized and calibrated product pixel value (DN)

This process does not include correction for the solar elevation angle. The following additional formula is used to obtain the true ToA reflectance:

$\rho\lambda = \rho\lambda'/\sin(\Theta_{SE})$

Where,

ρλ = ToA Planetary Reflectance with a correction for solar angle (unitless)

Θ_{SE} = Solar Elevation Angle

3.10 Knowledge-based image analysis

Knowledge based image analysis is a rules-based approach to multi-spectral image classification, post-classification refinement, and GIS modeling. In essence, expert classification system is a hierarchy of rules, or a decision tree, that describes the conditions under which a set of low level constituent information gets abstracted into a set of high level informational classes. In this approach, a knowledge is developed to improve IAPS detection, which includes a set of decision rules of identifying *Lantana* distribution in relation to its elevation, land use, climatic and spectral

characteristics. Using ERDAS imagine software's knowledge engineer and knowledge classifier tool, the decision rules are applied in order to identify the distribution of weed. The first component (knowledge engineer) provides a graphical user interface to build the knowledge base. A tree diagram represent the class definitions known as hypothesis, rules (conditional statements of variables), and variables (raster, vector, or scalar). The knowledge classifier executes the knowledge rules created in the knowledge engineer module and classify the image. The threshold values of the variable were determined on the basis of the ground reference data.

After running the model of knowledge based, the outcome of the model displayed as a binary data, which classifies the image into two classes, one is undefined and other is new hypothesis. The class undefined usually highlights the lacking or the absent of the data. The class new hypothesis represents presence data.

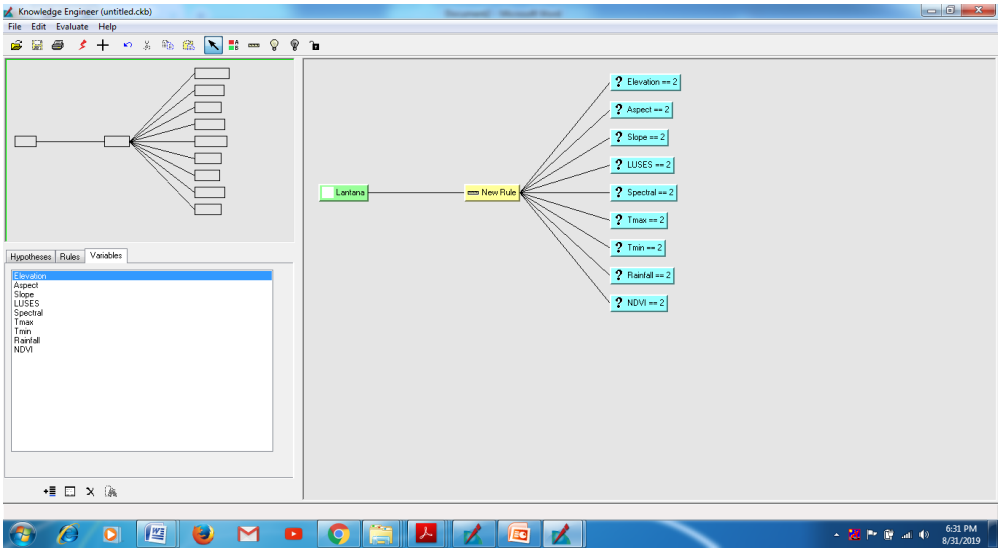

Figure 5: Rules built in the expert classifier in ERDAS imagine

Table1: Rules for knowledge engineer of class *Lantana camara*

Rules	Calculation	Suitable criteria	Source
Elevation	Reclassifying DEM file	70- <2000 m	Priyanka *et al.*, 2013
Aspect	Reclassifying DEM file	All aspect	Field observation
Slope	Reclassifying DEM file	All slope	Field observation
Tmax	Average analysis	35°C	Station based of DHM
Tmin	Average analysis	15°C	Station based of DHM
Precipitation	Average analysis	800-5000 mm	Station based of DHM
NDVI	(NIR - Red) / (NIR + Red)	0.2-0.5	NCAR, 2018
LUSES	Supervised classification (MLC)	Diverse habitat	Field observation
DN value	Band 5 isoclustering	0-255 (8 bit)	Isoclustering

3.11 Post classification validation

In this step accuracy assessment was performed through field validation. Accuracy assessment was carried out by using the principles proposed by Congalton and Green (2009). Accuracy assessment is about the verification of the classified data and is an important part of the workflow of this study. With an accuracy assessment, the quality of the classification is determined. In a classification process several errors can occur that can lead to insufficient results. Errors can occur from incorrect image registration, wrong interpretation of a class due to coarse resolution or insufficient training samples (Lu *et al.*, 2007).

3.11.1 Error matrix

There are several options to perform an accuracy assessment. An error matrix compares information from reference sites to information on the classified map for a number of sample areas. An error matrix is a square array of numbers set out in rows and columns that expresses the number of sample units assigned to a particular category in one classification relative to the number of sample units assigned to a particular category in another classification. In most cases, one of the classifications is considered to be correct (i.e., the reference data) and may be generated from ground observation, or ground measurement. The columns usually represent this reference data, while the rows indicate the classification generated from the remotely sensed data (i.e., the map). It should be noted that the reference data has often been referred to as the "ground truth" data. Reference data was collected from field visits to compare the classified data. An error matrix is a very effective way to represent map accuracy in that the individual accuracies of each category are plainly described along with both the errors of inclusion (commission errors) and errors of exclusion (omission errors) present in the classification. A commission error is simply defined as including an area in a category when it does not belong to that category. An omission error is excluding an area from the category to which it belongs. Each and every error is an omission from the correct category and a commission to a wrong category. In this study, there are two category or classes for the classification. They are 'Present' and 'Absent'. The ground truth data or the reference data for these category were collected from different area of interest (AOI) of the study area. The reference data were collected using an "ad-hoc" sampling design that is neither systematic nor random, instead emphasizing the opportunistic acquisition of ground

truth at sites that are readily accessible on the ground, readily interpretable in higher-resolution imagery.

Sample size must also weigh heavily in the development and interpretation of classification accuracy figures. As a broad guideline, it has been suggested that a minimum of 50 samples of each land cover class be included in the error matrix (Congalton and Green, 2009).

There are about 630 ground truth data for each category, collected from different AOI (Figs. 2 and 3) in between the year 2018 and 2019. The Kappa statistic (k) was calculated using the following equation:

3.11.2 Evaluating error matrices

The Kappa Coefficient is generated from a statistical test to evaluate the accuracy of a classification (Bishop *et al.,* 1975). Kappa essentially evaluates how well the classification performed as compared to just randomly assigning values, i.e., did the classification do better than random. The Kappa Coefficient can range from -1 to 1 (Table 3). A value of 0 indicated that the classification is no better than a random classification. A negative number indicates the classification is significantly worse than random. A value close to 1 indicates that the classification is significantly better than random.

The k ^ (“kappa” or “KHAT”) statistic is calculated by using following formula:.

$$KHAT = \frac{(n*SUM\ Xii)- SUM(Xi+ * X+i)}{n^2 –SUM\ (Xi+ * X+i)}$$

Where
SUM = sum across all rows in matrix

Xii = diagonal

Xi+ = marginal row total (row i)

X+i = marginal column total (column i)

n = number of observation

Table 2: Value range of kappa coefficient and its interpretation

Values	Interpretation
Smaller than 0.00	Poor agreement
0.00 to 0.20	Slight agreement
0.21 to 0.41	Fair agreement
0.41 to 0.60	Moderate agreement
0.61 to 0.80	Substantial agreement
0.81 to 1.00	Almost perfect agreement

3.12 Statistical analysis

The comparison of mean difference of normally distributed homogenous data was carried out by independent two sampled t-test having equal variances. The analysis was performed to compare the mean difference of area cover and accuracy between Landsat and Worldview 2 imageries ($p > 0.05$; data were considered as normal). All data were analyzed by using Microsoft Office Excel 2007, Statistical Package for Social Science (SPSS) Version 25.00.

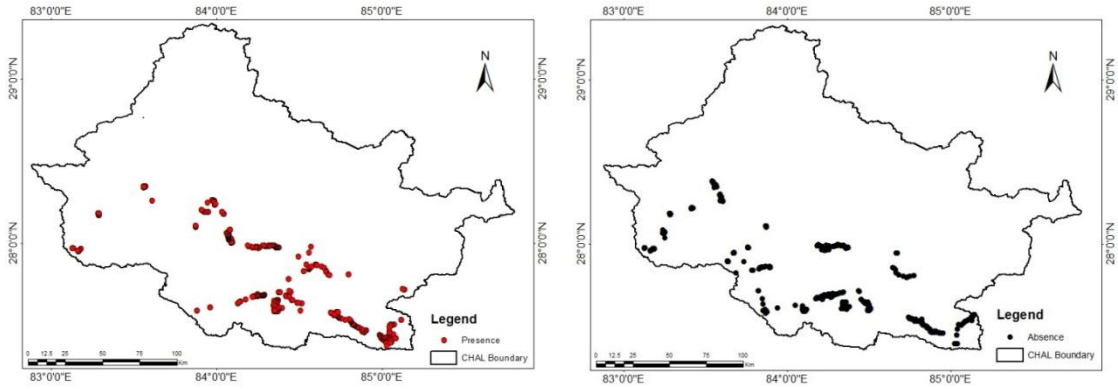

(a) (b)

Figure 6: Map showing the ground truth data of the category: (a) Presence and (b) Absence

4. RESULTS

4.1 *Lantana camara* cover in CHAL determined using Landsat images

The area invaded by the *Lantana camara* in CHAL showed the ascending order with the time series. The area covered by *L. camara* in CHAL was found to be lowest in the year 1992, i.e., 77.41 km^2 (0.24%) while the highest area covered was found in the year 2018, i.e., 877.26 km^2 (2.74%) (Table 3, Figure 7). In the year 1992, the area of invasion of *L. camara* was about 77.41 km^2 which was localized only in the eastern part of the Siwalik and Mid hills of the study area with the maximum elevation of 1425 m (Figs. 9 and 10). With the time elapsed the invasion was extended in the central and western part of the study area along with the altitudinal extension in the northern part with its maximum elevation 1618 m in the year 2018 (Fig. 11). The invasion was maximum in the year 2018 with the area cover of 877.26 km^2. The invasion of *L. camara* was mainly along roadside and on abandon land (Annex 10). The observation shows that most of distribution was concentrated in the anthropogenic landscape. During the 26-year period analysis, the cover of *L. camara* in the year 2018 was 11 times higher than in 1992.

Table 3: Area covered by *L. camara* in CHAL according to the image produced by knowledge based classification

SN	Year (AD)	Invaded area (km^2)	Cover percentage in CHAL
1	1992	77.41	0.24
2	2000	283.51	0.9
3	2009	455.21	1.45
4	2018	877.26	2.74

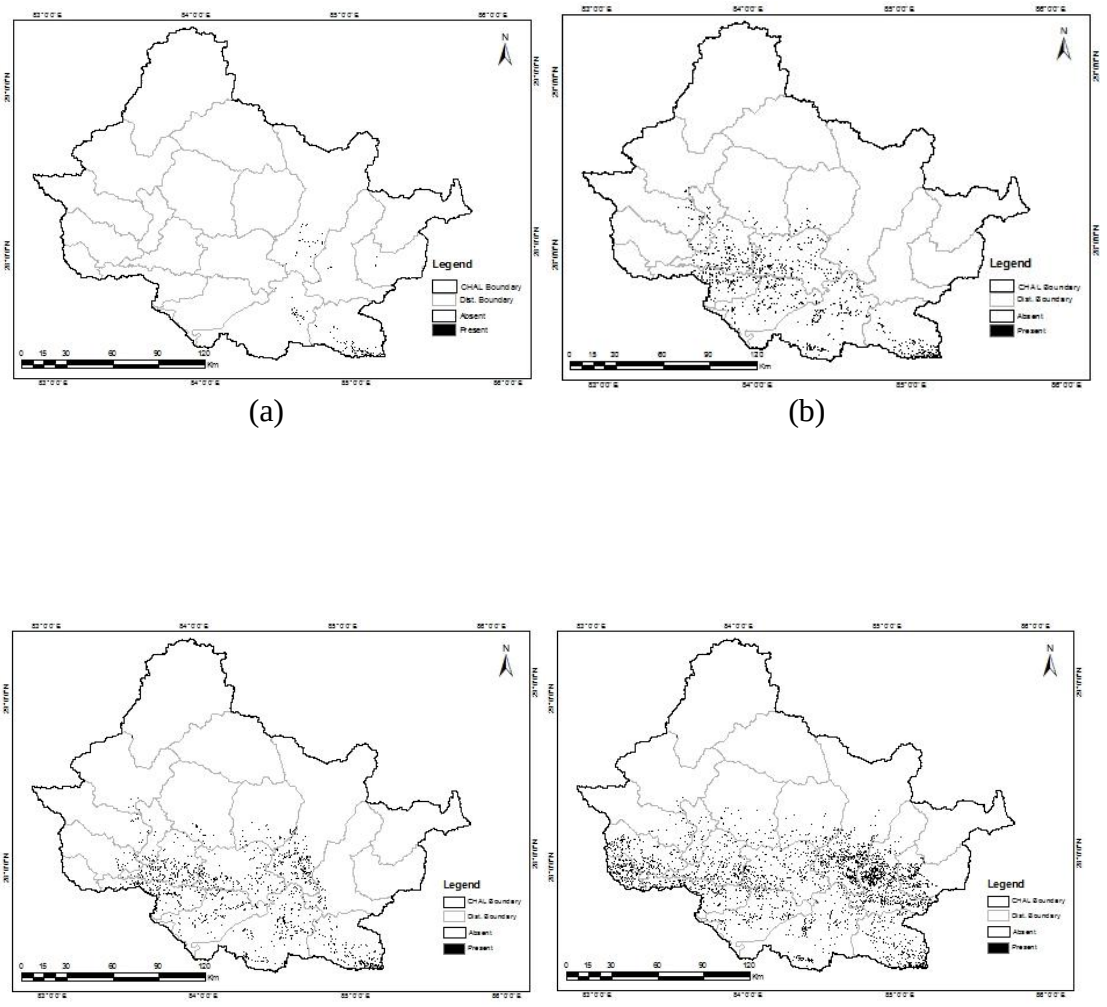

(a) (b)

(c) (d)

Figure 7: Spatial distribution of *L. camara* in the year: **(a)1992, (b) 2000, (c) 2009, (d) 2018**

4.2 *Lantana camara* cover in different physiographic zone of CHAL

The study area represent four of the five physiographic zone of Nepal, i.e., Siwalik (300-700 m), Middle Mountain (700-2000 m), High Mountain (2000-2500 m) and high himal (>2500 m). The highest percentage of invasion was found in the Middle mountain in the year 2000, 2009 and 2018 followed by Siwalik region except in 1992 the case is reversed in 1992 where Siwalik has the highest percentage of invasion followed by Middle mountain (Table 4). Spatial and temporal information from the map indicates that the distribution of *Lantana* was gradually spreading upward of the study area (Fig. 8, Annex 6).

Table 4. Area covered by *L. camara* in physiographic zone of CHAL

SN	Physiographic region	Cover (km^2)			
		1992	**2000**	**2009**	**2018**
1	Siwalik (300-700 m)	49.89 (64.4%)	89.48 (31.5%)	113.74 (24.9%)	109.97 (12.5%)
2	Middle mountain (700-2000 m)	27.42 (35.4%)	192.77 (67.9%)	338.44 (74.3%)	752.14 (85.7)
3	High mountain (2000-2500 m)	0.09 (0.1%)	1.24 (0.4%)	3.01 (0.6%)	15.13 (3.3%)
4	High himalalaya (>2500 m)	0.0	0.0	0.0	0.0

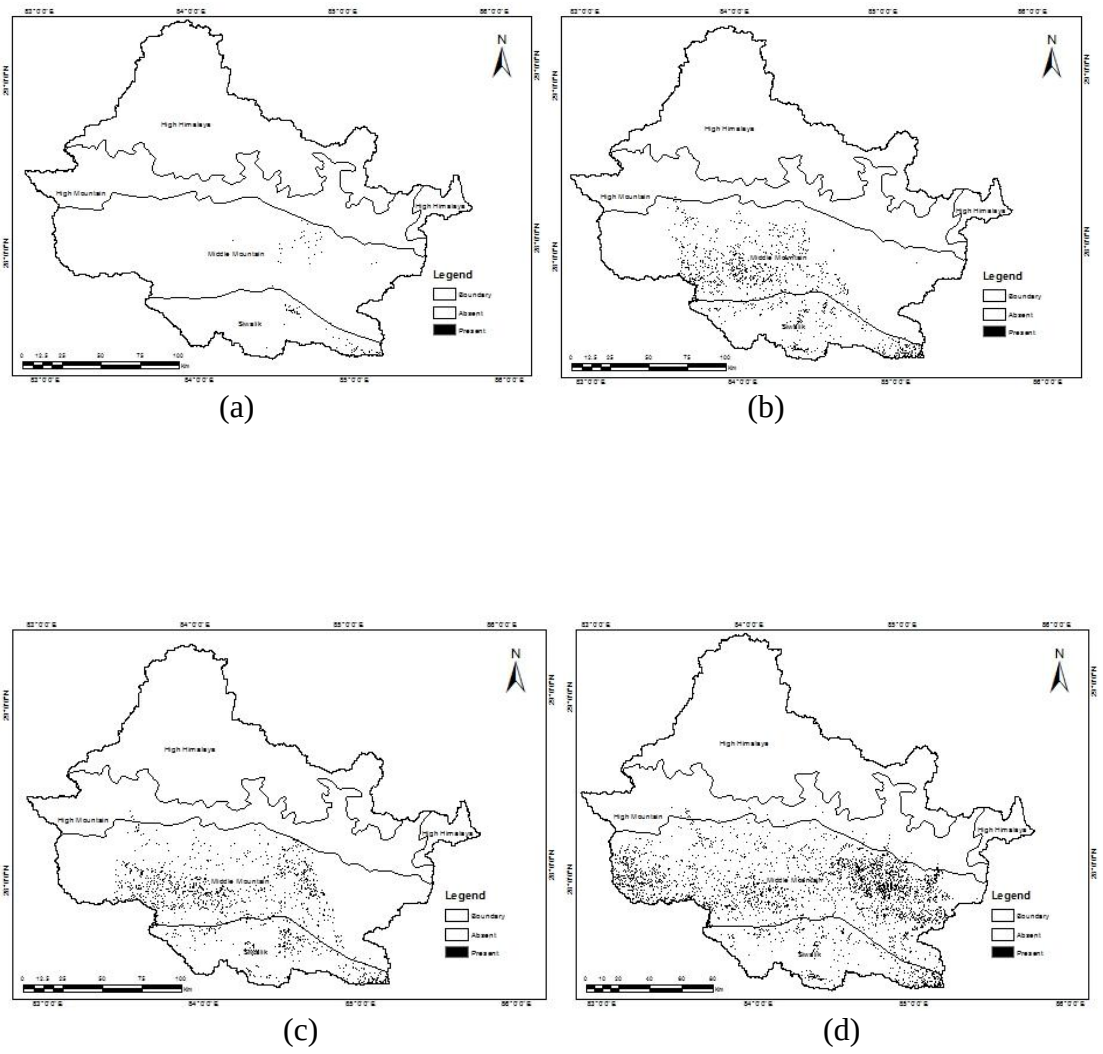

Figure 8: Distribution of *L. camara* in different physiographic zone of CHAL in the year **(a) 1992, (b) 2000, (c) 2009, (d) 2018**.

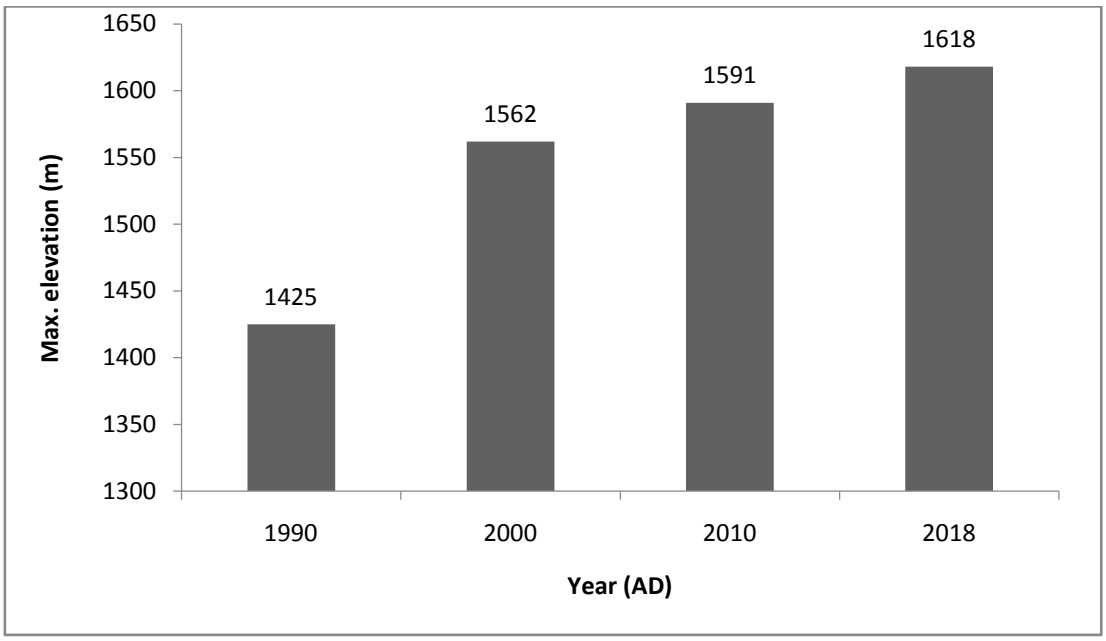

Figure 9: Time series plot for maximum elevation covered by *L. camara* from **1992-2018**

4.3 Comparison of *Lantana camara* cover in the selected area of interest estimated using Landsat and World view 2

The cover analysis of *L. camara* estimated from Landsat and WV2 images showed the differences. The difference in cover between Landsat and WV2 ranged from 0.18 km^2 (0.6%) in Beni Bazar, Myagdi to 1.03 (2.4%) in Rampur, Chitwan (Table 5, Fig. 10-12). The test of significance (P = 0.24) showed the insignificant difference in the mean cover between the Landsat and World view 2 imageries. The cover of *L. camara* in two different years (2008 and 2018) comparing distribution in Landsat and WV2 images (Table 6, Fig. 13-19). In both the images the cover was found to be high in 2018 as compared to 2008. The highest area cover was found to be 5.18 and 4.66 km^2 in the Landsat and WV2 images of Dharke, Dhading in the year 2018 while the lowest was found to be 1.16 and 1.02 km^2 in the Landsat and WV2 images of Hetauda, Makwanpur in the year 2018. During the 10 year (2008-2018) period analysis, the area cover increment ranged from 37-63% in Landsat whereas 34-54% in WV2 Images. The test of significance (P = 0.27 and P = 0.24) showed no difference in the mean cover between the Landsat and WV2 imageries in the year 2008 and 2018 (Annex 9). The highest percentage increment in Landsat image was observed in Muglin of Chitwan district whereas lowest was observed in Lekhnath-Kudule of Kaski district. Similarly in WV2 images the highest percentage increment was

observed in Dharke of Dhading district whereas lowest was observed in Lekhnath of Kaski district.

The column Landsat error (Table 5, 6) shows percentage error that in the Landsat images in comparison to WV2 images during classification of images. The results showed the Landsat error that ranged from 52.1 % in Rampur, Chitwan to 75% in Dulegauda, Tanahau (Table 5) where as error ranged from 11.1% in Dharke, Dhading to 51.6 % in Lekhnath, Kaski (Table 6). This information gives idea that Landsat images showed 11.1 to 51.6 times higher in percentage cover as compared to the WV2 images.

Table 5: Cover of *L. camara* in 2018 in the selected area of interest (AOI) estimated from Landsat and World view 2

Districts	**Area of interest (AOI)**	**Total area of AOI (km^2)**	**Cover (Landsat)**		**Cover (WorldView2)**		**Difference (%) (Landsat-WV2)**	**Landsat error (%)**
			Cover km^2	**Cover (%)**	**Cover km^2**	**Cover (%)**		
Chitwan	Rampur	42.764	2.99	7.0	1.96	4.6	2.4	52.1
Tanahau	Dulegauda-Bhimad	32.166	1.12	3.5	0.48	2.0	1.5	75.0
Myagdi	Benibazar	29.873	0.44	1.5	0.26	0.9	0.6	66.6
P-value					0.24			

Table 6: Cover of *L. camara* in 2008 and 2018 in the selected area of interest (AOI) estimated from Landsat and World view 2

Districts	Area of interest (AOI)	Total area of AOI (km^2)	Cover (%) Landsat		Cover (%) WV2		Difference (%) Landsat-WV2		Landsat error (%)	
			2008	2018	2008	2018	2008	2018	2008	2018
Dhading	Dharke	60.95	5.25	8.50	4.95	7.65	0.30	0.85	6.06	11.11
Nawalparasi	Devchuli	44.22	3.50	5.65	2.85	4.34	0.65	1.31	22.80	30.18
Makwanpur	Manahari	106.80	2.30	5.70	1.76	3.90	0.54	1.80	30.68	46.15
Makwanpur	Hetauda	54.30	3.92	5.95	3.51	5.23	0.41	0.72	11.68	13.76
Chitwan	Muglin	39.85	3.36	5.45	2.50	3.85	0.86	1.60	34.40	41.55
Tanahau	Ghasikuwa	75.34	3.26	5.29	2.90	4.35	0.36	0.94	12.41	21.60
Kaski	Lekhnath-Kudule	96.67	2.85	3.90	1.93	2.58	0.92	1.32	47.66	51.16

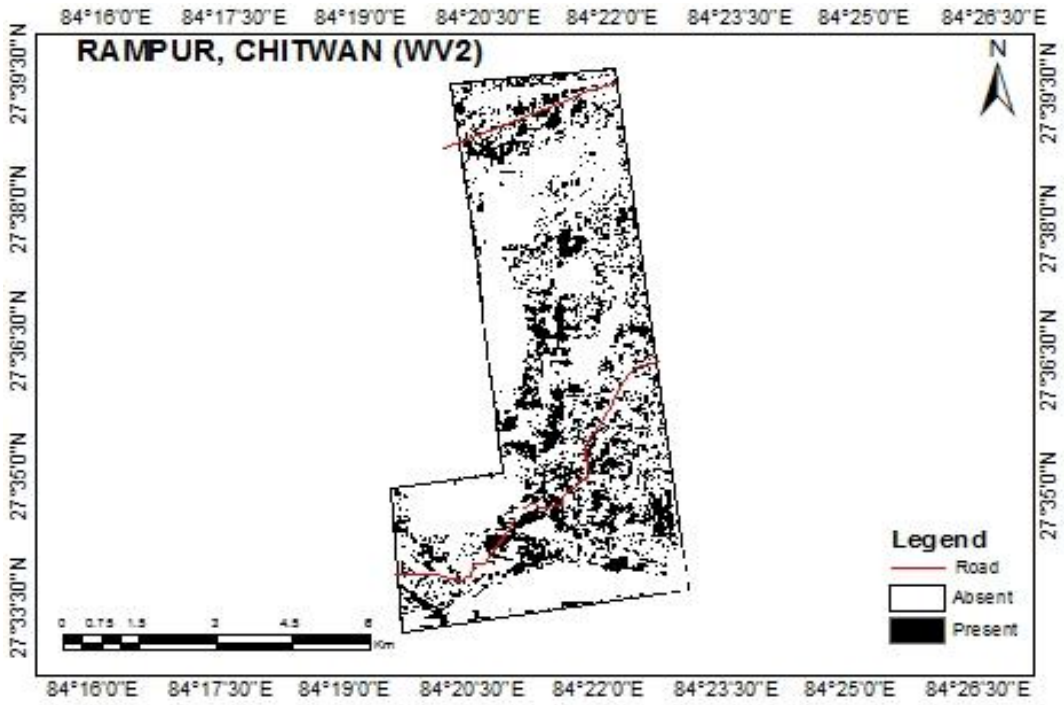

(a)

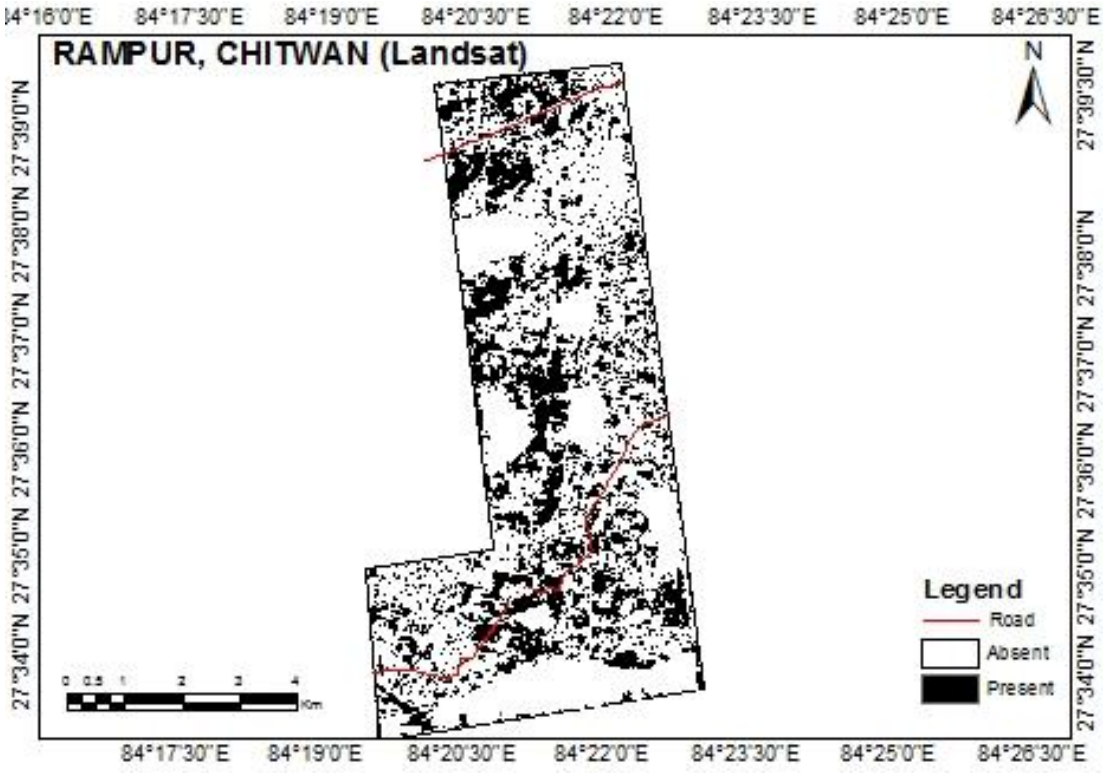

(b)

Figure 10: Comparison in distribution of *L. camara* in (a) World view-2 and (b) Landsat images of Chitwan in 2018

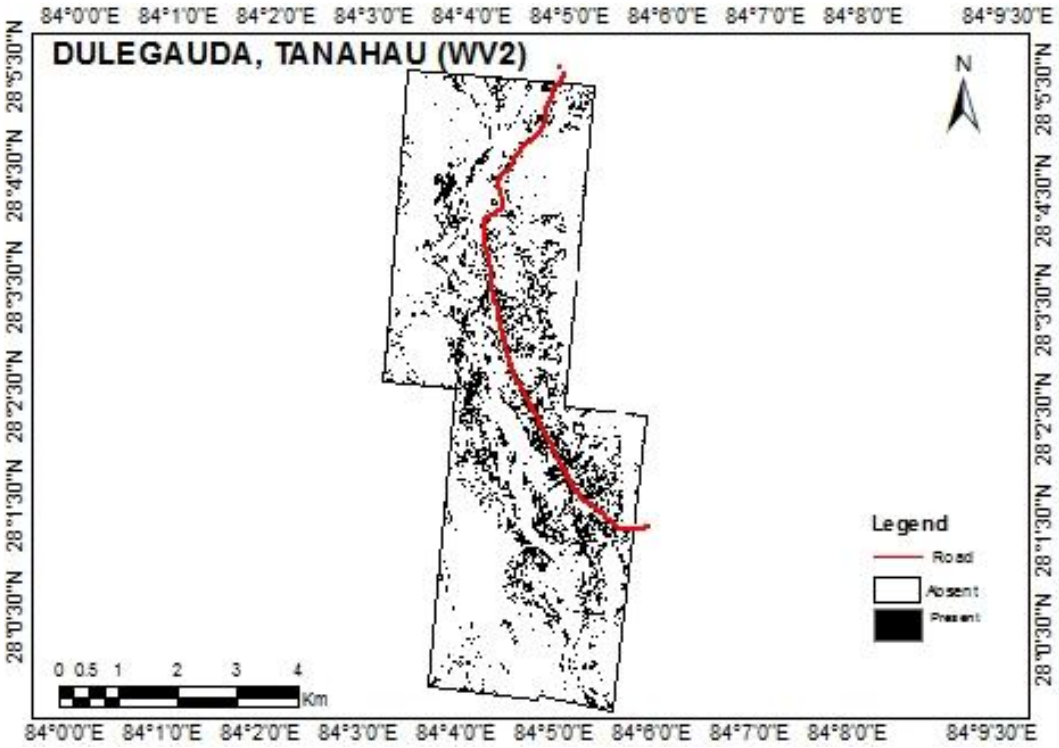

(a)

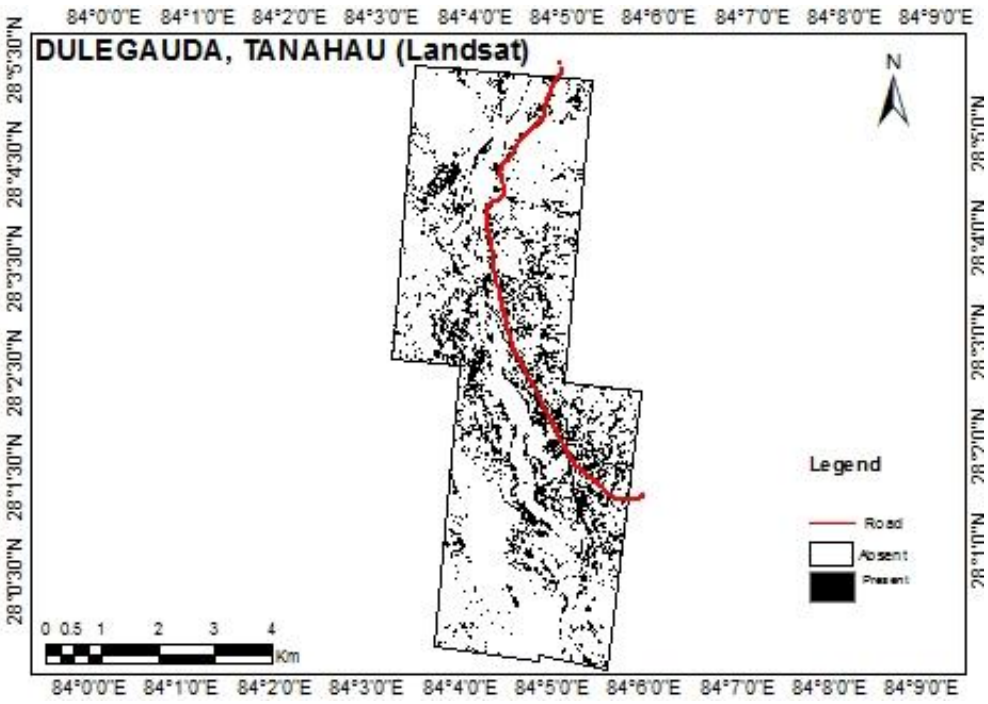

(b)

Figure 11: Comparison in distribution of *L. camara* in (a) World view-2 and (b) Landsat images of Tanahau in 2018

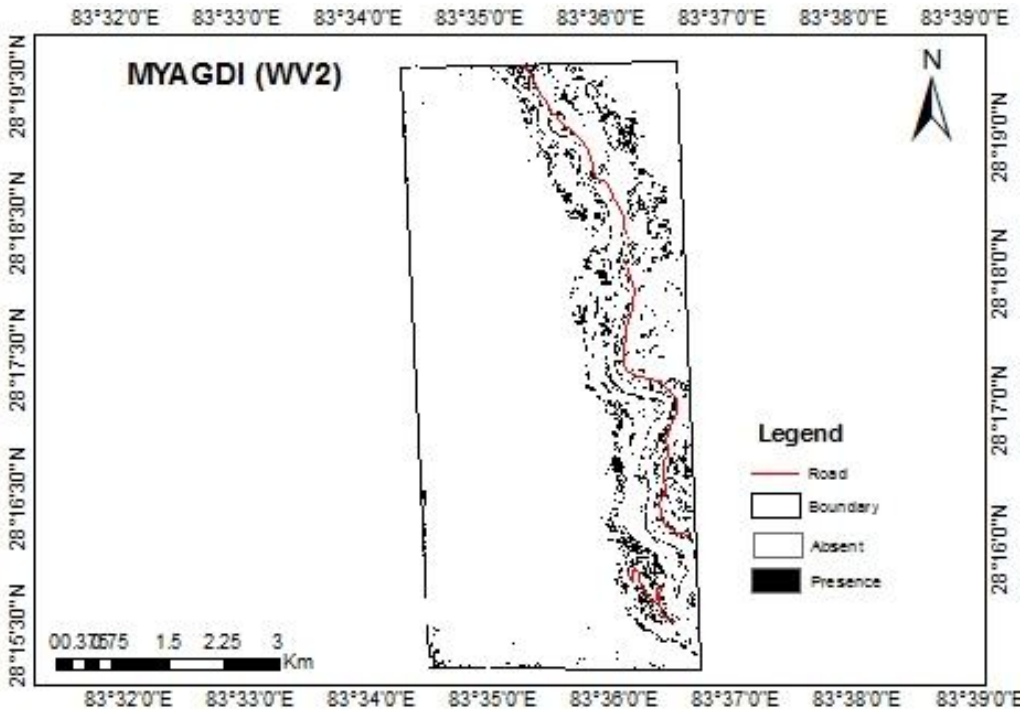

(a)

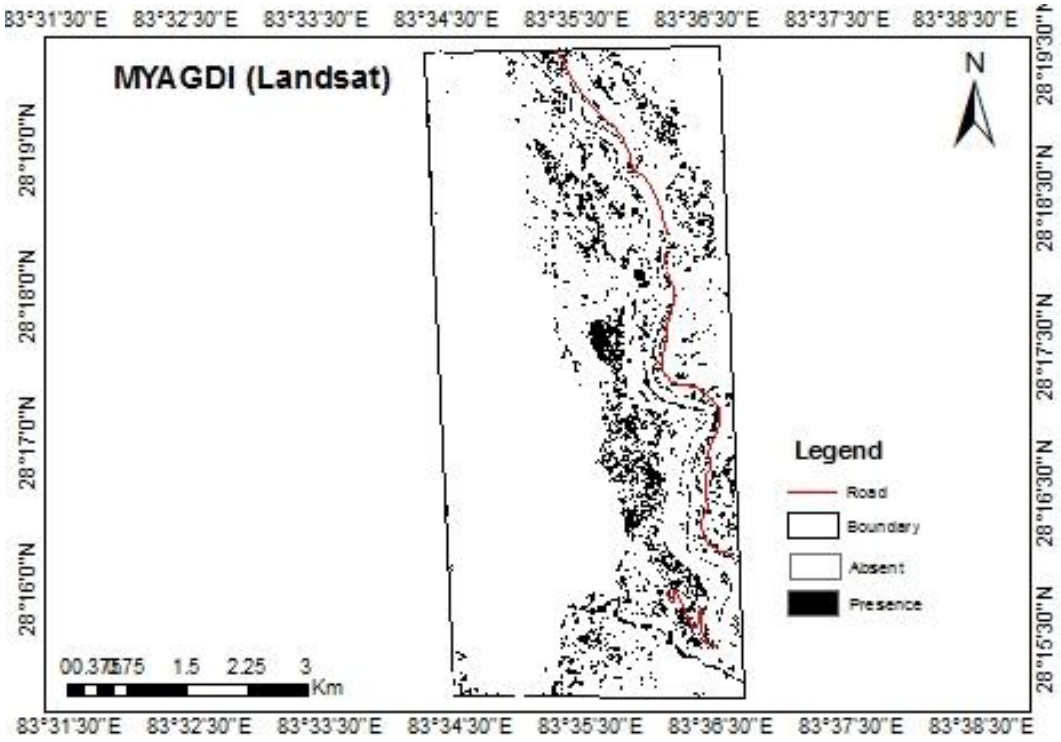

(b)

Figure 12: Comparison in distribution of *L. camara* in (a) World view 2 and (b) Landsat images of Myagdi district in 2018

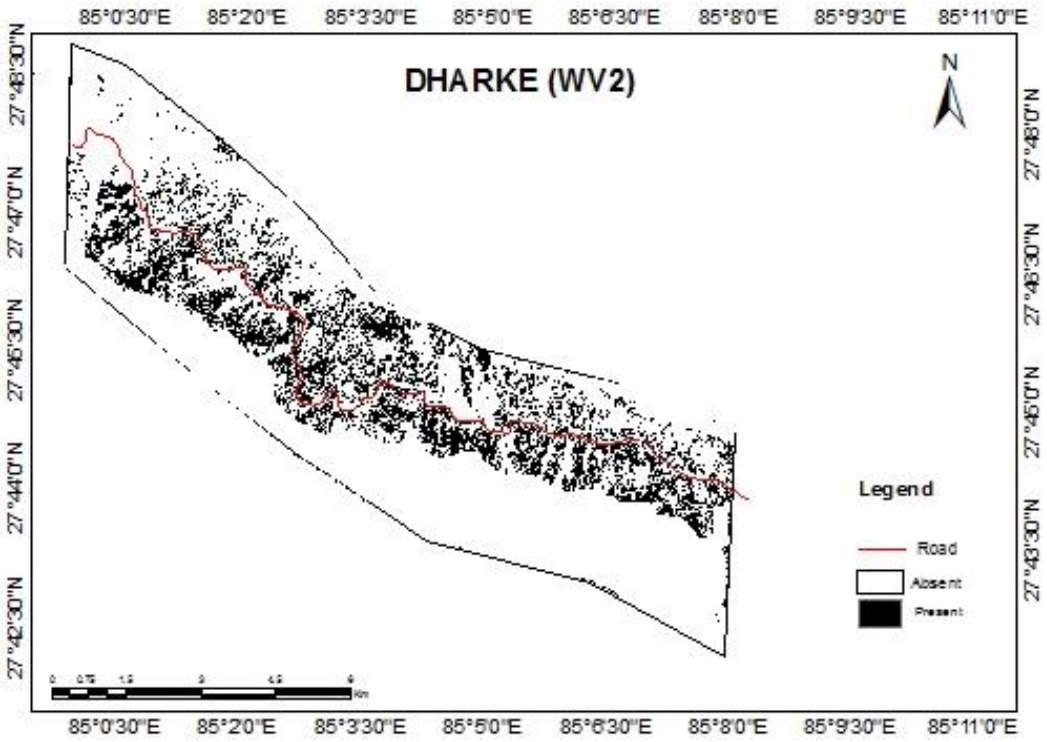

(a)

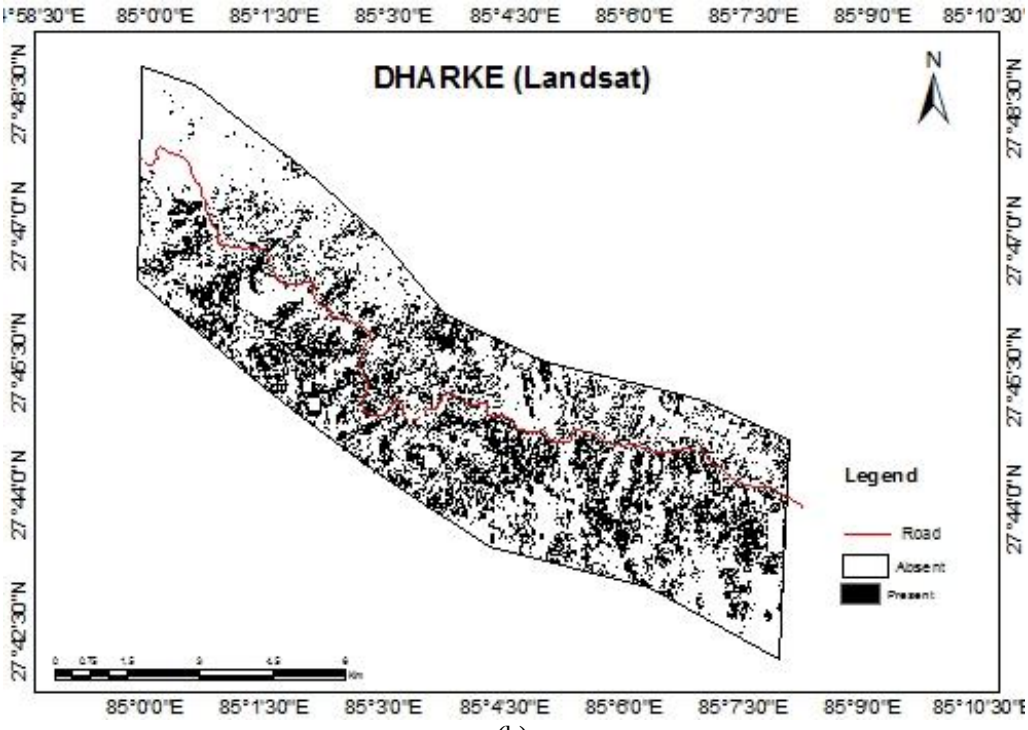

(b)

Figure 13: Comparison in distribution of *L. camara* in (a) World view 2 and (b) Landsat images of Dharke, Dhading in 2018

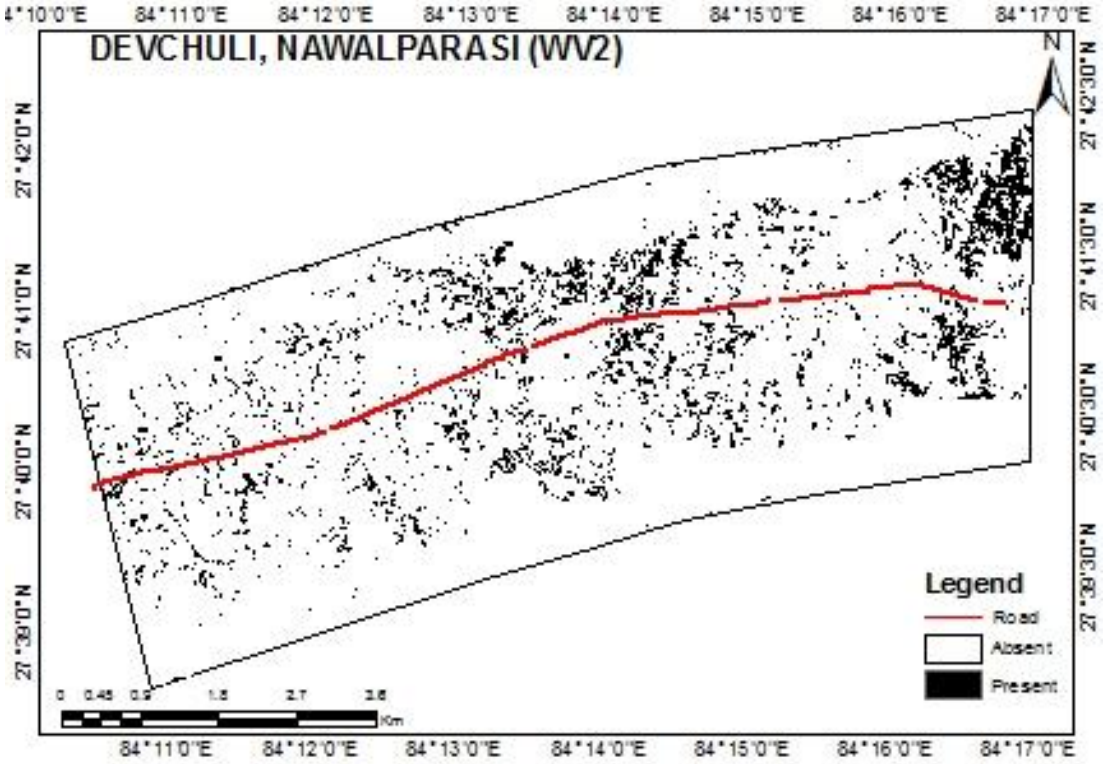

(a)

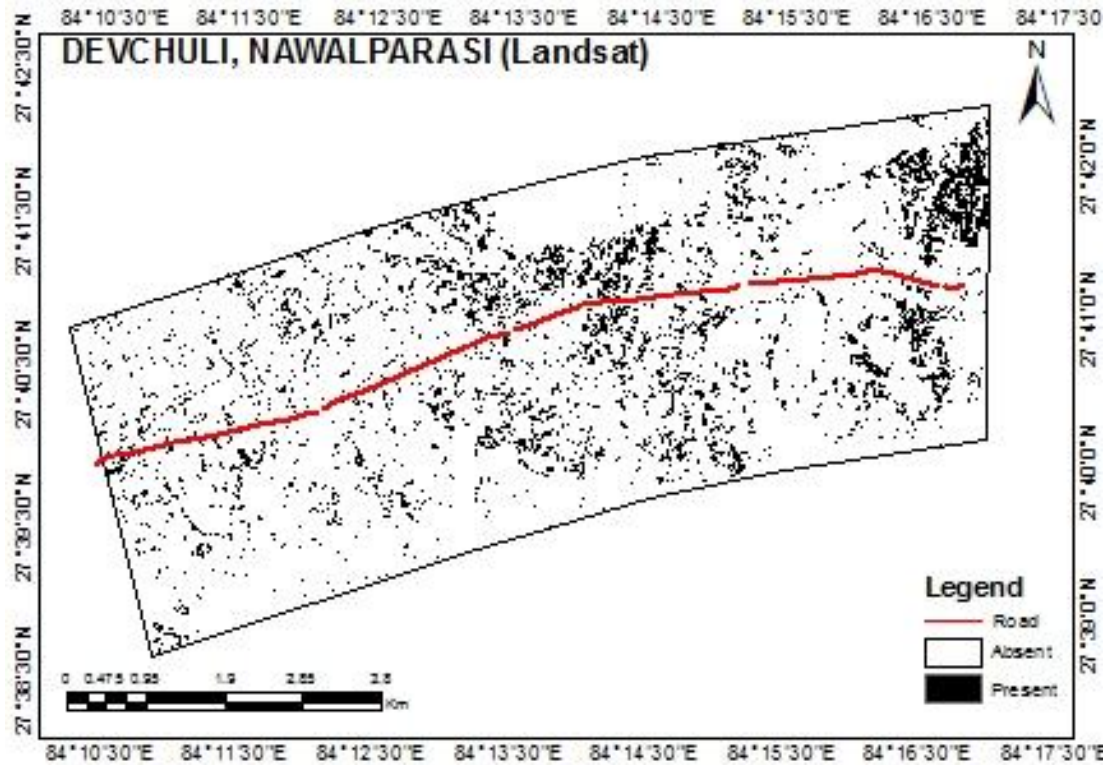

(b)

Figure 14: Comparison in distribution of *L. camara* in (a) World view 2 and (b) Landsat images of Devchuli, Nawalparasi district in 2018

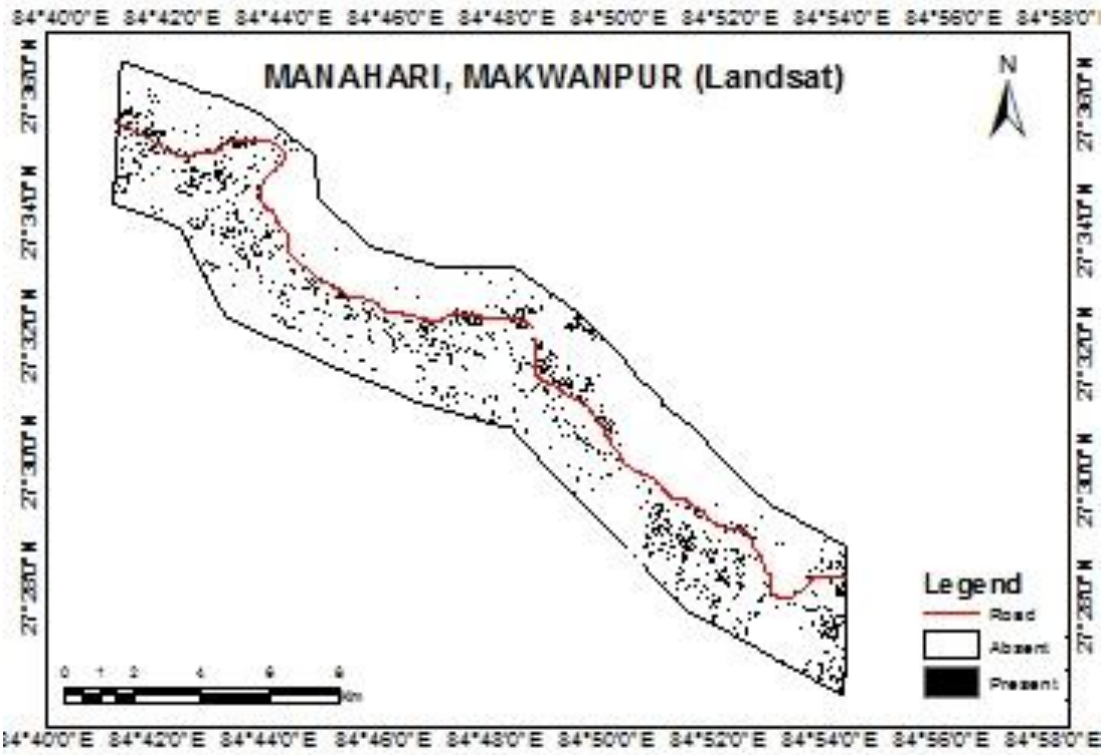

(a)

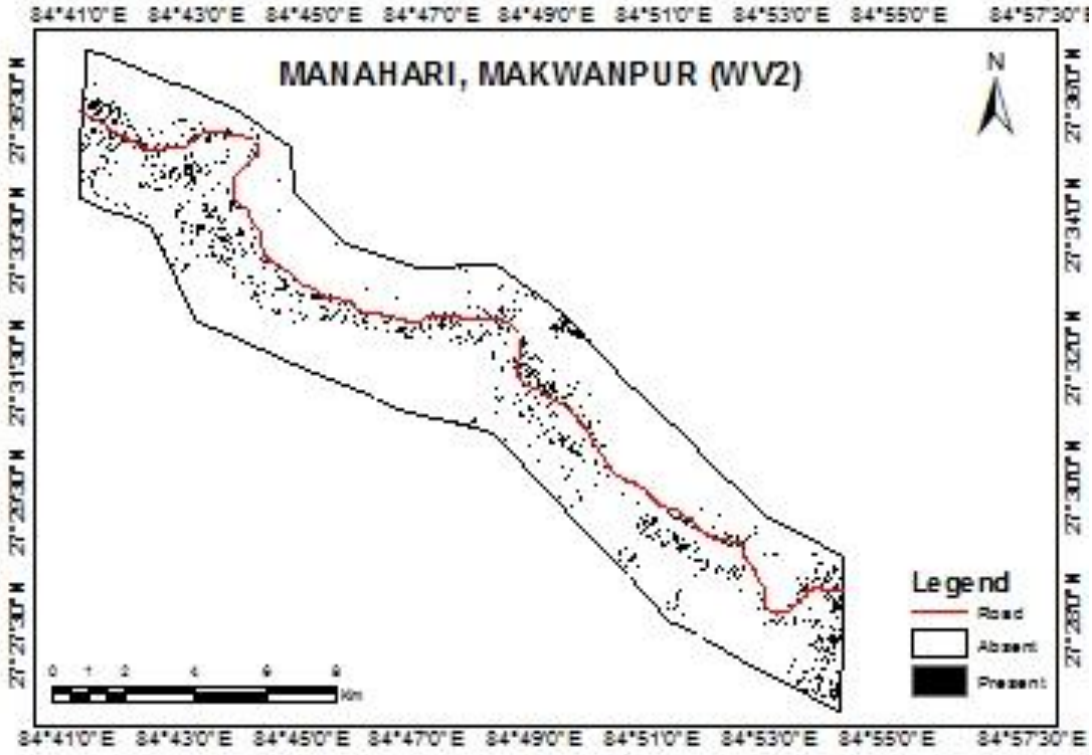

(b)

Figure 15: Comparison in distribution of *L. camara* in (a) World view 2 and (b) Landsat images of Manahari, Makwanpur districts in 2018

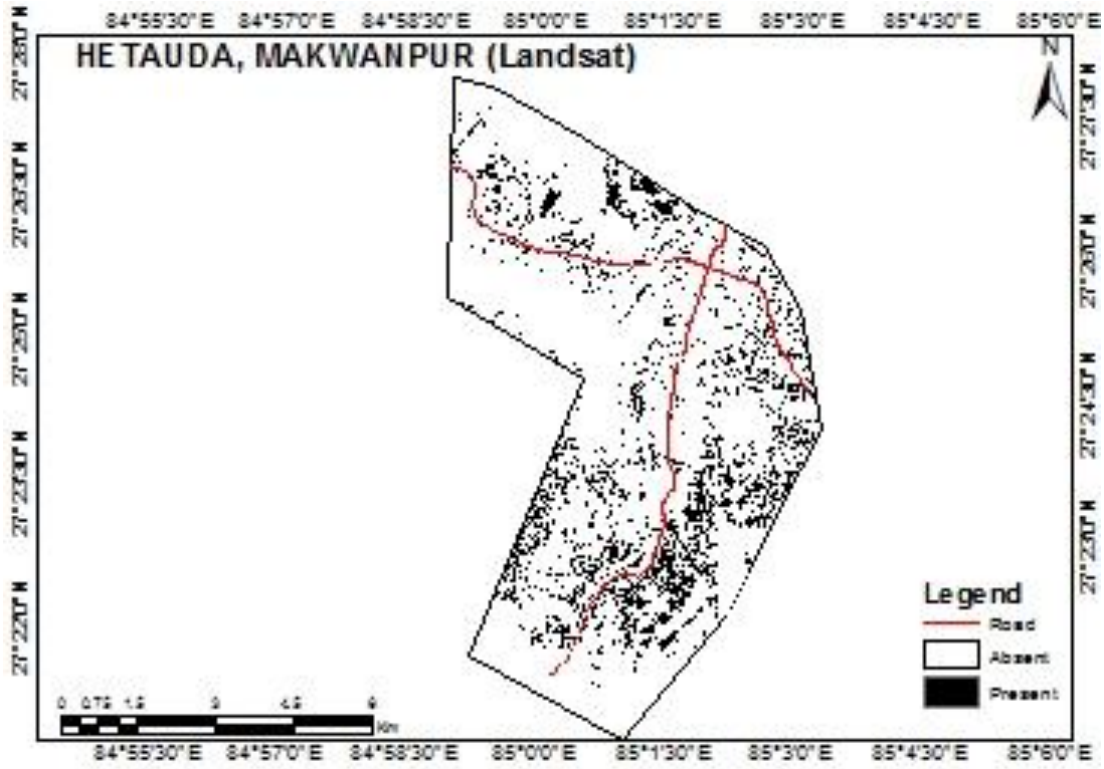

(a)

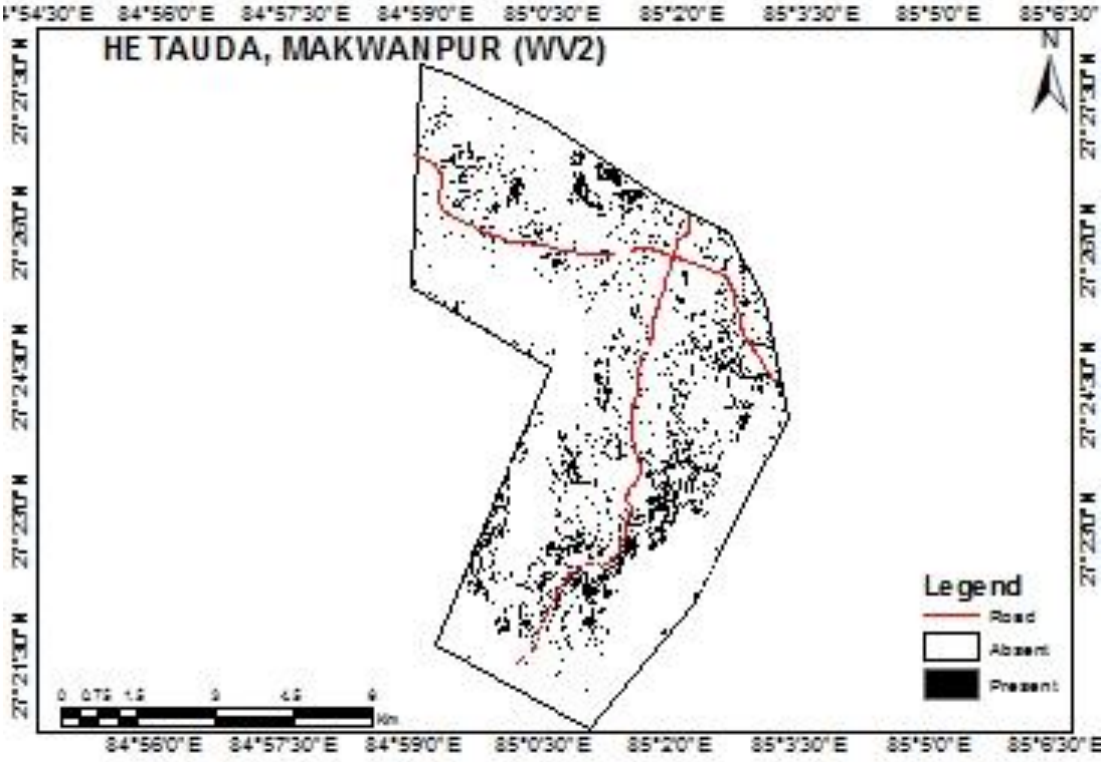

(b)

Figure 16: Comparison in distribution of *L. camara* in (a) World view-2) and (b) Landsat images of Hetauda, Makwanpur district in 2018

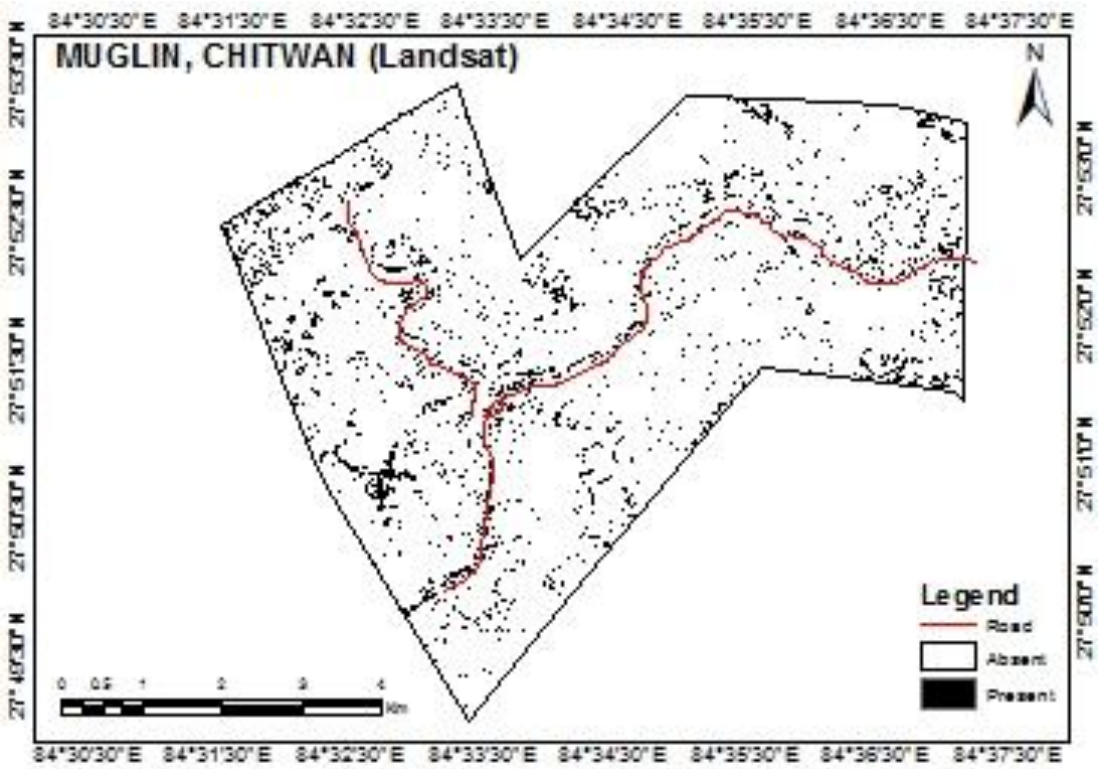

(a)

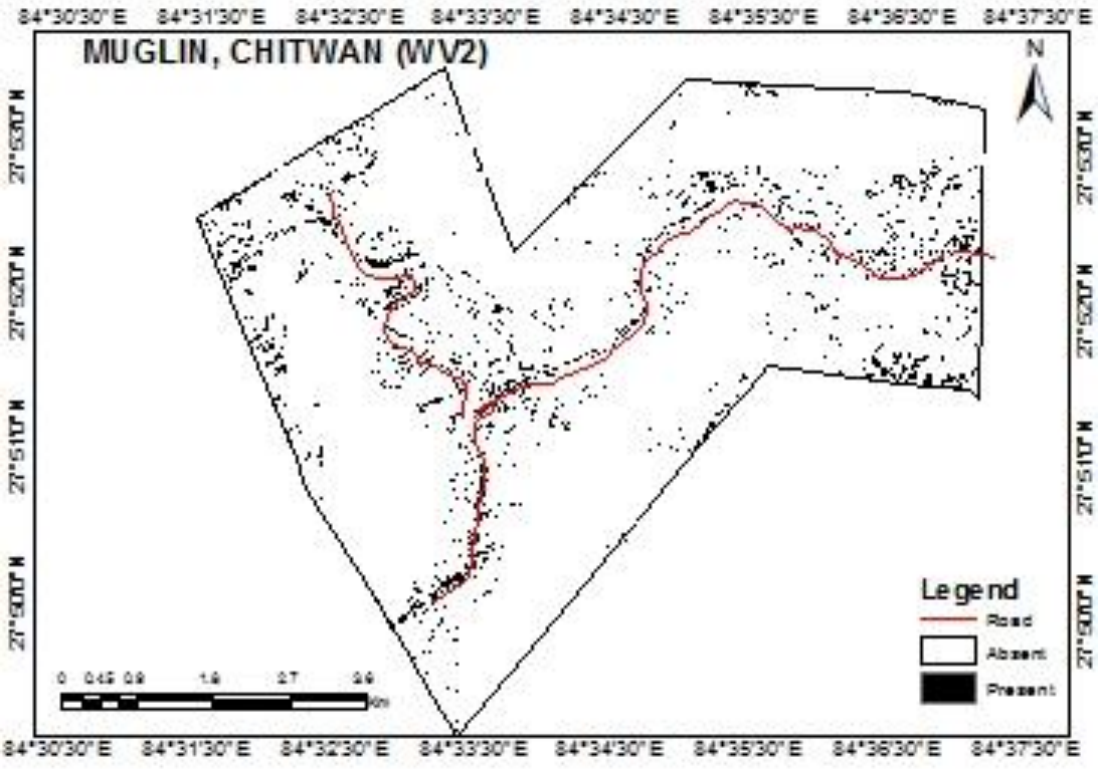

(b)

Figure 17: Comparison in distribution of *L. camara* in (a) World view-2 and (b) Landsat images of Muglin, Chitwan district in 2018

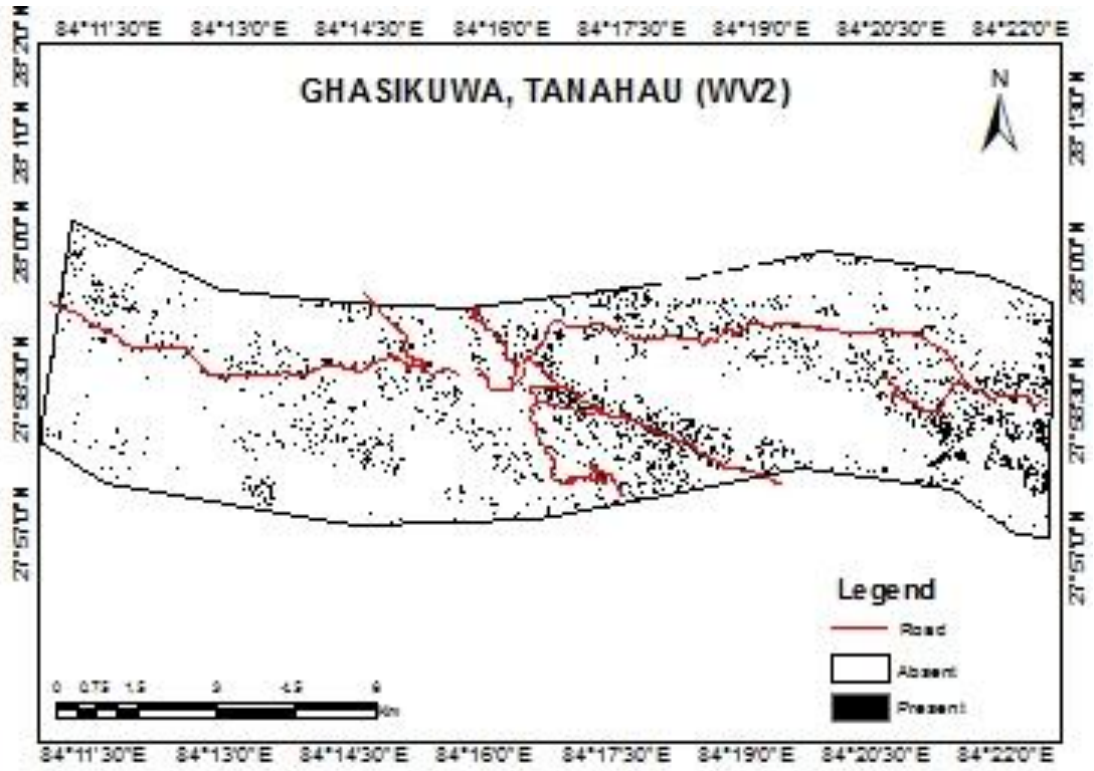

(a)

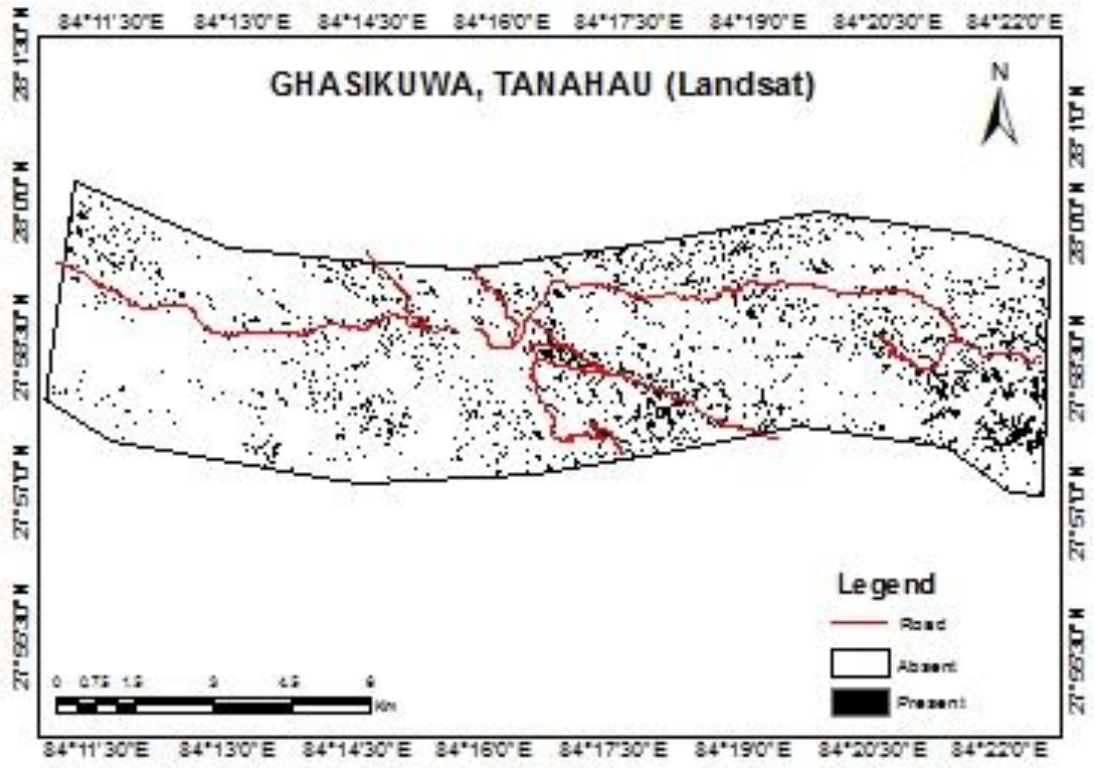

(b)

Figure 18: Comparison in distribution of *L. camara* in (a) World view-2 and (b) Landsat images of Ghasikuwa, Tanahau district in 2018

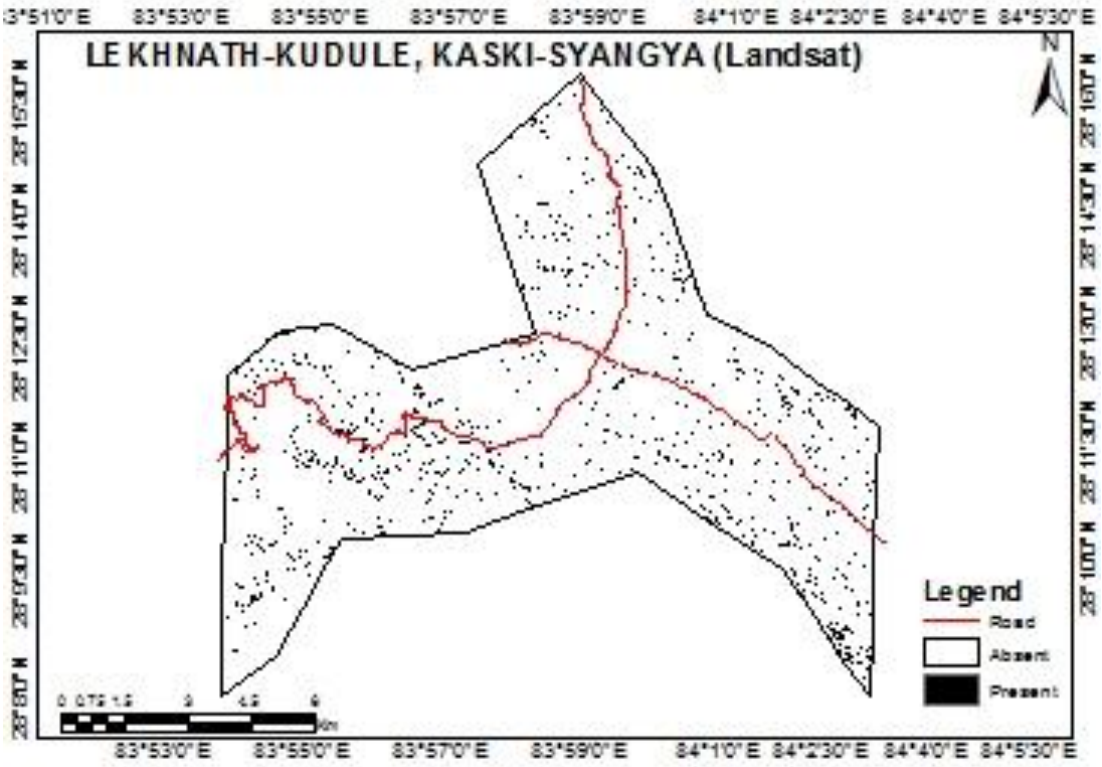

(a)

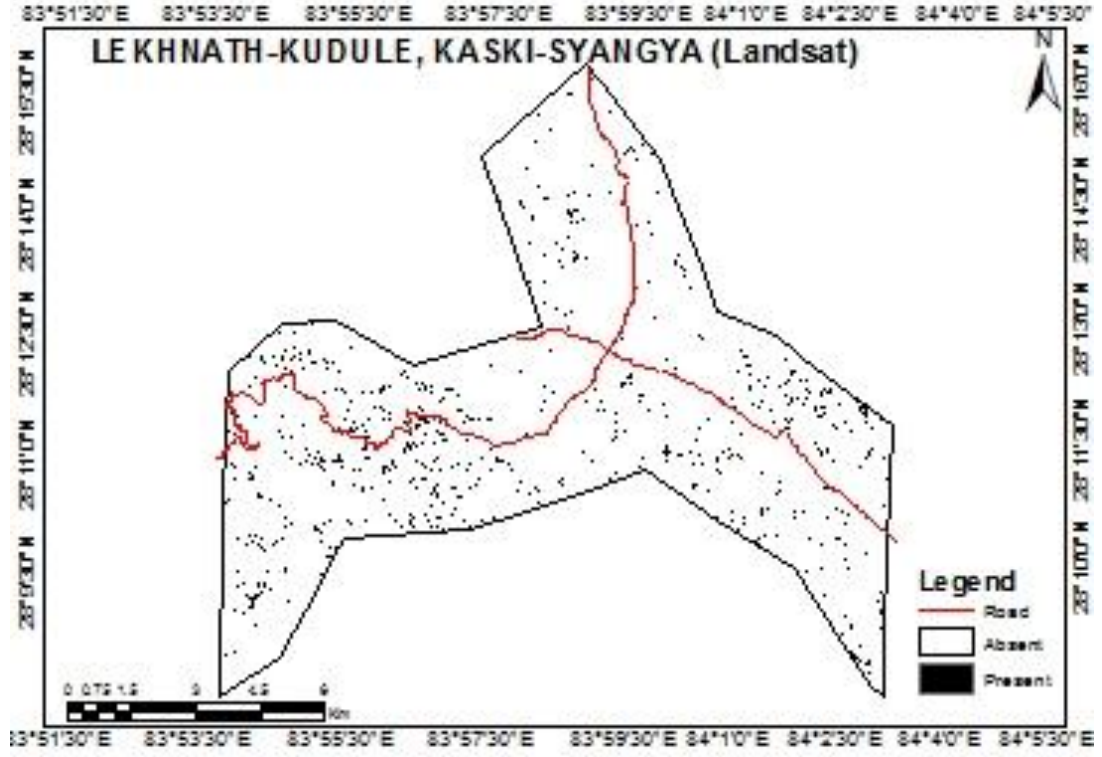

(b)

Figure 19: Comparison in distribution of *L. camara* in (a) World view-2 and (b) Landsat images of Kaski-Syangja district in 2018

4.4 Accuracy assessment

The classification result of the Landsat images was achieved satisfying accuracy results (Table 7). The overall accuracy is the total corrected prediction for both presence and absence coordinates where as kappa coefficient gives the insight of how well the classification performed as compared to just randomly assigning values. The overall accuracy in Landsat varied between 78 and 83% and kappa indices of 0.56 and 0.66. The highest overall accuracy was achieved in Makwanpur district where as lowest was achieved in Kaski district. The overall accuracy for the WV2 varied between 81 and 88% and kappa indices of 0.62 and 0.76. The significance test of accuracy between Landsat and WV2 ($p = 0.000075$) showed that the difference between the mean of accuracy of Landsat and WV2 was significantly different. On basis of Kappa value the image classification was moderate and substantial for most of Landsat images (value ranging from 0.4-0.8), for WV2 images, the classification was substantial (0.6-0.8). The highest overall accuracy was achieved in Nawalparasi district. For the year 2018, the knowledge based algorithm using Landsat images produced 77.25% overall accuracy and a Kappa index of 0.54 in CHAL.

Table 7: Classification accuracies for Landsat and World view 2 in area of interest (AOI) of 2018

Districts	Area of interest (AOI)	Overall accuracy (%)		Difference (%)	P- value	Kappa statistics (K)	
		Landsat	WV2			Landsat	WV2
Chitwan	Rampur	79.8	83.1	3.2		0.58	0.64
Tanahau	Dulegauda	81.0	85.0	4.0		0.62	0.70
Tanahau	Ghasikuwa	82.0	85.0	3.0		0.64	0.70
Dhading	Dharke	82.0	86.0	4.0	0.000075	0.62	0.72
Makwanpur	Hetauda	83.0	87.0	4.0		0.66	0.70
Makwanpur	Manahari	82.0	86.0	4.0		0.64	0.72
Chitwan	Muglin	79.0	83.0	4.0		0.58	0.66
Nawalparasi	Devchuli	81.0	88.0	7.0		0.62	0.76
Kaski-Syangja	Leknath-Kudule	78.0	81.0	3.0		0.56	0.62

5. DISCUSSION

5.1 Plant invasion and changes in land use/cover

Invasion is a common phenomenon in almost all ecosystems across the globe. The distribution map allows us to analyze the changes that occurred in the selected IAPS between 1992 and 2018, which is very useful for assessing the threat posed by invasive species. The results showed that the area covered by the *L. camara* was highest (2.74%) in the year 2018, followed by the year 2009 (1.45%), 2000 (0.9%) and 1992 (0.24%) based on Landsat images. Spatial and temporal information from the map indicates that *L. camara* gradually extends its occupancy towards the north and west sides of the study area (Fig. 10; Annex 6). According to Day *et al.* (2003), the distribution and density of *Lantana* is still increasing in many parts of the world, even in areas where it has been present for many years.

The area invaded by *L. camara* increased with the time period. The distribution area was the least in 1992 within the Siwalik and a few location of Middle Mountain. As the time passed, the invasion of *L. camara* goes on increasing covering new areas and elevation as observed in results. This was confirmed by post classification validation. Under this, the presence location from classified map were visited physically, interaction with the local people and reviewing literature.

The invasion is mainly influenced by three factors: the number of propagules entering the new environment (propagule pressure), the characteristics of the new species, and the susceptibility of the environment to invasion by new species (Lonsdale, 1999). After introduction, the dispersal and establishment of *L. camara* depends on availability of resources and anthropogenic activities via landscape transformation. Infrastructure development, increasing abandoned land in Middle Mountain have aided for more expansion of invasions. An analysis made by WWF (2013) about changes in major land use/land cover in the Chitwan Annapurna Landscape for the period 1990-2010 showed that some forest areas of the Siwalik has been degraded for infrastructure development, resettlement, urban expansion, and agriculture expansion. In the Middle Mountain, unplanned and unregulated construction of rural roads has

caused forest loss in many places. Frequent landscape fragmentation and local disturbances increases propagule pressure of invasive species (Waddel *et al*., 2020).

Climate change is likely to enhance the capacity of alien species to invade new areas, while simultaneously decreasing the resistance to invasion of natural communities by disturbing the dynamic equilibrium maintaining them (Thuiller *et al*., 2007). Climate change could potentially favor invasive non-native species by either creating more favourable environmental conditions for them, e.g., increasing fire frequency or by stressing native species to the point of being unable to compete against new invasive species (Brooks *et al*., 2004). The observation showed that most of the distribution concentrated in the anthropogenic landscape such as agro ecosystem, residential area and rangeland and in destructed area forest shrub land and abandoned area.

Nepal has undergone a significant transformation due to the developmental activities (Nepal, 2011; Lennartz, 2013). In the mountain and lowland regions of Nepal, newly built roads destabilize slopes and trigger landslides, creating bare ground suitable for colonization by the IAPS (Lennartz, 2013). Roads play a major role in the spread of alien species by facilitating dispersal pathways and by providing disturbed sites for percolation from roadsides into the natural adjacent vegetation (McDougall *et al.*, 2018). Besides this, rising temperature, altered precipitation, increased atmospheric carbon dioxide (CO_2), nitrogen (N) deposition and land use and land cover changes influence plant invasion(Vila *et al.*, 2007, Thuiller *et al*., 2007). The average temperature in every bioclimatic zone of CHAL has been increasing over the past five decades and 1999-2009 was a comparatively hotter decade at higher altitudes above 1000 m. On average, the temperature increased at a rate of 0.2°C to 0.27°C/ decade in different bioclimatic zones in CHAL between 1970-2019 (Luitel *et al.*, 2020).

5.2 Accuracy assessment

The overall accuracy of Landsat images was satisfactory despite its moderate spatial resolution as compared to high resolution World view 2 (WV2) images. The higher overall accuracy of World view 2 images is owing to its high spatial resolution.

Comparing the results of accuracy assessment of the World view 2 (WV2) and Landsat images, the effect of the better spatial resolution is evident for the WV2 image. The knowledge based classification in WV2 images achieved better accuracy than the classification based on Landsat images. In particular, the landuse and landcover (LULC) categories (forest, river, sand, cultivation, pond, snow, residential etc.) are very relevant from the classification point of view, so the ability of WV2 to separate these categories is very significant. A combination of high spatial resolution and the suitable spectral resolution, with 8 visible and near infrared bands in the WV2 image, seems to be crucial for the classification of the LULC categories. On the other hand, the archive of Landsat data is free and provides a long-time series of data (since the 1970s). So, it is necessary to analyze Landsat data when targeting homogenous stands over a large area (Huang *et al.*, 2009).

This error in Landsat is due to coarse spatial resolution of Landsat images and similarity in the spectral signatures in the NIR and visible portions of the electromagnetic spectrum in heterogeneous vegetation cover (Narumalani *et al.*, 2009). The Landsat error in classification is due to its coarse spatial resolution, compared to imagery from finer spatial resolution imagery like World view 2. The poor detection of *L. camara* in Landsat images could be attributed to the fact that, the spectral signature and the reflectance value of *L. camara* was developed from images composed of heterogeneous stands. Such stands of IAPS with similar reflectance would be difficult to detect unless they form dense monotypic stands (Bradley, 2014).

We found that WV2 data had better abilities in the classification of features (LULC) than Landsat data. WV2 is useful in small-scale case studies due to the better spatial resolution with a suitable spectral resolution and high cost (Immitzer and Atzberger, 2014). According to Griffiths *et al.* (2014) and Hais *et al.* (2009), Landsat data are suitable for large-scale case studies/regions.

Specifically, Piyasinghe *et al.* (2018) acquired high resolution multispectral World view 2 images for the mapping of *Austroeupatorium inulifolium* invasive species in Sri Lanka and tested the three classifier individually, i.e., unsupervised, supervised and knowledge based classification. The results presented by them showed overall classification accuracy of 100% with overall Kappa (K^) Statistics at 1.0. Producers and user accuracies of each classified class (Forests, *A. inulifolium* invaded areas, *C. nardus*-dominated grasslands etc.) showed a 100% accuracy. The present study also used the similar classification method as used by Piyasinghe *et al.* (2018) but in the present study the product of pixel based (unsupervised and supervised) classification were used as base map for the knowledge base classifier. The decision rules are applied to these base maps to identify species that are not able to be detected based on the pixel-based classification (Xu and Ji, 2014). Though the classification methods were similar but does not show the comparable results. The lower overall accuracy in the present study is due to lower spatial resolution of Landsat in compare to WV2 and the larger extent of the area under study.

Tarantino *et al.* (2019) performed species level mapping of *Ailanthus altissima* using the high spatial resolution image (WV2) involving both the knowledge driven and pixel based classification. The results presented by them showed the overall accuracy (OA) value of ≈ 91%, which is very close to the accuracy of WV2 in the present study. Their findings suggest that multi-temporal, very high resolution satellite imagery can be effective for species level mapping especially when airborne hyperspectral data are unavailable.

Ng *et al.* (2016) used Landsat 8 data for mapping *Prosopis* spp and evaluated the effectiveness of different methods. Their study show the overall accuracy of 74% when applying a pixel-based classification using a combination of the wet and dry season Earth observation data. Their results also suggest that the object-based mapping were less reliable due to the limitations in spatial resolution of the Landsat data (15-30 m) and problems in finding an appropriate segmentation scale.

Laba *et al.* (2008) applied a maximum-likelihood classification, with spatial resolution (2.4 m), to estimate the presence of multiple alien plants (*Lythrum salicaria*, *Phragmites australis* and *Trapa natans*) in diverse tidal wetlands of the

Hudson River National Estuarine Research Reserve, USA and was a relatively reliable data source for wetland non-native plant mapping (accuracy assessment ≥ 65%). Everrit *et al.* (2005) proved high accuracy (accuracy assessment ≥ 86%) in delineating an Indian grass (*Arundo donax*) along a riparian zone in Texas.

The development of models to depict future spread is a crucial research area. Various models have been developed; which use climatic and topographic variables as inputs to infer on future extent of IAPs (He *et al.,* 2011). Sensors and techniques used would also vary from region to region and would be dependent on various factors such as resource availability, terrain, IAPS present and vegetation type.

5.3 Management implication

Globally, plant invasions are growing in frequency and areal extent (Mack, 2000). These invasions need to be managed because they have serious consequences for biodiversity and the economy (Vilà *et al.,* 2011). Mapping is an important tool for managing plant invasions because it can identify where they are and how long they have been there. The effective management of IAPS relies on reliable maps of current location and prediction of future spread. Knowing the spatial distribution of invaders can help managers identify sites of invasion (Shaw, 2005), monitor the outcomes of management actions (Roura-Pascual *et al.,* 2009) and understand processes that operate at a landscape scale (Richardson 2011). Also, quantitatively documenting the change in areal extent of invasions is important for justifying and sustaining public support of management programs (Mack, 2000)

The present study shows that area of occupancy as well as the density of the weed goes on increasing temporally through which the factor affecting invasion can be known and thus provides a benchmark for monitoring future vegetation change. The results show the invaded area and the trend of invasion of IAPS which helps the land managers to direct resources towards curbing the spread of invasion. Further, our database allows for the identification of areas of high densities of weed, where managers can apply control measures and also areas where careful intervention may be required to conserve the native canopy species that coexist with non-native species.

6. CONCLUSION AND RECOMMENDATIONS

6.1 Conclusion

The main objective of this study was to determine the distribution of *Lantana camara* spatially and temporally in CHAL area. In this study, knowledge based classification approach using Landsat images was employed to determine the distribution of *Lantana camara* in CHAL area. The spatial extension of *Lantana camara* depicted in this study shows that the plant is spreading upward in the northern side mostly in the mid hills with the time and space. The knowledge based classification applied on World view 2 images produced the best results with higher classification accuracies in comparison to Landsat images. Overall accuracies of 77% was found in the present study using Landsat images of 2018. The highest overall accuracy was 88 and 83% in the selected area of interest of World view 2 and Landsat images, respectively. Landsat TM and World view 2 imageries have become invaluable source of data for detecting the spatial distribution of *L. camara* in the study area. Both historical time series of remotely sensed data present opportunities for characterizing habitat preferences. Though Landsat images showed higher coverages of the weed, however, it had given good results in deriving distribution of *L. camara* spatially and temporally.

6.2 Recommendations

Based on the results, followings are the recommendations:

- Use of satellite imageries for long term monitoring of invasive weed is recommended.
- The rate at which *L. camara* invasion is occurring shows the need for a monitoring and assessment of damage.
- The results of this study can have the following management implication.
- The results show the invaded area and the trend of invasion of IAPS which can help the land managers to direct resources towards curbing the spread of invasion.

- Provides improved information on the spatial segregation of IAPS which helps to know the factor affecting invasion like climatic, anthropogenic etc. on further research and thus provides a benchmark for monitoring future vegetation change.

REFERENCES

Aravind, N.A., Rao, D., Ganeshaiah, K.N., Shanker, R.U. and Poulsen, J.G. (2010). Impacts of the invasive plant, *Lantana camara*, on bird assemblages in Male Mahadeshwara Reserve Forest, South India. *Tropical Ecology*, **51,** 325-338.

Asner, G.P., Jones, M.O., Martin, R.E., Knapp, D.E. and Hughes, R.F. (2008). Remote sensing of native and invasive species in Hawaiian forests. *Remote Sensing of Environment*, **112**(5), 1912-1926.

Baral, S., Adhikari, A., Khanal, R., Malla, Y., Kunwar, R., Basnyat, B., Gauli, K. and Acharya, R.P. (2017). Invasion of alien plant species and their impact on different ecosystems of Panchase area, Nepal. *Banko Janakari*, **27,** 31-42.

Becker, T., Dietz, H., Billeter, R., Buschmann, H. and Edwards, P. (2005). Altitudinal distribution of alien plant species in the Swiss Alps. *Perspectives in Plant Ecology Evolution and Systematics*, **7,** 173-183.

Bellard, C., Thuiller, W., Leroy, B., Genovesi, P., Bakkenes, M. and Courchamp, F. (2013). Will climate change promote future invasions? *Global Change Biology*, **19,** 3740-3748.

Berry, Z.C., Wevill, K. and Curran, T.J. (2011). The invasive weed *Lantana camara* increases fire risk in dry rainforests by altering fuel beds. *Weed Research*, **51,** 525-533.

Berec, L., Kean, J.M., Epanchin-Niell, R., Liebhold, A.M. and Haight, R.G. (2015). Designing efficient surveys: spatial arrangement of sample points for detection of invasive species. *Biological Invasions*, **17,** 445-459

Bhagwat, S.A., Breman, E., Thekaekara, T., Thornton, T.F. and Willis, K.J. (2012). A Battle Lost? Report on two centuries of invasion and management of *Lantana camara* L. in Australia, India and South Africa. *PLoS ONE* **7,** e32407, https://doi.org/10.1371/journal.pone.0032407

Bhattarai, K.R., Maren, I.E. and Subedi, S.C. (2014). Biodiversity and invasibility: distribution patterns of invasive plant species in the Himalayas, Nepal. *Journal of Mountain Science*, **11,** 688-696.

Bishop, Y., Fienberg, S. and Holland, P.W. (1975). *Discrete Multivariate Analysis: Theory and Practice.* Cambridge: MIT Press.

Bista, D., Shrestha, S., Sherpa, P., Thapa, G.J., Kokh, M. and Lama, S.T. (2017). Distribution and habitat use of red panda in the Chitwan-Annapurna Landscape of Nepal. *PLoS ONE* **12**(10), e0178797, https://doi.org/10.1371/journal.pone.0178797

Bradley, B.A. (2014). Remote detection of invasive plants: A review of spectral, textural and phenological approaches. *Biological Invasions*, **16**(7), 1411-1425.

Bradley, B.A. and Marvin, D. (2011). Using expert knowledge to satisfy data needs: mapping invasive plant distributions in the western United States. *Western North American Naturalist*, **71**(3), 302-315.

Brooks, M.L., D'Antonio C.M., Richardson D.M., Grace, J., Keeley, J.E., Di Tomasso, J.M., Hobbs, R.J., Pellant, M. and Pyke, D. (2004). Effects of invasive alien plants on fire regimes. *BioScience*, **54,** 677–688

Calviño-Cancela, M., Méndez-Rial, R., Reguera-Salgado, J. and Martín-Herrero, J. (2014). Alien plant monitoring with ultralight airborne imaging spectroscopy. *PloS ONE*, **9**(7), e10238, https://doi.org/10.1371/journal.pone.0102381.

Carter, G.A., Lucas, K.L., Blossom, G.A., Lassitter, C.L., Holiday, D.M., Mooneyhan D.S., Fastring, D.R., Holcombe, T.R and Griffith, J.A. (2009). Remote sensing and mapping of tamarisk along the Colorado river, USA: A comparative use of summer acquired Hyperion, Thematic Mapper and Quick Bird data. *Remote Sensing*, **1**(3), 318-329.

Congalton, R.G. and Green, K. (2009). *Assessing the Accuracy of Remotely Sensed Data-Principles and Practices* (Second edition). Boca Raton: CRC Press, Taylor and Francis Group.

Cuneo, P., Jacobson, C.R. and Leishman, M.R. (2009). Landscape-scale detection and mapping of invasive African Olive (*Olea europaea* L. ssp. cuspidata Wall ex G.

Don Ciferri) in SW Sydney, Australia using satellite remote sensing. *Applied Vegetation*, **12,** 145-154.

Day, M., Wiley, C., Playford, J. and Zalucki, M. (2003). *Lantana Current Management Status and Future Prospects*. Canberra: Australian Center for International Agricultural Research, Australia.

Dobremez, J.F. (1976). *Le Nepal Ecologie et Phytogeography*. Paris: Editiion du Centre National de la Recherche Scientifique, France.

Doody, T.M., Lewis, M., Benyon, R.G. and Byrne, G. (2014). A method to map riparian exotic vegetation (*Salix* spp.) area to inform water resource management. *Hydrological Processes*, **28,** 3809-3823.

Evangelista, P.H., Stohlgren, T.J., Morisette, J.T. and Kumar, S. (2009). Mapping invasive Tamarisk (*Tamarix*): A comparison of single-scene and time-series analyses of remotely sensed data. *Remote Sensing*, **1**(3), 519-533.

Everitt, J.H., Yang, C. and Deloach, C.J. (2005). Remote sensing of giant reed with QuickBird satellite imagery. *Journa of Aquatic. Plant Management*, **43,** 81-85.

Everitt, J.H., Yang, C., Fletcher, R. and Deloach, C.J. (2008). Comparison of QuickBird and SPOT 5 satellite imagery for mapping giant reed. *Journal of Aquatic Plant Management*, **46,** 77-82.

Gavier-Pizarro, G.I., Kuemmerle, T., Hoyos, L.E., Stewart, S.I., Huebner, C.D., Keuler, N.S. and Radeloff, V.C. (2012). Monitoring the invasion of an exotic tree (*Ligustrum lucidum*) from 1983 to 2006 with Landsat TM/ETM+ satellite data and Support Vector Machines in Córdoba, Argentina. *Remote Sensing of Environment*, **122,** 134-145.

Ghulam, A., Porton, I. and Freeman, K. (2014). Detecting subcanopy invasive plant species in tropical rainforest by integrating optical and microwave (InSAR/PolInSAR) remote sensing data, and a decision tree algorithm. *ISPRS Journal of Photogrammetry and Remote Sensing*, **88,** 174-192.

Griffiths, P., Kuemmerle, T., Baumann, M., Radeloff, V.C., Abrudan, I.V., Lieskovsky, J., Munteanu, C., Ostapowicz, K. and Hostert, P. (2014). Forest

disturbances, forest recovery, and changes in forest types across the Carpathian ecoregion from 1985 to 2010 based on Landsat image composites. *Remote Sensing. Environment,* **151,** 72-88.

Hais, M., Langhammer, J., Jirsova, P. and Dvorak, L. (2009). Deforestation development dynamics in central part of the Sumava Mountains between 1985 and 2007 based on Landsat TM/ETM+ satellite data. Acta University, Carolina. *Geography,* **45,** 1-2.

He, K.S., Rocchini, D., Neteler, M. and Nagendra, H. (2011). Benefits of hyperspectral remote sensing for tracking plant invasions. *Diversity and Distributions,* **17**(3), 381-392.

Higgins, S.I., Richardson, D.M., Cowling, R.M. and Trinder-Smith, T.H. (1999). Predicting the landscape-scale distribution of alien plants and their threat to plant diversity. *Conservation Biology,* **13**(2), 303-313.

Hishe, S., Lyimo, J. and Bewket, W. (2017). Effects of soil and water conservation on vegetation cover : a remote sensing based study in the Middle Suluh Valley, northern Ethiopia. *Environmental System Research,* **6**(1), 1-16.

Huang, C.Y. and Asner, G.P. (2009). Applications of remote sensing to alien invasive plant studies. *Sensors* (*Basel, Switzerland),* **9**(6), 4869-4889.

Immitzer, M. and Atzberger, C. (2014). Early detection of bark beetle infestation in Norway spruce (*Picea abies* L.) using World view 2 data. *Photogrammatic Fernerkund. Geoinformation,* **5,** 351-367.

IUCN. (2017). Invasive Alien Species and Climate Change. International Union for Conservation of Nature (IUCN) Issues Brief, November. www.iucn.org/ resources/issues-briefs/invasive-alien-species-and-climate-change.

Jevon, T. and Shackleton, C.M. (2015). Integrating local knowledge and forest surveys to assess *Lantana camara* impacts on indigenous species recruitment in Mazeppa Bay, South Africa. *Human Ecology,* **43,** 247-254.

Joshi, C., de Leeuw, J., Skidmore, A.K., van Andel, J., Lekhak, H.D. and van Duren, I. (2005). Remote sensing and GIS for mapping and management of invasive shrub *Chromolaena odorata* in Nepal. *Proceedings of Eighth AGILE Conference on Geographic Information Science* (pp. 71-80). Estoril: Portugal.

Joshi, C., de Leeuw, J., van Andel, J., Skidmore, A.K., Lekhak, H.D., van Duren, I.C. and Norbu, N. (2006). Indirect remote sensing of a cryptic forest understorey invasive species. *Forest Ecology and Management,* **225**(1-3), 245-256.

Kent, R. and Dorward, A. (2015). Livelihood responses to *Lantana camara* invasion and biodiversity change in southern India: application of an asset function framework. *Regional Environmental Change,* **15,** 353-364.

Kimothi, M.M. and Dasari, A. 2010. Methodology to map the spread of an invasive plant (*Lantana camara L.*) in forest ecosystems using Indian remote sensing satellite data. *International Journal of Remote Sensing,* **31,** 3273-3289.

Laba, M., Downs, R., Smith, S., Welsh, S., Neider, C., White, S., Richmond, M., Philpot, W. and Baveye, P. (2008). Mapping invasive wetland plants in the Hudson River National Estuarine Research Reserve using QuickBird satellite imagery. *Remote Sensing of Environment,* **112,** 286-300.

Lennartz, T. (2013). Constructing roads—constructing risks? Settlement decisions in view of landslide risk and economic opportunities in Western Nepal. *Mountain Research and Development,* **33**(4), 364-371.

Levine, J.M. and D'antonio, C.M. (2003). Forecasting biological invasions with increasing international trade. *Conservation Biology,* **17,** 322-326.

Lillesand, M.T., KIefer, W.R. and Chipman, N.J. (2008). *Remote Sensing and Image.* (6th edn.). Hoboken: John Wiley & Sons.

Lillesand, T.M. and Kieffer, R.W. (1994). *Remote Sensing and Image Interpretation*. (3rd edition). New York: John Wiley and Sons, USA.

Lonsdale, W.M. (1999). Global patterns of plant invasions and the concept of invisibility. *Ecology,* **80,** 1522-1536.

Lowe, S., Browne, M., Boudjelas, S. and DePoorter, M. (2000). *100 of the World's Worst Invasive Alien Species: A Selection from the Global Invasive Species Database*. The Invasive Species Specialist Group (ISSG), a specialist group of the Species Survival Commission (SSC) of the World Conservation Union (IUCN), New Zealand.

Lu, D. and Weng, Q. (2007). A survey of image classification methods and techniques for improving classification performance. *International Journal of Remote Sensing*, **28,** 823-870.

Luitel, D.R., Jha, P.K., Siwakoti, M., Shrestha, M.L. and Munniappan, R. (2020). Climatic Trends in Di_erent Bioclimatic Zones in the Chitwan Annapurna Landscape, Nepal. *Climate*, **8**(136), 1-18

Mack, R.N. (2000). Assessing the extent, status, and dynamism of plant invasions: current and emerging approaches. In: Mooney H. and Hobbs R.J. (Eds). *Invasive species in a changing world* (pp.141–168). Island Press, Washington, DC.

Mack, R.N. and Smith, M.C. (2011). Invasive plants as catalysts for the spread of human parasites. *NeoBiota*, **9,** 13-29.

Mack, R.N., Holle, B.V. and Meyerson, L.A. (2007). Assessing invasive alien species across multiple spatial scales: working globally and locally. *Frontiers in Ecology and the Environment*, **5**, 217-220.

Maharjan, S., Shrestha, B.B., Joshi, M. D., Devkota, A., Muniappan, R., Adiaga, A. and Jha, P.K. (2019). Predicting suitable habitat of an invasive weed *Parthenium hysterophorous* under future climate scenarios in Chitwan-Annapurna Landscape, Nepal. *Journal of Mountain Science*, **16(10),** 2243-2256

McDougall, K.L., Lembrechts, J., Rew, L.J., Haider, S., Cavieres, L.A., Kueffer, C. and Alexander, J.M. (2018). Running off the road: Roadside non-native plants invading mountain vegetation. *Biological Invasions*, **20,** 3461-3473.

MFSC. (2015). *Strategy and Action Plan 2016-2025: Chitwan-Annapurna Landscape*. Kathmandu: Ministry of Forest and Soil Conservation (MFSC), Nepal.

Morais, M., Marchante, E. and Marchante, H. (2007). Big troubles are already here: Risk assessment protocol shows high risk of many alien plants present in Portugal. *Journal for Nature Conservation,* **35,** 1-12.

Mullerova, J., Pergl, J. and Pysek, P. (2013). Remote sensing as a tool for monitoring plant invasions: Testing the effects of data resolution and image classification approach on the detection of a model plant species *Heracleum mantegazzianum* (giant hogweed). *International Journal of Applied Earth Observation and Geoinformation,* **25,** 55-65.

Murphy, S.T., Subedi, N., Gnawali, S.R., Lamichhane, B.R., Upadhyay, G.P., Kock, R. and Amin, R. (2013). Invasive *Mikania* in Chitwan National Park, Nepal: The threat to the greater one-horned rhinoceros *Rhinoceros unicornis* and factors driving the invasion. *Oryx,* **47,** 361-368.

Mutanga, O., van Aardt, J. Van. and Kumar, L. (2009). Imaging spectroscopy (hyperspectral remote sensing) in southern Africa : An overview. *South African Journal of Science,* **105,** 193-198.

Nagendra, H. and Rocchini, D. (2008). High resolution satellite imagery for tropical biodiversity studies: The devil is in the detail. *Biodiversity and Conservation,* **17,** 3431-3442.

Nanjappa, H.V., Saravanane, P. and Ramachandrappa, B.K. (2005). Biology and management of *Lantana camara* L.—A review. *Agricultural Reviews,* **26,** 272-280.

Narumalani, S., Mishra, D.R., Wilson, R., Reece, P. and Kohler, A. (2009). Detecting and mapping four invasive species along the floodplain of North Platte River, Nebraska. *Weed Technology,* **23**(1), 99-107.

NCAR. (2018). *The Climate Data Guide: NDVI: Normalized-Difference-Vegetation-Index: NOAA AVHRR***.** National Center for Atmospheric Research Staff (Eds).

climatedataguide.ucar.edu/climate-data/ndvi-normalized-difference-vegetation-index-noaa-avhrr.

Ng, W.T., Meroni, M., Immitzer, M., Bock, S., Leonardi, U., Rembold, F., Gadain, H. and Atzberger, C. (2016). Mapping *Prosopis* spp with Landsat 8 data in arid environments: Evaluating effectiveness of different methods and temporal imagery selection for Hargesia Somaliland. *International Journal of Applied Earth Observational and Geoinformation,* **53,** 76-89.

Nepal, S.K. (2011). Mountain tourism and climate change: Implications for the Nepal Himalaya. *Nepal Tourism and Development Review,* **1**(1), 1-14.

Noonan, M. and Chafer, C. 2007. A method for mapping the distribution of willow at a catchment scale using bi-seasonal SPOT5 imagery. *Weed Research,* **47,** 173–181.

Paini, D.R., Sheppard, A.W., Cook, D.C., De Barro, P.J., Worner, S.P. and Thomas, M.B. (2016). Global threat to agriculture from invasive species. *Proceedings of the National Academy of Sciences*, **113**(27), 7575-7579.

Parsons, W.T. and Cuthbertson, E.G. (2001). Common *Lantana*. In Parsons W.T. and Cuthbertson, E.G. (Eds.), *Noxious Weeds of Australia* (pp. 627-632). Melbourne: CSIRO Publishing.

Piyasinghe, I., Gunatilake, J. and Madawala, H. (2018). Mapping the distribution of invasive shrub *Austroeupatorium inulifolium* (Kunth) RM King & H. Rob: A case study from Sri Lanka. *Ceylon Journal of Science,* **47**(1), 95-102.

Pocock, M.J.O., Roy, H.E., Preston, C.D. and Roy, D.B. (2015). The Biological Records Centre: a pioneer of citizen science. *Biological Journal of the Linnaean Society,* **115,** 475-493

Poudel, A.S., Shrestha, B.B., Joshi, M. D., Muniappan, R., Adiaga, A., Venkatramanan, S. and Jha, P.K. (2020). Predicting the current and future distribution of the invasive weed *Ageratina adenophora* in the Chitwan-Annapurna Landscape, Nepal. *Mountain Research and Development*, **40(2),** 61-71.

Priyanka, N. and Joshi, P. (2013). Modeling spatial distribution of *Lantana Camara*— A comparative study. *Canadian Journal of Basic and Applied Sciences*, **1,** 100-117.

Pyšek, P., Richardson, D.M., Rejmánek, M., Webster, G.L., Williamson, M. and Kirschner, J. (2004). Alien plants in checklists and floras: Towards better communication between taxonomists and ecologists. *Taxon*, **53**, 131–143.

Reichard, S.H. and White, P. (2001). Horticulture as a pathway of invasive plant introductions in the United States: most invasive plants have been introduced for horticultural use by nurseries, botanical gardens, and individuals. *Bioscience*, **51,** 103-113.

Roura-Pascual, N., Richardson, D.M., Krug, R.M., Brown, A., Chapman, R.A., Forsyth, G.G., Le Maitre, D.C., Robertson, M.P., Stafford, L., Van Wilgen, B.W., Wannenburgh, A. and Wessels, N. (2009). Ecology and management of alien plant invasions in South African fynbos: Accommodating key complexities in objective decision making. *Biological Conservation,* **142,** 1595–1604.

Rowlinson, L., Summerton, M. and Ahmed, F. (1999). Comparison of remote sensing data sources and techniques for identifying and classifying alien invasive vegetation in riparian zones. *Water SA*, **25**(4), 497-500.

Roy, H.E. (2015). The contribution of volunteer recorders to our understanding of biological invasions. *Biological Journal of the Linnaean Society*, **115,** 678 – 689

Ruwanza, S. and Shackleton, C.M. (2016). Effects of the invasive shrub *Lantana camara* on soil properties in the Eastern Cape, South Africa. *Weed Biology and Management*, **16,** 67-79.

Seebens, H., Blackburn, T.M., Dyer, E.E. and Genovesi, P. (2017). No saturation in the accumulation of alien species worldwide. *Nature Communications,* **8**, 14435. **DOI**:10.1038/ncomms14435

Sharma, G.P., Raghubanshi, A.S. and Singh, J.S. (2005). *Lantana* invasion: An overview, *Weed Biology and Management*, **5**(4), 157-165.

Shaw, D.R. (2005). Translation of remote sensing data into weed management decisions. *Weed Science,* **53,** 264–273.

Shouse, M., Liang, L. and Fei, S. (2013). Identification of understory invasive exotic plants with remote sensing in urban forests. *International Journal of Applied Earth Observation and Geoinformation,* **21,** 525-534.

Shrestha, B.B. (2016). Invasive alien plant species in Nepal. In Jha, P.K., Siwakoti, M. and Rajbhandari, S. (Eds.). *Frontiers of Botanty* (pp. 269-284). Kirtipur: Central Department of Botany, Tribhuvan University, Kathmandu.

Shrestha, B.B. (2019). Management of invasive alien plants in Nepal: Current practices and future prospects. In Garkoti, S.C., Van Bloem, S.J, Fulé, P.Z and Semwal, R.L. (Eds). *Tropical Ecosystems: Structure, Functions and Challenges in the Face of Global Change* (pp. 45-46). Springer Nature Singapore Pte Ltd.

Shrestha, B.B., Budha, P.B., Wong, L.J. and Pagad, S. (2019). *Global Register of Introduced and Invasive Species-Nepal*. Version 2.4. Invasive Species Specialist Group ISSG. Checklist dataset, https://doi.org/10.15468/4r0kkr accessed via GBIF.org on 2019-07-01.

Shrestha, B.B., Shabbir, A. and Adkins, S.W. (2015). *Parthenium hysterophorus* in Nepal: A review of its weed status and possibilities for management. *Weed Research,* **55,** 132-144.

Shrestha, B.B., Shrestha, U.B., Sharma, K.P., Thapa-Parajuli, R.B., Devkota, A. and Siwakoti, M. (2019). Community perception and prioritization of invasive alien plants in Chitwan-Annapurna Landscape, Nepal. *Journal of Environmental Management*, **229,** 38-47.

Tarantino, C., Casella, F., Adamo, M., Lucas, R., Beierkuhnlein, C. and Blonda, P. (2019). *Ailanthus altissima* mapping from multi-temporal very high resolution satellite images. *ISPRS Journal of Photogrammetry and Remote Sensing,* **147,** 90-103.

Te Beest, M., Cromsigt, J., Ngobese, J. and Olff, H. (2012). Managing invasions at the cost of native habitat? An experimental test of the impact of fire on the

invasion of *Chromolaena odorata* in a South African savanna. *Biological Invasions,* **14,** 607-618.

Thuiller, W., Richardson, D.M. and Midgley, G.F. (2007). Will climate change promote alien plant invasions? In Nentwig, W. (Ed.), *Ecological Studies,* **193**, 197-211, Springer-Verlag Berlin Heidelberg.

Tittensor, D.P., Walpole, M., Hill, S.L., Boyce, D.G., Britten, G.L., Burgess, N.D., Butchar, S.H.M., Leadley, P.W., Regan, E.C., Alkemade, R., Baumung, R., Bellard, C., Bouwman, L., Bowles-Newark, N.J., Chenery, A.M., Cheung, W.W.L., Christensen, V., Cooper, H.D.., Crowther, A.R., Dixon, M.J.R., Galli, A., Gaveau, V., Gregory, R.D., Gutierrez, N.L., Hirsch, T.L., Höft, R., Januchowski-Hartley, S.R., Karmann, M., Krug, C.B., Leverington, F.J., Loh, J., Lojenga, R.K., Malsch, K., Marques, A., Morgan, D.H.W., Mumby, P.J., Newbold, T., Noonan-Mooney, K., Pagad, S.N., Parks, B.C., Pereira, H.M., Robertson, T., Rondinini, C., Santini, L., Scharlemann, J.P.W., Schindle, S., Sumaila, U.R., Teh, L.S.L., van Kolck, J., Visconti, P. and Ye, Y. (2014). A mid-term analysis of progress toward international biodiversity targets. *Science,* **346,** 241-244.

Tiwari, S., Adhikari, B., Siwakoti, M. and Subedi, K. (2005). *An Inventory and Assessment of Invasive Alien Plant Species of Nepal*. Kathmandu: IUCN Nepal.

Tucker, C.J. (1979). Red and photographic infrared linear combination for monitoring vegetation. *Remote Sensing of Environment*, **8,** 127-150.

Underwood, E., Ustin, S. and Di Pietro, D. (2003). Mapping nonnative plants using hyperspectralimagery. *Remote Sensing Environment*, **86**(2), 150-161.

van den Berg, E., Kotze, I. and Beukes, H. (2014). Detection, quantification and monitoring of Prosopis in the Northern Cape Province of South Africa using remote sensing and GIS. *South African Journal of Geomatic,s* **2**(2), 68-81.

van Wilgen, B.W., Reyers, B., Le Maitre, D.C., Richardson, D.M. and Schonegevel, L. (2008). A biome-scale assessment of the impact of invasive alien plants on ecosystem services in South Africa. *Journal of Environmental Management*, **89**(4), 336-349.

Vilà, M., Basnou, C., Pyšek, P., Josefsson, M., Genovesi, P., Gollasch, S. and Hulme, P.E. (2010). How well do we understand the impacts of alien species on ecosystem services? A pan-European, cross-taxa assessment. *Frontiers in Ecology and the Environment,* **8**(3), 135-144.

Vila, M., Corbin, J.D., Dukes, J.S., Pino, J. and Smith, S.D. (2007). Linking plant invasions to global environmental change. In Canadell, J., Pataki, D., Pitelka, L. (Eds.). *Terrestrial Ecosystems in a Changing World* (pp. 93-102), Springer-Verlag, Berlin Heidelberg.

Vilà, M., Espinar, J.L., Hejda, M., Hulme, P.E., Jarošík, V., Maro, J.L., Pergl, J., Schaffner, U., Sun, Y. and Pyšek, P. (2011). Ecological impacts of invasive alien plants: a meta-analysis of their effects on species, communities and ecosystems. *Ecology Letters,* **14,** 702–708.

Waddel, E.H., Banin, L.F., Fleiss, S., Hill, J.K., Hughes, M., Jelling, A., Yeong, K.L., Ola, B.B., Sailim, A.B., Tangah, J. and Chapman, D.S. (2020). Land-use change and propagule pressure promote plant invasion in tropical rainforest remnants. *Landscape Ecology*, **35,** 1891-1906.

Wittenberg, R. and Cock, M.J.W. (2001). *Invasive Alien Species: A Toolkit of Best Prevention and Management Practices*. U.K.: CAB International, Wallingford.

WWF. (2013). Chitwan-Annapurna Landscape biodiversity important areas and linkages. WWF Nepal, *Hariyo Ban Program*.

Xie, Z., Roberts, C. and Johnson, B. (2008). *Object-based target search using remotely sensed data*: A case study in detecting invasive exotic Australian Pine in south Florida. *ISPRS Journal of Photogrammetry & Remote Sensing,* **63,** 647-660.

Xu, X. and Ji, W. (2014). Knowledge-based algorithm for satellite image classification of urban wetlands. *Proceedings of the International Conference of Computational Methods in Sciences and Engineering* (pp. 285-288). Athens, Greece.

Yang, J., Townsen, R.D. and Daneshfar, B. (2005). A GIS-based approach to river network floodplain delineation, *WIT Transactions on Ecology and the Environment*, **83,** 1743-3541.

ANNEXES

Annex 1: Checklist for data collection

Checklist									**Remarks**
Locality									
Management- 1 = Chemical, 2 = Physical, 3 = Biological, 4 = no management, 5 = other									
Magnitude - 1 = Low, 2 = Moderate, 3 = Dense, 4 = Just invaded, 5 = absent									
SN	**Latitude**	**Longitude**	**Elevation**	**Aspect**	**Slope**	**Species**	**Associated species**	**Landuse**	**Magnitude**	**Management**
						Lantana camara				

Annex 2: Climatological statistics of CHAL and outside CHAL for the year:

A. 1990

Station ID	Station name	District	Latitude	Longitude	rainfall	tmax	tmin
303	Jumla	Jumla	27.28333	82.16667	618.2	23.46693	9.348051
310	Dipal Gaun	Jumla	26.26667	83.21667	760.42	24.46959	9.29382
409	Khajura (Nepalganj)	Banke	26.1	81.78333	1234.94	33.48104	21.91676
416	Nepalgunj (Reg.Off.)	Banke	28.06667	81.61667	1308.96	33.08363	23.37841
420	Nepalgunj Airport	Banke	28.1	81.66667	1308.96	33.08363	23.37841
601	Jomsom	Mustang	28.78333	83.71667	124.48	20.19333	8.999048
604	Thakmarpha	Mustang	28.75	83.7	271.22	19.30476	9.537619
605	Baglung	Baglung	28.26667	83.6	1672.42	31.22571	18.92857
607	Lete	Mustang	28.63333	83.6	1028.76	19.30476	9.537619
609	Beni Bazar	Myagdi	28.35	83.56667	1255.92	31.02063	19.95794
612	Mustang (Lomangthang)	Mustang	29.18333	83.96667	88.34	17.19667	3.089286
614	Kushma	Parbat	28.21667	83.7	2256.76	30.58214	18.475
616	Gurja Khani	Myagdi	28.6	83.21667	1474.82	31.02063	19.95794
623	Dhiee	Mustang	29.1	84	151.8	17.19667	3.089286
633	Chhoser	Mustang	29.18333	83.98333	151.8	17.19667	3.089286
702	Tansen	Palpa	27.86667	83.53333	814.16	27.425	18.25571
706	Dumkauli	Nawalparasi	27.68333	84.21667	2069.24	32.71143	22.74857
708	Parasi	Nawalparasi	27.53333	83.66667	1757.86	32.71143	22.74857
715	Khanchikot	Arghakhanchi	27.93333	83.15	1490.98	21.94	18.92857
716	Taulihawa	Kapilbastu	27.55	83.06667	1425.76	33.67984	15.36571
725	Tamghas	Gulmi	28.06667	83.25	1579.56	24.69714	22.7203
728	Semari	Nawalparasi	27.53333	83.75	1401.68	35.30857	15.23714
802	Khudi Bazar	Lamjung	28.28333	84.36667	2993.74	29.14857	22.43238
804	Pokhara Airport	Kaski	28.21667	84	3452.8	28.83143	19.42881
805	Syangja	Syangia	28.1	83.88333	2454.78	29.84143	18.67143
806	Larke Samdo	Gorkha	28.66667	84.61667	871.2	29.84143	18.11143
808	Bandipur	Tanahun	27.93333	84.41667	1431.12	20.19333	8.962857
809	Gorkha	Gorkha	28	84.61667	1262.28	28.65952	18.80476
810	Chapkot	Syangja	27.88333	83.81667	1800.68	31.74571	20.90571
811	Malepatan (Pokhara)	Kaski	28.11667	84.11667	3334.1	28.99881	18.36488
814	Lumle	Kaski	28.3	83.8	5040.5	22.06571	14.86286
815	Khairini Tar	Tanahun	28.03333	84.1	2118.68	31.85086	20.03486

816	Chame	Manang	28.55	84.23333	615.66	19.56571	8.962857
817	Damauli	Tanahun	27.96667	84.28333	1477.46	20.19333	8.962857
832	Dandaswara	Syangja	28.08333	83.91667	2454.78	29.84143	18.67143
866	Pokhara Reg. Off.	Kaski	28.21667	83.98333	3452.8	28.83143	19.42881
902	Rampur	Chitawan	27.61667	84.41667	1638.8	32.91143	21.65657
905	Daman	Makwanpur	27.6	85.08333	1384.92	20.26429	11.34286
906	Hetaunda N.F.I.	Makwanpur	27.41667	85.05	2019.7	30.95381	20.76
918	Birganj	Parsa	27	84.86667	391.62	35.30857	20.76
927	Bharatpur	Chitawan	27.66667	84.43333	1638.8	32.91143	21.65657
1001	Timure	Rasuwa	28.28333	85.38333	1062.62	20.36714	12.53
1004	Nuwakot	Nuwakot	27.91667	85.16667	1450.4	29.67857	19.83095
1007	Kakani	Nuwakot	27.8	85.25	2619.08	21.45524	13.99143
1009	Chautara	Sindhupalchok	27.78333	85.71667	405.2	27.52246	15.90936
1016	Sarmathang	Sindhupalchok	27.95	85.6	275.3667	27.52246	15.90936
1027	Bahrabise	Sindhupalchok	27.78333	85.9	781.04	27.52246	15.90936
1030	Kathmandu Airport	Kathmandu	27.7	85.36667	285.86	27.52246	15.90936
1039	Panipokhari (Kathmandu)	Kathmandu	27.73333	85.33333	312.525	26.29874	16.17431
1055	Dhunche	Rasuwa	28.1	85.3	1781.467	22.08222	12.53
1057	Pansayakhola	Nuwakot	28.01667	85.11667	2963.62	20.36714	13.85162
1062	Sangachok	Sindhupalchok	27.7	85.71667	241.42	30.23647	18.84843
1071	Buddhanilakantha	Kathmandu	27.78333	85.36667	317.82	25.9213	13.94737
	Mustang	Mustang	29.329	83.966	88.34	17.19667	3.089286

B. 2000

Station ID	Station name	District	Latitude	Longitude	rainfall	tmax	tmin
303	Jumla	Jumla	27.283333	82.166667	622.86	23.717977	9.8688803
310	Dipal Gaun	Jumla	26.266667	83.216667	813.72	24.714434	9.5074858
409	Khajura (Nepalganj)	Banke	26.1	81.783333	1274.1	33.183583	23.229797
416	Nepalgunj (Reg.Off.)	Banke	28.066667	81.616667	1352.86	33.135047	24.101344
420	Nepalgunj Airport	Banke	28.1	81.666667	1353.46	33.247664	22.778411
601	Jomsom	Mustang	28.783333	83.716667	165.84	20.357143	10.334286
604	Thakmarpha	Mustang	28.75	83.7	266.46	19.548	9.7731429
605	Baglung	Baglung	28.266667	83.6	2139.2667	29.789286	18.692857
607	Lete	Mustang	28.633333	83.6	1126.1	19.020571	10.503905
609	Beni Bazar	Myagdi	28.35	83.566667	1488.68	30.400952	17.019524
612	Mustang (Lomangthang)	Mustang	29.183333	83.966667	209.85	19.020571	10.503905
614	Kushma	Parbat	28.216667	83.7	2691.54	30.4	19.189286
616	Gurja Khani	Myagdi	28.6	83.216667	1347.12	30.400952	18.388571
623	Dhiee	Mustang	29.1	84	148.53333	20.642857	7.8428571
633	Chhoser	Mustang	29.183333	83.983333	148.53333	20.642857	7.8428571
702	Tansen	Palpa	27.866667	83.533333	1290	26.166667	19.189683
706	Dumkauli	Nawalparasi	27.683333	84.216667	2538.74	32.474286	23.16
708	Parasi	Nawalparasi	27.533333	83.666667	1893.42	32.474286	23.16
715	Khanchikot	Arghakhanchi	27.933333	83.15	1558.26	22.025	13.216667
716	Taulihawa	Kapilbastu	27.55	83.066667	1247.22	32.688949	22.635412
725	Tamghas	Gulmi	28.066667	83.25	1911.5	24.642857	16.208571
728	Semari	Nawalparasi	27.533333	83.75	2148.74	34.215143	22.96781
802	Khudi Bazar	Lamjung	28.283333	84.366667	3200.5	29.422857	19.562857

804	Pokhara Airport	Kaski	28.216667	84	4422.42	28.962857	19.251429
805	Syangja	Syangia	28.1	83.883333	3185.36	29.177143	18.802857
806	Larke Samdo	Gorkha	28.666667	84.616667	554.32	29.177143	18.802857
808	Bandipur	Tanahun	27.933333	84.416667	1398.42	30.512571	21.368571
809	Gorkha	Gorkha	28	84.616667	1474.14	28.769643	18.55
810	Chapkot	Syangja	27.883333	83.816667	1907.48	30.431429	20.802857
811	Malepatan (Pokhara)	Kaski	28.116667	84.116667	4064.84	29.04219	19.188571
814	Lumle	Kaski	28.3	83.8	5773.5	22.58	15.377143
815	Khairini Tar	Tanahun	28.033333	84.1	2476.98	30.512571	21.368571
816	Chame	Manang	28.55	84.233333	553.28	19.037143	8.4657143
817	Damauli	Tanahun	27.966667	84.283333	1939.8	30.512571	21.368571
832	Dandaswara	Syangja	28.083333	83.916667	3386.9667	29.177143	18.802857
866	Pokhara Reg. Off.	Kaski	28.216667	83.983333	4422.42	28.962857	19.251429
902	Rampur	Chitawan	27.616667	84.416667	2331.34	33.137143	22.72
905	Daman	Makwanpur	27.6	85.083333	2004.62	21.614857	11.968571
906	Hetaunda N.F.I.	Makwanpur	27.416667	85.05	2810.24	31.751429	20.362857
918	Birganj	Parsa	27	84.866667	326.5	34.215143	22.96781
927	Bharatpur	Chitawan	27.666667	84.433333	1421.05	33.137143	22.72
1001	Timure	Rasuwa	28.283333	85.383333	580.94	21.614857	11.968571
1004	Nuwakot	Nuwakot	27.916667	85.166667	2163.98	29.646286	19.990857
1007	Kakani	Nuwakot	27.8	85.25	3055.52	21.7	14.348571
1009	Chautara	Sindhupalchok	27.783333	85.716667	425.38	27.902243	16.860654
1016	Sarmathang	Sindhupalchok	27.95	85.6	644.96	27.902243	16.860654
1027	Bahrabise	Sindhupalchok	27.783333	85.9	636.16	27.902243	16.860654
1030	Kathmandu Airport	Kathmandu	27.7	85.366667	351.9	27.902243	16.860654
1039	Panipokhari (Kathmandu)	Kathmandu	27.733333	85.333333	346.4	27.360476	17.139346
1055	Dhunche	Rasuwa	28.1	85.3	1754.02	22.653571	13.310714
1057	Pansayakhola	Nuwakot	28.016667	85.116667	3461.2	21.258095	10.328571
1062	Sangachok	Sindhupalchok	27.7	85.716667	320.44	30.4	19.189286
1071	Buddhanilakantha	Kathmandu	27.783333	85.366667	431.8	26.292012	14.14782
	Mustang	Mustang	29.329	83.966	209.85	19.020571	10.503905

C. 2010

Station ID	Station name	District	Latitude	Longitude	rainfall	tmax	tmin
303	Jumla	Jumla	27.283333	82.166667	698.32	24.078785	9.7472897
310	Dipal Gaun	Jumla	26.266667	83.216667	572.3	24.873223	8.5723578
409	Khajura (Nepalganj)	Banke	26.1	81.783333	1221.36	33.659272	22.537505
416	Nepalgunj (Reg.Off.)	Banke	28.066667	81.616667	1179	33.206558	23.542673
420	Nepalgunj Airport	Banke	28.1	81.666667	1425.78	33.68028	22.457757
601	Jomsom	Mustang	28.783333	83.716667	207.24	20.488571	8.9571429
604	Thakmarpha	Mustang	28.75	83.7	302.98	20.531429	9.1114286
605	Baglung	Baglung	28.266667	83.6	1598.04	29.335238	18.267143
607	Lete	Mustang	28.633333	83.6	1163.66	19.202857	9.5342857
609	Beni Bazar	Myagdi	28.35	83.566667	1518.48	30.12	18.808571
612	Mustang (Lomangthang)	Mustang	29.183333	83.966667	164.22	17.92	4.56
614	Kushma	Parbat	28.216667	83.7	2100.6	31.068571	18.048571
616	Gurja Khani	Myagdi	28.6	83.216667	1902.74	20.534286	8.9661905
623	Dhiee	Mustang	29.1	84	38.54	17.92	4.56

633	Chhoser	Mustang	29.183333	83.983333	164.22	17.92	4.56
702	Tansen	Palpa	27.866667	83.533333	1474.04	29.04	15.648571
706	Dumkauli	Nawalparasi	27.683333	84.216667	2111.04	32.737143	22.868571
708	Parasi	Nawalparasi	27.533333	83.666667	1044.92	41.1	24.1
715	Khanchikot	Arghakhanchi	27.933333	83.15	1593.1	22.939286	15.592857
716	Taulihawa	Kapilbastu	27.55	83.066667	1450.46	33.492951	22.725195
725	Tamghas	Gulmi	28.066667	83.25	1652.42	25.000238	15.777143
728	Semari	Nawalparasi	27.533333	83.75	1805.84	34.037143	20.757143
802	Khudi Bazar	Lamjung	28.283333	84.366667	2952.8	29.674286	18.237143
804	Pokhara Airport	Kaski	28.216667	84	3267.46	29.42	19.054286
805	Syangja	Syangia	28.1	83.883333	2566.84	29.148571	18.954286
806	Larke Samdo	Gorkha	28.666667	84.616667	557.425	26.832143	16.417857
808	Bandipur	Tanahun	27.933333	84.416667	1842	27.385714	18.532143
809	Gorkha	Gorkha	28	84.616667	1617.1	29.754286	19.955714
810	Chapkot	Syangja	27.883333	83.816667	1705.16	31.528571	20.537143
811	Malepatan (Pokhara)	Kaski	28.116667	84.116667	3364.88	29.697143	18.925714
814	Lumle	Kaski	28.3	83.8	5162.7	23.725714	14.78
815	Khairini Tar	Tanahun	28.033333	84.1	1878.36	31.582857	21.045714
816	Chame	Manang	28.55	84.233333	672.08	20.45	5.5821429
817	Damauli	Tanahun	27.966667	84.283333	1398.12	32.468571	20.237143
832	Dandaswara	Syangja	28.083333	83.916667	2676.26	26.832143	16.417857
866	Pokhara Reg. Off.	Kaski	28.216667	83.983333	3059.76	29.627976	19.816667
902	Rampur	Chitawan	27.616667	84.416667	1680.64	32.645714	21.314286
905	Daman	Makwanpur	27.6	85.083333	915.85	22.119048	13.455714
906	Hetaunda N.F.I.	Makwanpur	27.416667	85.05	2114.1	31.697143	20.971429
918	Birganj	Parsa	27	84.866667	197.72	40.322581	23.209677
927	Bharatpur	Chitawan	27.666667	84.433333	1770.18	33	22.461905
1001	Timure	Rasuwa	28.283333	85.383333	976.4	24.888571	14.19619
1004	Nuwakot	Nuwakot	27.916667	85.166667	1264.92	30.288095	19.381905
1007	Kakani	Nuwakot	27.8	85.25	2525.68	22.011429	13.848571
1009	Chautara	Sindhupalchok	27.783333	85.716667	190.14	28.039087	16.717078
1016	Sarmathang	Sindhupalchok	27.95	85.6	748.62	21.673585	12.849057
1027	Bahrabise	Sindhupalchok	27.783333	85.9	334.275	29.562489	16.609942
1030	Kathmandu Airport	Kathmandu	27.7	85.366667	287.84	28.476449	16.819252
1039	Panipokhari (Kathmandu)	Kathmandu	27.733333	85.333333	307.6	29.209917	18.514261
1055	Dhunche	Rasuwa	28.1	85.3	2031.4	22.527714	13.705238
1057	Pansayakhola	Nuwakot	28.016667	85.116667	2676.54	22.011429	13.848571
1062	Sangachok	Sindhupalchok	27.7	85.716667	207.26	29.562489	16.609942
1071	Buddhanilakantha	Kathmandu	27.783333	85.366667	402.06	27.266174	13.515944
		Mustang	Mustang	29.329	164.22	17.92	4.56

D. 2016

Station ID	Station name	District	Latitude	Longitude	Rainfall	tmax	tmin
303	Jumla	Jumla	27.283333	82.166667	575.56667	24.617445	10.066942
310	Dipal Gaun	Jumla	26.266667	83.216667	650.66667	25.892475	9.3637284
409	Khajura (Nepalganj)	Banke	26.1	81.783333	1338.7	34.128232	20.952522
416	Nepalgunj (Reg. Off.)	Banke	28.066667	81.616667	1286.4667	33.557499	23.798582
420	Nepalgunj Airport	Banke	28.1	81.666667	1369.4333	34.120249	22.568761

601	Jomsom	Mustang	28.783333	83.716667	194.30	20.87	9.50
604	Thakmarpha	Mustang	28.75	83.7	254.97	21.17	7.84
605	Baglung	Baglung	28.266667	83.6	1774.70	29.40	18.92
607	Lete	Mustang	28.633333	83.6	994.73	19.61	9.96
609	Beni Bazar	Myagdi	28.35	83.566667	1454.53	31.27	21.73
612	Mustang (Lomangthang)	Mustang	29.183333	83.966667	158.06667	18.121429	5.3357143
614	Kushma	Parbat	28.216667	83.7	2332.93	31.02	18.18
616	Gurja Khani	Myagdi	28.6	83.216667	528.17	22.22	7.47
623	Dhiee	Mustang	29.1	84	49.20	18.121429	5.3357143
633	Chhoser	Mustang	29.183333	83.983333	158.07	18.12	5.34
702	Tansen	Palpa	27.866667	83.533333	1218.30	28.73	17.60
706	Dumkauli	Nawalparasi	27.683333	84.216667	2156.50	35.27	23.37
708	Parasi	Nawalparasi	27.533333	83.666667	1327.23	34.01	22.51
715	Khanchikot	Arghakhanchi	27.933333	83.15	1221.73	23.80	15.35
716	Taulihawa	Kapilbastu	27.55	83.066667	1215.3667	33.402181	23.137072
725	Tamghas	Gulmi	28.066667	83.25	1577.97	25.78	15.78
728	Semari	Nawalparai	27.533333	83.75	1321.87	34.66	22.51
802	Khudi Bazar	Lamjung	28.283333	84.366667	2520.27	30.67	19.81
804	Pokhara Airport	Kaski	28.216667	84	3418.43	29.78	17.69
805	Syangja	Syangia	28.1	83.883333	2612.63	31.17	19.23
806	Larke Samdo	Gorkha	28.666667	84.616667	366.37	29.885714	19.261905
808	Bandipur	Tanahun	27.933333	84.416667	1241.40	28.31	19.13
809	Gorkha	Gorkha	28	84.616667	1299.00	30.83	20.53
810	Chapkot	Syangja	27.883333	83.816667	1364.70	31.95	20.78
811	Malepatan (Pokhara)	Kaski	28.116667	84.116667	3721.87	29.89	19.26
814	Lumle	Kaski	28.3	83.8	4767.47	22.46	15.26
815	Khairini Tar	Tanahun	28.033333	84.1	1942.73	32.31	21.30
816	Chame	Manang	28.55	84.233333	3042.4	26.228571	16.361905
817	Damauli	Tanahun	27.966667	84.283333	1088.50	33.45	21.79
832	Dandaswara	Syangja	28.083333	83.916667	3042.40	26.23	16.36
866	Pokhara Reg. Off.	Kaski	28.216667	83.983333	3721.8667	29.885714	19.261905
902	Rampur	Chitawan	27.616667	84.416667	1841.97	32.88	21.67
905	Daman	Makwanpur	27.6	85.083333	549.73333	20.10	8.00
906	Hetaunda N.F.I.	Makwanpur	27.416667	85.05	1959.03	31.61	21.24
918	Birganj	Parsa	27	84.866667	216.3	35.391057	24.319122
927	Bharatpur	Chitawan	27.666667	84.433333	2011.03	33.40	22.53
1001	Timure	Rasuwa	28.283333	85.383333	549.73	26.71	16.19
1004	Nuwakot	Nuwakot	27.916667	85.166667	1320.73	29.88	20.24
1007	Kakani	Nuwakot	27.8	85.25	1805.23	22.99	15.03
1009	Chautara	Sindhupalchok	27.783333	85.716667	474.6	25.860523	16.265364
1016	Sarmathang	Sindhupalchok	27.95	85.6	817.9	18.407588	10.608183
1027	Bahrabise	Sindhupalchok	27.783333	85.9	468.3	30.224019	15.715477
1030	Kathmandu Airport	Kathmandu	27.7	85.366667	274.63333	28.192523	16.953029
1039	Panipokhari (Kathmandu)	Kathmandu	27.733333	85.333333	244.96667	30.210148	17.796365
1055	Dhunche	Rasuwa	28.1	85.3	1390.70	22.94	13.58
1057	Pansayakhola	Nuwakot	28.016667	85.116667	1372.40	22.93	14.52
1062	Sangachok	Sindhupalchok	27.7	85.716667	250.5	25.860523	16.265364

1071	Buddhanilakantha	Kathmandu	27.783333	85.366667	493.6	25.939344	15.243333
	Mustang	Mustang	29.329	83.966	2332.9333	31.02381	18.17619

Annex 3: Data sources for Landsat images

Year	Row/path	Acquisition date	Instrument	Source
1992	142/040	1992/11/15	Thematic Mapper (TM)	https://earthexplorer.usgs.gov/
	142/041	1992/11/15		
	143/040	1992/11/06		
	141/041	1992/11/08		
	142/040	1992/11/29		
1999	141/040	1999/10/27	Thematic Mapper (TM)	https://earthexplorer.usgs.gov/
	141/041	1999/10/27		
	142/041	1999/12/05		
	143/043	1999/12/28		
	143/040	1999/10/27		
	142/040	1999/12/05		
2009	142/041	2009/10/29	Thematic Mapper (TM)	https://earthexplorer.usgs.gov/
	143/041	2009/11/05		
	142/040	2009/10/29		
	141/040	2009/11/23		
	143/040	2009/11/05		
	141/041	2009/11/23		
2018	141/041	2018/06/25	Operational Land Imager (OLI)	https://earthexplorer.usgs.gov/
	141/040	2018/06/25		
	142/040	2017/06/13		
	142/041	2016/06/10		
	143/040	2017/06/04		

Annex 4: Data sources for WV2 images

Districts	Raster	Acquisition Date
Chitwan	18JAN22050352-M2AS_R1C1-011412008070_01_P001	2018
	18JAN22050352-M2AS_R1C2-011412008070_01_P001	2018
	18JAN22050250-M2AS-058370866010_01_P001	2018
	17NOV20051739-M2AS_R1C1-011412008010_01_P001	2017
	17NOV20051739-M2AS_R1C2-011412008010_01_P001	2017
	10NOV02050845-M2AS_R1C1-011412008140_01_P001	2010
	10NOV02050845-M2AS_R1C2-011412008140_01_P001	2010
	10NOV02050845-M2AS_R1C3-011412008140_01_P001	2010
	10NOV02050845-M2AS_R1C4-011412008140_01_P001	2010
	10NOV02050845-M2AS_R2C2-011412008140_01_P001	2010
	10NOV02050845-M2AS_R2C3-011412008140_01_P001	2010
	10NOV02050845-M2AS_R2C4-011412008140_01_P001	2010
Dhading	18APR14053230-M2AS_R1C1-011412018020_01_P001	2018

	18APR14053230-M2AS_R1C2-011412018020_01_P001	2018
	18APR14053230-M2AS_R2C1-011412018020_01_P001	2018
	18APR14053230-M2AS_R2C2-011412018020_01_P001	2018
	18APR14053230-M2AS_R2C3-011412018020_01_P001	2018
	18APR14053230-M2AS_R3C2-011412018020_01_P001	2018
	18APR14053230-M2AS_R3C3-011412018020_01_P00	2018
	10APR24051303-M2AS_R1C1-011412008050_01_P001	2010
	10APR24051303-M2AS_R1C2-011412008050_01_P001	2010
	10APR24051303-M2AS_R2C1-011412008050_01_P001	2010
	10APR24051303-M2AS_R2C2-011412008050_01_P001	2010
	10APR24051303-M2AS_R2C3-011412008050_01_P001	2010
Gorkha	16FEB21051047-M2AS_R1C1-011412008110_01_P001	2016
	16FEB21051047-M2AS_R1C2-011412008110_01_P001	2016
	16FEB21051047-M2AS_R2C1-011412008110_01_P001	2016
	11MAR22050837-M2AS_R1C1-011412008120_01_P001	2011
	11MAR22050837-M2AS_R1C2-011412008120_01_P001	2011
	11MAR22050837-M2AS_R2C1-011412008120_01_P001	2011
Kaski	18MAR09051004-M2AS_R1C2-011412018030_01_P001	2018
	18MAR09051004-M2AS_R1C3-011412018030_01_P001	2018
	18MAR09051004-M2AS_R2C1-011412018030_01_P00	2018
	18MAR09051004-M2AS_R2C2-011412018030_01_P001	2018
	18MAR09051004-M2AS_R2C3-011412018030_01_P001	2018
	18MAR09051004-M2AS_R2C4-011412018030_01_P001	2018
	18MAR09051004-M2AS_R3C1-011412018030_01_P00	2018
	18MAR09051004-M2AS_R3C2-011412018030_01_P001	2018
	18MAR09051004-M2AS_R3C3-011412018030_01_P001	2018
	18MAR09051004-M2AS_R3C4-011412018030_01_P001	2018
	18MAR09051004-M2AS_R4C1-011412018030_01_P001	2018
	17DEC09052020-M2AS-058496162010_01_P0021	2017
	12MAY15052059-M2AS_R1C1-011412008030_01_P001	2012
	12MAY15052059-M2AS_R1C2-011412008030_01_P001	2012
	12MAY15052059-M2AS_R2C1-011412008030_01_P001	2012
	12MAY15052059-M2AS_R2C2-011412008030_01_P001	2012
	12MAY15052059-M2AS_R2C3-011412008030_01_P001	2012
Makwanpur	17NOV30050815-M2AS_R1C1-011412008100_01_P001	2017
	17NOV30050815-M2AS_R1C2-011412008100_01_P001	2017
	17NOV30050815-M2AS_R2C1-011412008100_01_P001	2017
	17NOV30050815-M2AS_R2C2-011412008100_01_P001	2017
	18JAN22050233-M2AS_R1C1-011412008060_01_P001	2018
	18JAN22050233-M2AS_R1C2-011412008060_01_P001	2018
	18JAN22050233-M2AS_R2C1-011412008060_01_P001	2018
	18JAN22050233-M2AS_R2C2-011412008060_01_P001	2018
	18JAN22050233-M2AS_R2C3-011412008060_01_P001	2018
	18JAN22050233-M2AS_R3C3-011412008060_01_P001	2018

	09DEC02050534-M2AS_R1C1-011412008090_01_P001	2009
	09DEC02050534-M2AS_R2C1-011412008090_01_P00	2009
	10DEC16051138-M2AS_R1C1-011412008080_01_P001	2010
	10DEC16051138-M2AS_R1C2-011412008080_01_P001	2010
Nawlparasi	18JAN25052515-M2AS_R1C1-011412018040_01_P001	2018
	18JAN25052515-M2AS_R1C2-011412018040_01_P001	2018
	18JAN25052515-M2AS_R1C3-011412018040_01_P001	2018
	18JAN25052515-M2AS_R2C1-011412018040_01_P001	2018
	18JAN25052515-M2AS_R2C2-011412018040_01_P001	2018
	17DEC06053039-M2AS-059477838020_01_P001	2017
	10NOV05051952-M2AS-011412008020_01_P001	2010
	10NOV05051931-M2AS-011412008020_01_P002	2010
Tanahau	18MAR19050245-M2AS_R1C1-011412008130_01_P001	2018
	18MAR19050245-M2AS_R1C2-011412008130_01_P001	2018
	18MAR19050245-M2AS_R1C3-011412008130_01_P001	2018
	18MAR16052211-M2AS-011412008130_01_P002	2018
	17DEC09052001-M2AS-058496164010_01_P001	2017
	09FEB14050434-M2AS_R1C1-011412008150_01_P001	2009
	09FEB14050434-M2AS_R1C2-011412008150_01_P001	2009
	09FEB14050434-M2AS_R1C3-011412008150_01_P001	2009
	09FEB14050434-M2AS_R1C4-011412008150_01_P00	2009
	09FEB14050434-M2AS_R2C3-011412008150_01_P001	2009
	09FEB14050434-M2AS_R2C4-011412008150_01_P001	2009
Myagdi	18NOV06051534-M2AS-059477838010_01_P001	2018

Annex 5: Landuse and landcover map

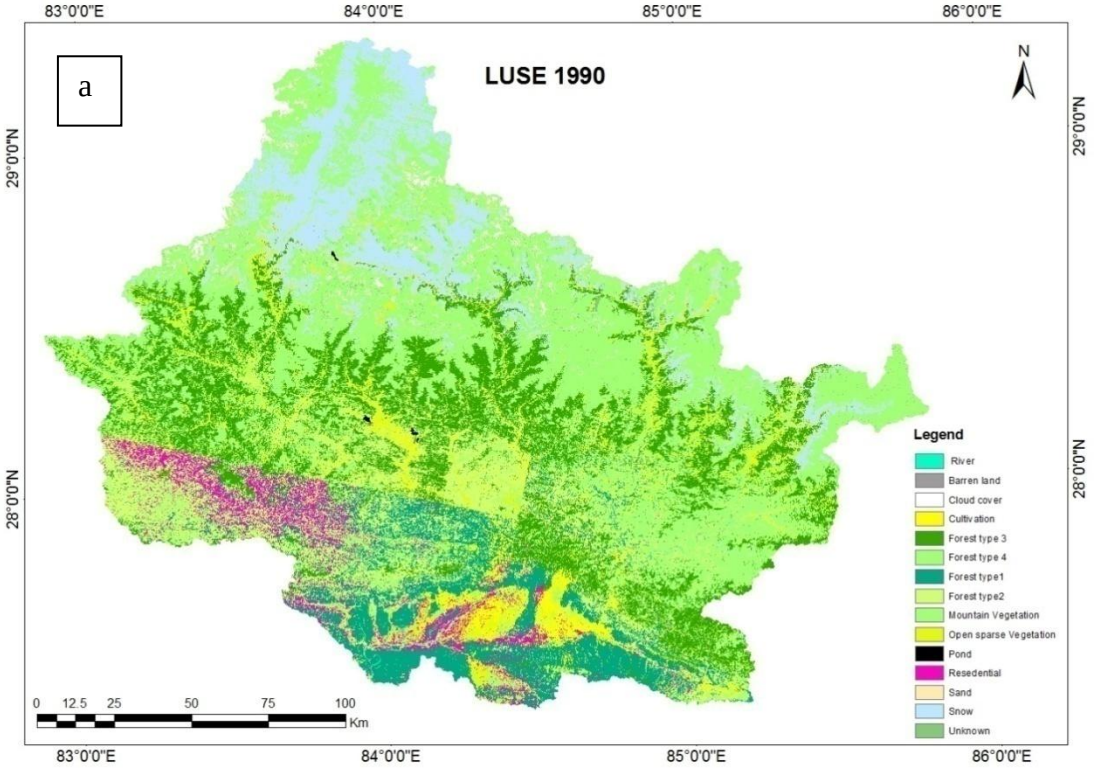

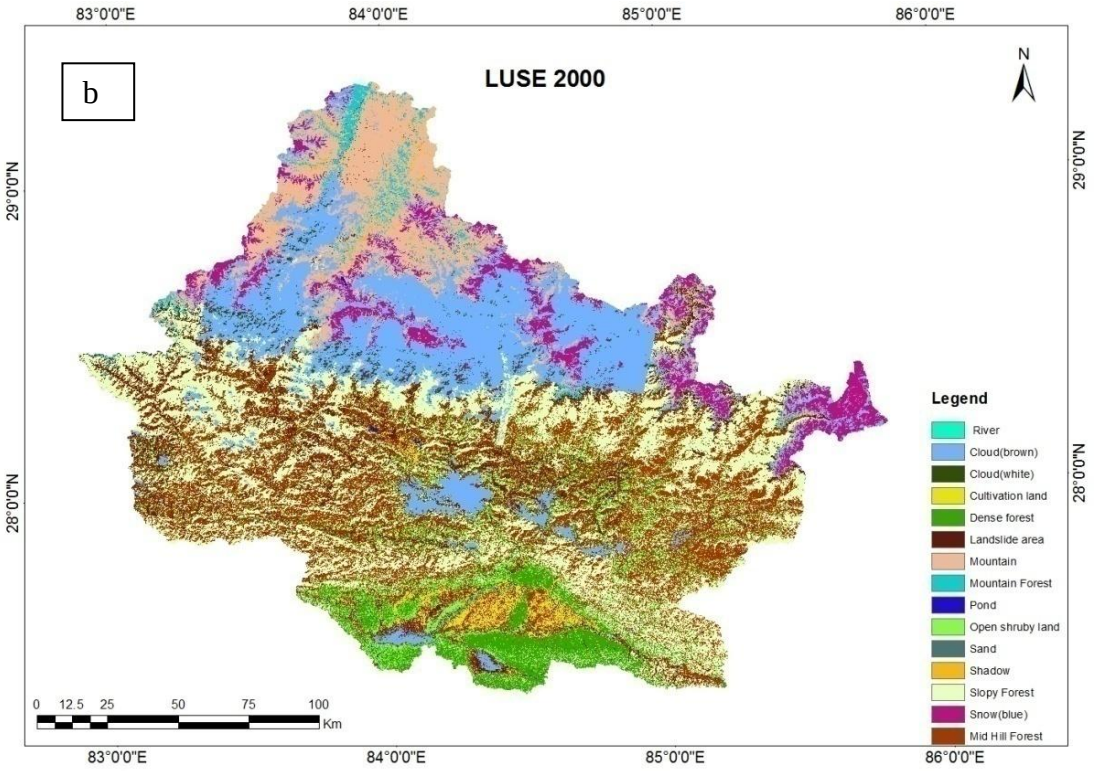

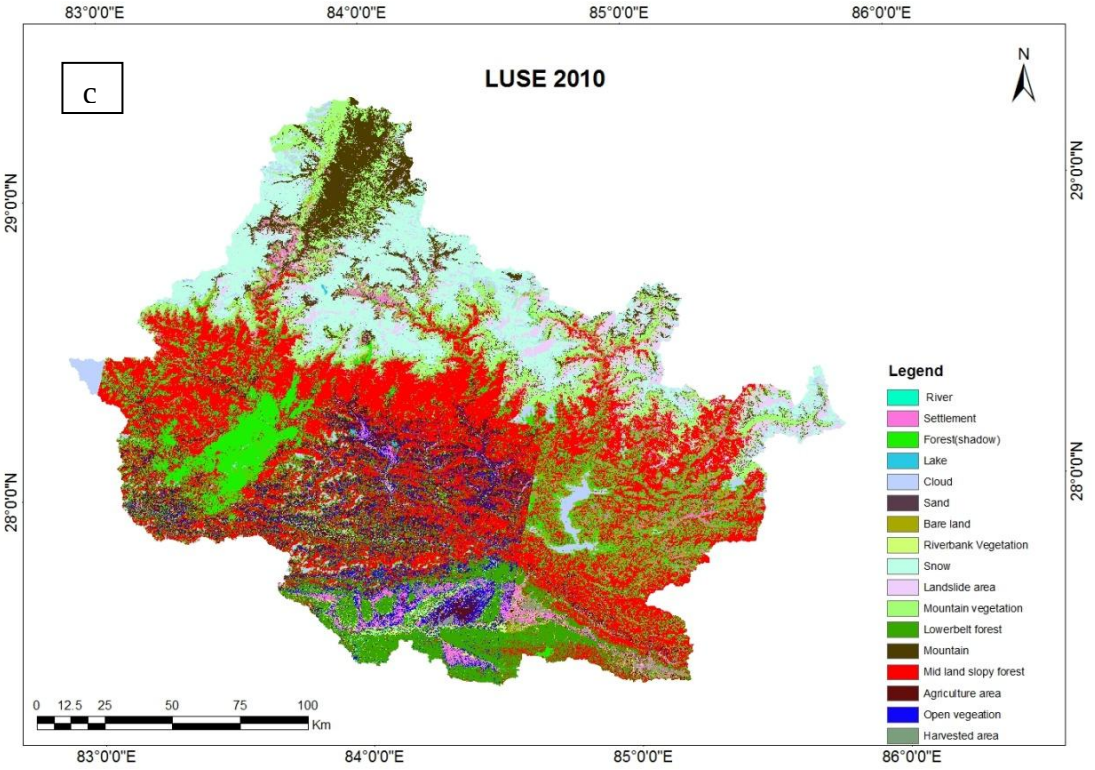
c
LUSE 2010
N
83°0'0"E
84°0'0"E
85°0'0"E
86°0'0"E
29°0'0"N
28°0'0"N
Legend
River
Settlement
Forest(shadow)
Lake
Cloud
Sand
Bare land
Riverbank Vegetation
Snow
Landslide area
Mountain vegetation
Lowerbelt forest
Mountain
Mid land slopy forest
Agriculture area
Open vegeation
Harvested area
0 12.5 25 50 75 100
Km

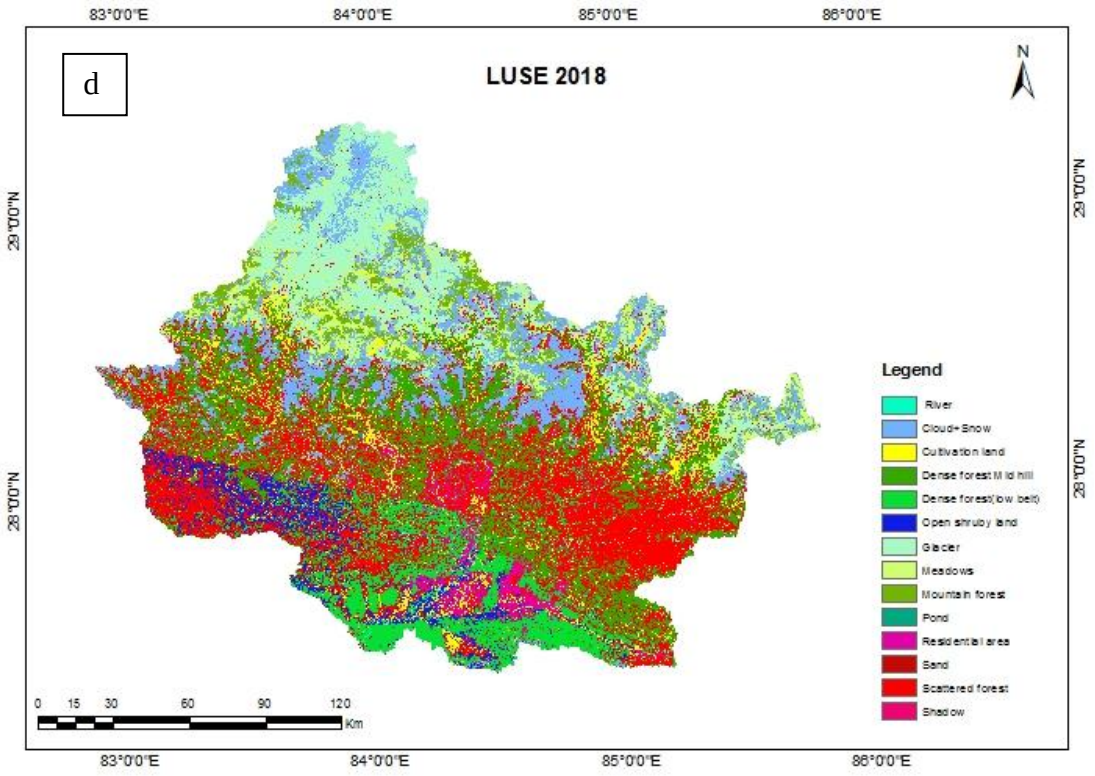
d
LUSE 2018
N
83°0'0"E
84°0'0"E
85°0'0"E
86°0'0"E
29°0'0"N
28°0'0"N
Legend
River
Cloud+Snow
Cultivation land
Dense forest Mid hill
Dense forest(low belt)
Open shruby land
Glacier
Meadows
Mountain forest
Pond
Residential area
Sand
Scattered forest
Shadow
0 15 30 60 90 120
Km

Annex 6: Elevational range covered by *Lantana camara*

SN	Year (AD)	Minimum elevation (m)	Maximum elevation (m)	Range	Mean
1	1990	193	1425	1232	492.61
2	2000	136	1562	1426	742.69
3	2010	146	1591	1445	698.26
4	2018	143	1618	1475	874.46

Annex 7: Summary of classification accuracies for Landsat images of CHAL

Site	Year	Overall accuracy (%)	User accuracy (%)		Producer accuracy (%)		Error of ommission		Error of commission		Kappa Statistics (k)
			Absent	Present	Absent.	Present.	Absent.	Present.	Absent	present	
CHAL	2018	77.25	78.38	76.21	75.27	79.23	0.24	0.2	0.21	0.2	0.54

Annex 8: Summary of classification accuracies for Landsat and World view 2 images of the year 2018

Districts	Sites	Class	Landsat				Digital globe			
			Producer's	User's	Com. Error	Omi. Error	Producer's	User's	Com. Error	Omi. Error
Chitwan	Rampur	Absent	79.3	70.7	0.29	0.2	82.7	75	0.25	0.17
		Present	80.2	86.5	0.13	0.19	83.3	88.88	0.11	0.16
Tanahau	Dulegauda	Absent	79.6	84.9	0.15	0.2	82.3	89.4	0.10	0.17
		Present	82.9	77.0	0.22	0.17	88.2	80.5	0.19	0.11
Tanahau	Ghasikuwa	Absent	80.0	83.3	0.16	0.20	86.0	84.3	0.15	0.14
		Present	84.0	80.7	0.19	0.16	84.0	85.7	0.14	0.16
Dhading	Dharke	Absent	80.0	83.3	0.16	0.20	84.0	87.5	0.12	0.16
		Present	84.0	80.7	0.19	0.16	88.0	84.6	0.15	0.12
Makwanpur	Hetauda	Absent	80.0	83.3	0.12	0.20	84.0	87.5	0.12	0.16
		Present	84.0	80.7	0.15	0.16	88.0	84.6	0.15	0.12
Makwanpur	Manahari	Absent	82.0	83.6	0.16	0.18	86.0	87.7	0.12	0.14
		Present	84.0	82.3	0.17	0.16	88.0	86.2	0.13	0.12
Chitwan	Muglin	Absent	78.0	79.5	0.2	0.22	84.0	82.3	0.17	0.16
		Present	80.0	78.4	0.21	0.20	82.0	83.6	0.16	0.18
Nawalparasi	Devchuli	Absent	78.0	82.9	0.17	0.22	86.0	89.5	0.1	0.14
		Present	84.0	79.2	0.2	0.16	90.0	86.5	0.13	0.10
Kaski-	Leknath-	Absent	76.0	79.1	0.2	0.24	78.0	82.9	0.17	0.22
Syangja	Kudule	Present	80.0	76.9	0.1	0.20	84.0	79.2	0.20	0.16

Com. Error - Commission Error, Omi. Error - Omission Error

Annex 9: Comparison on P-value of area cover between Landsat and WV2 for the year 2008 and 2018

AOI	Total Area of AOI (km^2)	Landsat (2008) Area(km^2)	WV2(2008) Area(km^2)	Landsat (2018) Area(km^2)	WV2(2018) Area(km^2)
Dharke	60.95	3.19	3.01	5.18	4.66
Devchuli	44.22	1.54	1.26	2.49	1.91
Manahari	106.8	2.45	1.87	6.08	4.16
Hetauda	54.3	2.12	1.90	3.09	2.83
Muglin	39.85	1.33	0.99	2.17	1.53
Ghasikuwa	75.34	2.45	2.18	3.98	3.27
Lekhnath	96.67	2.75	1.86	3.77	2.49
P- value		**0.27**		**0.24**	

Annex 10: Photoplates

Dense patch (>5*5)

Moderate patch (5*5)

Low patch (2*2)

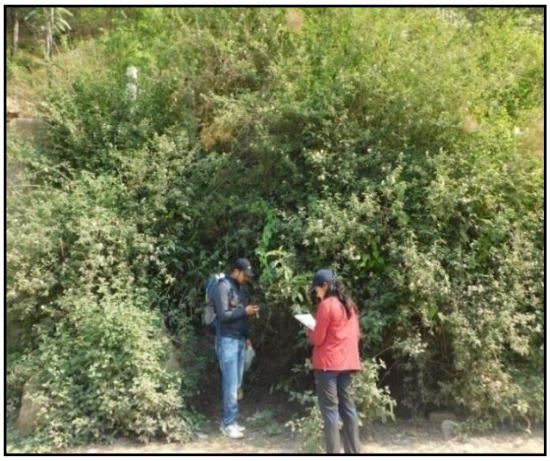

Data collection at Roadside

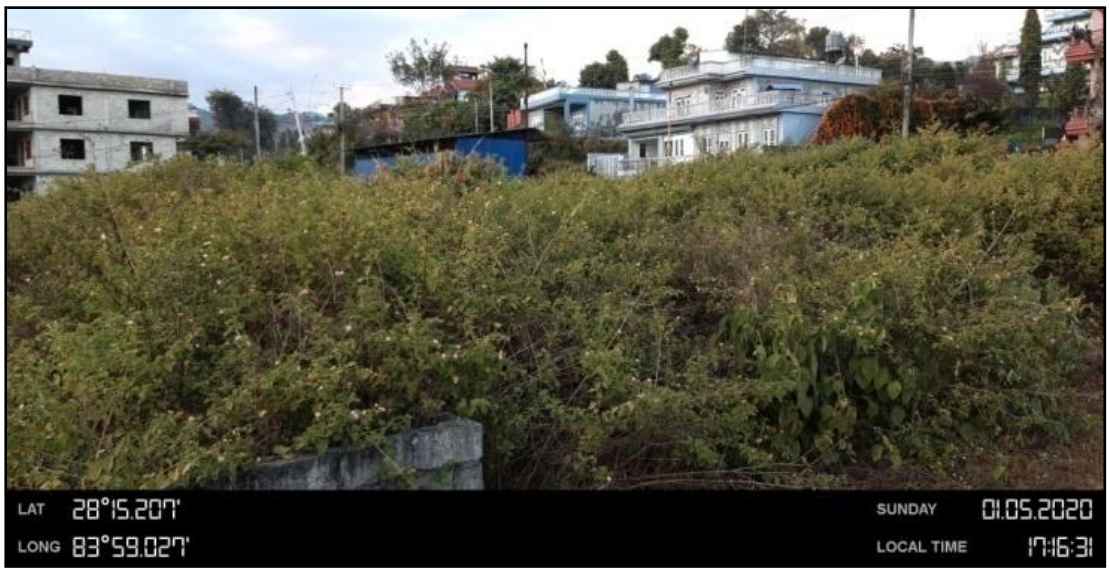

Dense patch invaded by *Lantana camara*

Dense patch of *Lantana camara* along Roadside

Absent point for *Lantana camara*

Interaction with local people

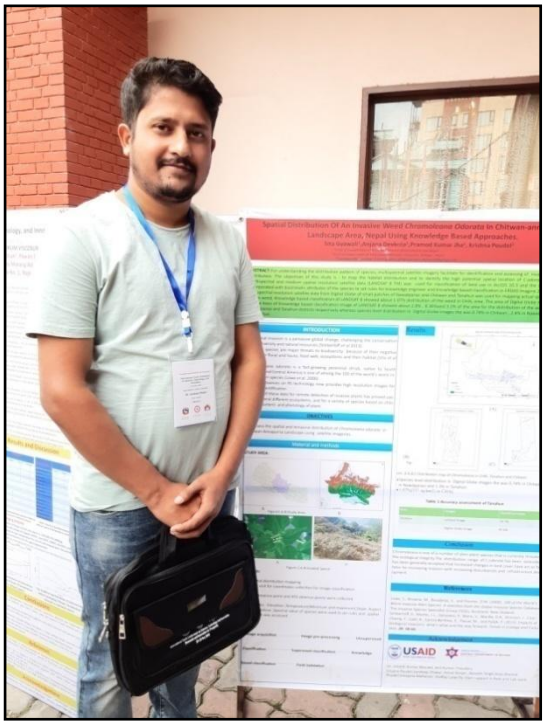

Participation on conference conducted by NAST

Participation on conference on 'NCIBP 2020'